The Pennsylvania State University

The Graduate School

College of Health and Human Development

OPTIMALITY AND STABILITY OF INTENTIONAL AND UNINTENTIONAL ACTIONS DURING MULTI-FINGER FORCE-MOMENT PRODUCTION

A Thesis in

Kinesiology

by

Behnoosh Parsa

Submitted in Partial Fulfillment

of the Requirements

for the Degree of

Master of Science

August 2016

The thesis of Behnoosh Parsa was reviewed and approved* by the following:

Mark L. Latash
Distinguished Professor of Kinesiology
Thesis Advisor

Robert L. Sainburg
Professor of Kinesiology and Neurology

Stephen J. Piazza
Professor of Kinesiology, Mechanical Engineering, and Orthopedics and Rehabilitation

Vladimir Zatsiorsky
Professor of Kinesiology

*Signatures are on file in the Graduate School

ABSTRACT

This thesis investigates intentional and unintentional human actions during multi-finger isometric force-moment production tasks. In the first study, a multi-finger isometric force-moment task was used for studying the nature of force and moment unintentional drift, and the force-moment stabilizing synergies. In this experiment subjects were utilizing visual feedback to maintain a certain amount of force and moment. At some point after subjects had stabilized their performance at the target, either force, or moment, or both feedbacks were turned off. The finger forces were studied under the uncontrolled-manifold and referent configuration hypothesis. This study showed that the absolute value of force and moment drops without visual feedback. However, drifts in individual finger forces could be in different directions; in particular, fingers that produced moments of force against the required total moment showed an increase in their forces. The force/moment drift was associated with a drop in the index of synergy stabilizing performance under visual feedback. The drifts in directions that changed performance (non-motor equivalent) and in directions that did not (motor equivalent), were of about the same magnitude. The results suggest that control with referent coordinates is associated with drifts of those referent coordinates toward the corresponding actual coordinates of the hand – a reflection of the natural tendency of physical systems to move toward the minimum of potential energy. The interaction between drifts of the hand referent coordinate and referent orientation led to counter-directional drifts in individual finger forces. The results also demonstrate that the sensory information used to create multi-finger synergies is necessary for their presence over the task duration.

In the second study, subjects performed a set of force-moment tasks with different levels of force and moment. These data were used to compute a cost function using the analytical inverse optimization method. Then, the subjects were asked to produce accurate force-moment tasks with a non-preferred sharing among the fingers. This was done by asking the subjects to reduce the middle finger force to half of its magnitude during the comfortable task performance. Adding this new constraint to an ongoing task resulted in a drop of variance within the uncontrolled manifold leading to a decline in the synergy index. Then, the visual feedback was removed for one, two, or all three of the main variables (force, moment, and middle finger force). The studies showed that the observed drift in performance variables was due to two processes, a drift of the referent coordinate toward the actual coordinate leading to a decrease in the finger forces, and a movement in the space of finger forces in a direction that did not affect the performance, but it reduced the cost of performing the task. Overall, these results fit naturally the scheme of hierarchical control using changes in referent coordinates for relevant variables.

TABLE OF CONTENTS

LIST OF FIGURES

LIST OF TABLES

ACKNOWLEDGEMENTS

Firstly, I would like to express my sincere gratitude to my advisor Prof. Mark Latash for the continuous support of my Master study and related research, for his patience, motivation, and immense knowledge. His guidance helped me in all the time of research and writing of this thesis. I could not have imagined having a better advisor and mentor for my Master study.

Besides my advisor, I would like to thank the rest of my thesis committee: Prof. Vladimir Zatsiorsky, Prof. Stephen J. Piazza, and Prof. Robert L. Sainburg, for their insightful comments and encouragement, but also for the questions which incented me to widen my research from various perspectives.

Last but not the least, I would like to thank my family: my parents and my sister for supporting me spiritually throughout writing this thesis and my life in general.

Chapter 1

Introduction

It has been observed that turning off the visual feedback while a person is producing a constant total force in isometric condition with the help of visual feedback leads to a drift in force without the subject being aware of the force drop. The drift is sometimes as large as 30% percent of the initial force level over 20-30 s. This phenomenon has been studied in two main ways. First, this phenomenon has been interpreted as a reflection of a limitation of working memory with the possible contribution of fatigue (Slifkin et al. 2000, Vaillancourt and Russell 2002). A few recent studies questioned this interpretation (Ambike et al. 2015; Jo et al. 2015), in particular, based on an observation that resting for a similar time interval does not result in a consistent change in the force level reproduced without visual feedback after the rest interval.

An alternative explanation has been suggested based on an approach to human motor action as reflections of natural motion of a physical/physiological system (including both neural and muscle elements and the external forces) toward its most stable state corresponding to the minimum of potential energy (Latash 2010; Ambike et al. 2015).). According to this view, the phenomenon of unintentional drift can be interpreted based on two concepts. The first concept suggests that the control of the voluntary actions is performed by changing the referent configurations (RCs) of the involved effectors (Feldman and Levin 1995; Feldman 2015). For example, when squeezing an object in the hand, the RC of the hand is situated inside the squeezed object. The squeezing force is then determined by the distance between the actual configuration of the hand (AC) and RC. The second is the idea of synergic control of redundant systems (note that all natural actions involve redundant sets of effectors, Bernstein 1967) based on the principle of abundance (Latash 2012). Within this scheme, producing a constant force by an effector is associated with setting its RC (and possibly apparent stiffness, Latash and Zatsiorsky 1993) and keeping it unchanged with the help of visual feedback. When the feedback becomes unavailable, RC drifts toward the actual coordinates and causes a slow decrease of the produced force. This hypothetical mechanism has been referred to as RC-back-coupling (Reschechtko et al. 2014; Ambike et al. 2015; Zhou et al. 2015). For instance, force production by a finger in isometric conditions is associated with setting a referent coordinate for the fingertip and a magnitude of apparent stiffness (k, which is also a reflection of shifts in spatial RCs for the participating muscles) (Pilon et al. 2007; Feldman 2015; Ambike et al. 2016b). Given the constant actual coordinate of the effector (AC), force magnitude $F = k(RC - AC)$. A slow drop in force means that RC drifts toward AC (for simplicity, we do not consider here possible changes in k).

The concepts of RC and synergic control were used to explain the overall change in the salient performance variable and its stability as reflected, for example, in the structure of inter-trial variance within the space not affecting the performance (UCM) and orthogonal to that space (ORT). In this study, we focus on the third characteristic of actions by abundant systems, namely the average across trials sharing of the salient performance variable among the elements. We consider only the systems where effects of the individual variables on the performance variable are additive, such as producing a total force and a total moment with four fingers. Sharing has been addressed based on optimality principles (reviewed in Prilutsky and Zatsiorsky 2002). Recently, a method of analytical inverse optimization (ANIO) has been introduced (Terekhov et al. 2010) that allows computing a cost function based on observed behavior of a redundant system over a broad range of task constraint values.

The present study was primarily motivated by the fact that none of the studies of four finger isometric force-moment production tasks in the concept of unintentional drifts have focused on the direction of the change in total force and moment magnitudes. The change in force and moment sometimes reported in studies concerning other questions. The other important motivation was that human actions have been mainly studied in biomechanics and motor control within the optimization concepts. That is human actions have been considered to be optimal and follow optimization criterion. However, by observing the phenomenon of unintentional drift in performance variables, it seems that we are facing a violation from the optimality.

1.1 Goals of This Study

There are two main goals for this study: the first is to examine the RC-back coupling interpretation of the unintentional drift for a four-finger isometric force-moment production task. In this part, the direction of the spontaneous drift in the space of finger forces was also explored. The second is to investigate if the unintentional drift is leading to minimization of a cost function defined using ANIO. Moreover, the effect of an additional constraint (prescribing force by the middle finger) was also investigated as part of the second goal. The following specific hypotheses were studied.

1.1.1 Exploring the interpretation of the unintentional drift for a four-finger total force-moment task

1- We expected that drifts of RC toward the actual coordinate (AC) and of referent orientation (RO) toward the actual orientation (AO) would lead to a parallel drop in both total force (F_{TOT}) and total moment (M_{TOT}) magnitudes.

2- Depending on the role of individual fingers in the M_{TOT} production, some fingers are expected to show a drift toward lower forces (fingers that contribute to M_{TOT} production in the initial condition) while others may show a drift to higher forces (fingers that act against the instructed M_{TOT}, "moment antagonists", Zatsiorsky et al. 2002)

3- Several recent studies have shown that synergies stabilizing salient performance variables persist during unintentional movements (or force changes) in response to a transient external perturbation (Wilhelm et al. 2013; Zhou et al. 2014). While no studies explored synergies during spontaneous force drift, we hypothesized that synergies would indeed persist during F_{TOT} and M_{TOT} drifts.

4- A spontaneous drift in a performance variable, $F_{TOT,}$ and M_{TOT} is expected to lead to an increase in the corresponding variance component in the ORT space (V_{ORT}) compared to the condition with feedback.

1.1.2 Unintentional drift of the performance variables and the cost drift in the presence of a new constraint

1- Unintentional changes in performance variables during continuous static task without visual feedback are duo to two processes. First, there is RC-back-coupling leading to a drift of the RC towards the actual coordinate of the effector. Second, there is a drift within the UCM toward a minimum of the cost function reflected in coordinated drifts of the elemental variables.

2- We predicted that F_{TOT} would drop (similarly to Vaillancourt and Russell 2002; Ambike et al. 2015a) while M_{TOT} drift would depend on the initial magnitude and direction of M_{TOT} and directed toward its zero magnitude corresponding to the horizontal actual orientation of the hand.

3- Considering a new constrain on the middle finger force, after visual feedback had been turned off, the forces drift towards their preferred sharing pattern.

1.1.3 Structure of variance and motor equivalence in the presence of a new constraint

1- Stability of performance variables would be selective even when the magnitudes of those variables drift unintentionally.
2- We also explored whether the stability of a variable depended on the number of explicit task constraints.

1.2 Related Publications

The procedures and data in this thesis have been described in three journal articles. The exploration of the RC-back-coupling interpretation of the unintentional drift for a four-finger isometric total force-moment production task is in the press in *Journal of Neurophysiology* under the title of "**On the Nature of Unintentional Action: A Study of Force/Moment Drift during Multi-Finger Task**" by Behnoosh Parsa, Daniel J. O'Shea, Vladimir M. Zatsiorsky, Mark L. Latash. The Unintentional drift of the performance variables and the cost drift in the presence of a new constraint is in the press in *Journal of Experimental Brain Research* under the title of "**Optimality and stability of intentional and unintentional actions: I. Origins of drifts in static performance**" by Behnoosh Parsa, Alexander Terekhov, Vladimir M. Zatsiorsky, Mark L. Latash. The Structure of variance and motor equivalence in the presence of a new constraint is in the press in *Journal of Experimental Brain Research* under the title of "**Optimality and stability of intentional and unintentional actions: II. Motor equivalence and structure of variance**" by Behnoosh Parsa, Vladimir M. Zatsiorsky, Mark L. Latash.

Chapter 2

Literature Review

2.1 Motor Variability

It was first emphasized by Bernstein 1947 that repetition of the same movement never leads to same actions, and he named this phenomenon “repetition without repetition”. However, this aspects of motor variability have been viewed by researchers in many ways. Some viewed it as an existing “noise” in human actions which makes it harder to be studied. Later at the end of the nineteenth century, researchers started to view this phenomenon with more appreciation. Woodworth, for instance, performed a series of studies on the relations between accuracy requirements and speed of movement (reviewed in Newell and Vaillancourt 2001).

More recently, researchers started to study motor variability to explore synergies in human actions (Latash 2006). A system has synergy when its elements compensate each other’s shortcomings when they are performing a particular task. A critical component to a synergy is that it can change its functioning in a task-specific way, in other words, it forms a new set of rules for its elements to work together for performing a different task. The hand can open can lids, turn a screwdriver, write with the pen, and play music.

As it was mentioned, one of the features of synergy is that effects of deviations in the contribution of one of the elements are compensated by adjustments in the contributions of other elements. This gives the system flexibility to stabilize important performance variables. Hence, an analysis of patterns of variability of elements of a system may reveal if its elements are working with a synergy and what that synergy is trying to accomplish. A promising computational method to analyze variability within elemental variables for studying synergy has been developed by Gregor Schoner (1995) and tested experimentally (Scholz and Schoner 1999). They called this approach the uncontrolled manifold (UCM) hypothesis.

2.2 Uncontrolled Manifold Hypothesis

Numerous elements involved in performing a task are not a source of computational problems for the nervous system but a useful, flexible apparatus that requires proper organization (Latash 2006). This is known as the principle of abundance presented by Gelfand and Tsetlin (1966) to describe essential properties of structural units like the human body. If we introduce the organization of human actions by a

hierarchical structure the notion of "principle of abundance" indicates that within the hierarchical organization, a functional goal is formulated by an upper level of the hierarchy, but this formulation does not suppress the freedom of the elements at the lower level of the hierarchy.

The question is how the elements of a structural unit organize their action to fulfill a goal set by CNS. According to the principle of abundance, biological systems control their essential functions using hierarchically organized multi-level structure, and in the case of facing a redundant problem, it chooses a family of solutions solving the problem within an acceptable margin of error. This seems to conflict with the optimization approaches addressing the mathematical problems of redundancy; however, researchers believe in this method say that they think those families of the solution is derived by an optimal criterion by the nervous system (Latash 2006).

To quantify the behavior of these families of the solution and find criteria for studying the synergy occurring in human action, Schoner introduced the uncontrolled manifold hypothesis. To illustrate this hypothesis, imagine we asked a person to produce 40 N force by two fingers (F_1 and F_2). Figure 2-1 shows three possible outcomes of such experiment. In the left panel, the data distributed evenly between the two fingers (a circular distribution). This means if one finger introduces an error in total force production, the other finger will, with equal probability, reduce the error or amplify it. Therefore, we can say that there is no synergy between two fingers that try to stabilize their total force production. In panel B, data distribution forms an ellipse elongated along the $F_1 + F_2 = 40$ N line. In such distribution if one finger produces more force the other finger is more likely to produce less force. Therefore, this relationship reduces the probability of the occurrence of an error in the total force. In another word, the co-variation of finger forces distributed in this way stabilizes the total force value and may be interpreted as a force-stabilizing synergy.

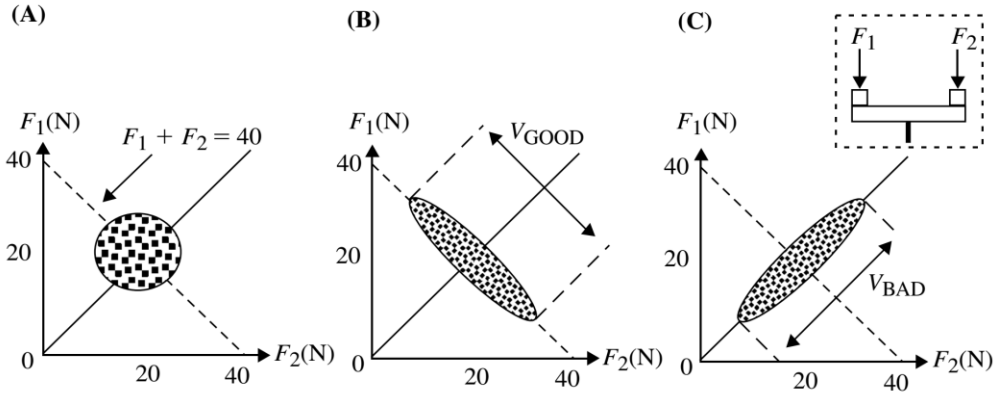

Figure 2-1. Clouds of data points measured in several trials for producing a total force of 40 N. (A) the data points may form a circular cloud about a certain average sharing of total force between the two fingers. Alternatively, the data point may form an ellipse elongated along the line $F_1+F_2=40$ (the dashed slanted line, B) or elongated perpendicular to this line (the solid slanted line, C). Variance along the dashed line does not affect total force (good variance, V_{GOOD}) while variance along the solid line does (bad variance, V_{BAD}). This figure was taken from the book Synergy by Mark Latash 2006, page122.

Another possible elliptical distribution is shown in panel C. this ellipse is elongated along a line with positive slope, which means if one finger accidentally produces more force the other finger tends to produce a higher force than its average contribution. This is no force-stabilizing synergy; however, it can be a different synergy stabilizing total moment generated by the two fingers about a pivot located between the points of force application as it is depicted in Figure 2-1.

To quantify synergies, several indices have been used based on the amounts of variance per dimension (per degrees of freedom) within the UCM and within its orthogonal complement. Normalizing the variance by dimension is necessary to make these indices comparable across subspaces of different dimensionalities. In the example above, the dimensionality of each subspace is unity. The variances computed within the UCM, and ORT has been named differently such as V_{GOOD} and V_{BAD}, goal-equivalent and non-goal-equivalent, and V_{UCM} and V_{ORT}, respectively. In the following chapters, I am going to call these V_{UCM} and V_{ORT}.

The index that I used in the following studies is $(V_{UCM} - V_{ORT})/V_{TOT}$, where V_{TOT} is the sum of the two variance components. I did not divide these terms by their dimensionality, but they should be divided. This index can be positive, zero, or negative. It being positive reflects a synergy stabilizing the performance variable corresponding to the UCM used for the analysis. When it is zero or negative we do not have a synergy; however, for the contrary case we can say that it might be a synergy with respect to another UCM or in another word, it is a synergy stabilizing another performance variable which was not asked from subjects to perform.

I would like to summarize the features of UCM hypothesis through the following points:

1- This hypothesis assumes a multi-level hierarchical control. The controller uses an apparently redundant set of elements to ensure stable performance with respect to a task and the elements that are either united or not united into an apt synergy.

2- We can examine the presence of synergy and its strength by an index defined by relative magnitudes of V_{UCM} and V_{ORT}. As these variances represent the extent of the variability observed in the performance variables, the presence of synergy does not necessarily ensure high accuracy. While a non-synergetic behavior might be very accurate.

3- This method is based on the assumption that the system of interest is behaving linearly, or it is possible to approximate it with a linear relation. Therefore, we are limited in designing experiments in that we have to make them very simple.

2.3 Referent Configurations and Equifinality

The Referent Configuration (RC) Hypothesis (Feldman 2009) provides a physical representation for observations in human actions. This hypothesis is based on the assumption that human actions must be controlled by the modifications in some specific parameters in the system. This is not a far fetched assumption as we see the interaction forces and moments emerge in all physical systems as a consequence of a set of physical parameters they have.

On the other hand, the Referent Configuration (RC) Hypothesis can be viewed as a generalization of the EP hypothesis from a single muscle up to an arbitrarily large muscle actuated system engaged in the intentional movement. The RC hypothesis conceptualizes the high-level neural variables set by the motor system as relating to referent body configurations which are task-specific. In an assumed hierarchical system, the few-to-many mappings lead to other RCs at lower levels, down to that of individual alpha-motoneuronal pools, where the relevant RC is equivalent to the threshold of the tonic stretch reflex, as in Feldman's lambda-model (1986).

The actualization of the RC will lead either to the movement toward the RC or force production (if movement toward the RC is blocked); hence, both movement and force production are outcomes of the same neural processes. Therefore, accepting this assumption means that as long as the RC is held constant (the subject of this experiment is to continue the task in the same way they were doing it before the visual feedback was turned off), a system will produce the same force-moment as it was before the feedback goes off. However, recent studies (Ambike et al 2014a; Ambike et al 2014b; Wilhelm et al 2013; Zhou et al 2014b), have showed systematic violations of equifinality that point toward the utility of an addition to the RC Hypothesis according to the notion of "RC back-coupling," (Reschechtko et al 2014) a phenomenon in which the Referent Configuration seems to move toward the body's actual configuration.

2.4 Motor Redundancy and Optimization

As was briefly mentioned, there are usually more effector than the physical (mathematical) relations that describe the task performed by humans. The approaches that have been considered to deal with this problem can be categorized into three groups: reducing the number of effectors or in other word simplifying the problem, using various optimization methods to find the best solution solving the problem (Foster et al. 2004, Jiang and Mirka 2007, Herzog and Binding 1992, Buchanan et al. 2004, Buchanan et al. 1996, Berret et al. 2011), and using inverse optimization methods trying to find the best rule for finding that optimal

solution (Liu et al. 2005, Bottasso et al. 2006, Siemienski 2006, Mombaur et al. 2010, Terekhov et al. 2010, Terekhov and Zatsiorsky 2011, Zou et al. 2012).

All of these methods are useful in their way; however, the latter seems very promising to find a mathematical logic behind the human decision making. The goal of an inverse optimization method is to approximate a cost function that given the constraints reproduces the observed optimal solutions. Because of the complexity of the inverse optimization problems usually they are solved using numerical methods (Liu et al. 2005, Bottasso et al. 2006, Siemienski 2006, Mombaur et al. 2010). Achieving a global solution for an inverse optimization problem has never been easy and required stochastic approaches, such as simulated annealing and genetic algorithm, which cost a considerable time for a complex problem of human movement. However, under some circumstances, a simplified problem can be defined that is analytically solvable (Terekhov et al. 2010, Terekhov and Zatsiorsky 2011, Park et al. 2010 and 2012).

2.5 The Human Hand

The human hand is important complex parts of the body responsible for many important daily actions. In almost all of our daily activities, we rely on the dexterity and help the hands provide for us. Moreover, the human hand is also redundant system but in the case of isometric force-moment production as we are studying here it shows a limited degree of redundancy, which is very helpful especially when we were implementing the ANIO. By using hand force-moment production, we could form a problem which obeyed the acceptable form for the Analytical Inverse Optimization Method. The following sections characterize the anatomy of the human hand with some considerations which must be made when we are investigating finger force production as a result of these anatomical features.

2.5.1 Anatomy of the Human Hand

In this subsection, I described the related skeletal, and muscular properties of the human hand.

2.5.1.1 Skeletal Anatomy of the Hand

The forearm, wrist, and fingers of the human hand are formed from 29 bones. The distal aspects of the radius and ulna, as well as the eight carpal bones (two rows of four bones), form the wrist. The wrist allows movement in two planes: flexion/extension (range of motion: 70°-90° of flexion and 65°-85° of extension) and abduction/adduction (15°-25°/25°- 45° respectively). Both of these movements occur

between the distal aspect of the radius and the proximal row of carpal bones. Each finger has three joints. From proximal to distal these joints are the: metacarpalphalangeal (MCP), proximal interphalangeal (PIP), and distal interphalangeal (DIP) joints. The MCPs permit movement in two planes: flexion/extension (85°-100°/0-40° respectively) and abduction/adduction. As MCP joints deviate from the neutral position in one plane of motion, their range of motion (ROM) in the other plane of motion decreases (Schultz et al. 1987). In contrast to the two planes of motion afforded by the MCPs, the PIPs and DIPs can only flex and extend plane; PIPs can move from full extension to 90°-120° of flexion while DIPs can move from full extension to 80°-90° of flexion. The preceding information is summarized from Napier (1980).

2.5.1.2 Muscles of the Hand

Hand has *extrinsic* and *intrinsic* muscles named according to their function and where they are located. *Extrinsic* muscles originate outside of the hand and insert inside of it; *intrinsic* muscles originate and insert within the hand. The *intrinsic* muscles are responsible for precise movements of fingers while the extrinsic muscles produce the more potent, gross movements (Freivalds, 2004). The extrinsic muscles of the hand can be differentiated according to anterior and posterior musculature. The anterior muscles are finger flexors, and the posterior muscles are finger extensors. The experimental task presented here explicitly concerns finger flexion only. The extrinsic flexors are flexor digitorum profundus (FDP) and flexor digitorum superficialis (FDS). The muscle bellies of FDP and FDS do no reside in the hand but rather insert into the digits using long tendons; this method of connection reduces the bulk of the hand. FDP tendons are connected to the distal phalanges and can be used to flex the fingers without loading while FDS tendons insert into the medial phalanges and are recruited for tasks which require additional force production. Additionally, the FDP is composed of two divisions: radial and ulnar. Disregarding the thumb, the index finger is the most independent of the four fingers; some of the independence of the index finger can be attributed to the fact that the radial FDP connects only to it while the ulnar division of the FDP connects to the middle, ring, and little fingers. The intrinsic muscles of the hand are grouped topologically according to the digits they move: thenar muscles for an extension, ab- and adduction of the thumb; hypothenar for little finger flexion and adduction; and midpalmar muscles for MCP flexion and ab- and adduction. Each of these groups is composed of multiple muscles for each digit.

2.5.1.3 Mechanoreceptors

Mechanoreceptors are responsive to any kind of mechanical stimuli such as pressure or skin deformation. They differ in size, receptive field, the rate of adaptation, location in skin, and physiological properties. There are four types of mechanoreceptors: Meissner's corpuscles, Pacinian corpuscles, Merkel's disks, and Ruffini endings.

Mechanoreceptors are generally specialized to certain stimuli. Merkel's disks and Ruffini endings detect contact forces, while, Meissner's corpuscles and Pacinian corpuscles sense vibration. The special resolution shows the number of receptors found in the locus, and it depends on the skin location. The size of the receptive field depends on how deep in the skin the particular receptor type lies, the deeper the receptor lies, the larger the receptive field. Type-I receptors have large receptive fields and low spatial resolution, while type-II receptors have small receptive fields and good spatial resolution.

Receptors are divided into two categories based on their speed of adaptation. Slowly adapting (SA) receptors detect contact stimulus; for example, pressure and skin stretch. Rapidly adapting (RA) receptors detect only short pulses such as initial contact and vibration.

In the brain, the sensation is determined by the combined input from all type of receptors. In the following table, the properties of the four mechanoreceptors are summarized.

Table 2-1. Mechanoreceptors properties.

Receptors	**Rate of adaptation**	**Location**	**Receptive field**	**Stimulus frequency**	**Function**
Merkel's disks	SA-I	Shallow	2-3 mm	0-30 Hz	Pressure; edges and intensity
Ruffini endings	SA-II	Deep	>10 mm	0-15 Hz	Directional skin stretch, tension
Meissner's corpuscles	RA-I	Shallow	3-5 mm	10-60 Hz	Local skin deformation, low-frequency vibratory sensations
Pacinian corpuscles	RA-II	Deep	>20 mm	80-400 Hz	Unlocalized high-frequency vibration; tool use

2.5.2 The Interdependence of Finger Forces

The interdependence of finger forces is a well-known phenomenon. This phenomenon is called *enslaving* (Li et al. 1998; Zatsiorsky et al. 2000). Enslaving results from the anatomy of the human hand. The described shared musculature among the fingers, as well as friction between connective tissues, is partially responsible for this unintentional force production. Moreover, there are neural reasons for enslaving: the cortical representation of the digits is not completely differentiated. However, enslaving has been shown to change over long time periods with training (Slobonov et al. 2002), healthy aging (Shinohara et al. 2003, 2004), and with onset of neurological disorder (Park et al. 2012), enslaving has generally been

assumed to be stable over short periods of time. Based on this assumption, a definition of *finger modes* (Zatsiorsky et al. 2008; Danion et al. 2003) was introduced to present a hypothetical elemental variable which reflects the motor system's *intended* finger force recruitment, rather than the actual peripheral output of the system which reflects enslaving. In the first study presented in this thesis both finger forces and finger, modes were analyzed.

Chapter 3

Methodology

In this chapter, I will briefly discuss the main computational methods used in the following chapters.

3.1 Enslaving and Finger Modes

Even when a person tries to press down with one fingertip, other fingers produce involuntary force that has been called a lack of individualization or enslaving (Kilbreath and Gandevia 1994; Zatsiorsky et al. 2000; Schieber and Santello 2004). This phenomenon is due to both peripheral connections among the fingers such as shared muscles and inter-digit tendinous connections, and neural factors such as overlapping cortical representations for individual fingers (Leijnse et al. 1993). Various computational methods have been presented to quantify the enslaving. In this thesis a linear regression of F_{TOT} against individual finger forces was performed:

$$F_{i,j} = F_i^0 + k_{i,j} \times F_{TOT,j} \quad (3\text{-}1)$$

where *i*, *j* are indicating fingers (I – index, M – middle, R – ring, and L – little), $F_{TOT,j}$ is the total force produced by all fingers when finger *j* was the instructed finger, and $F_{i,j}$ is the force produced by finger *i* when *j* was the instructed finger. The values of $k_{i,j}$ arranged into the 4×4 enslaving matrix, **E**. The intercept values, F_i^0 were very small and not analyzed here. The inverse of **E** was used to compute hypothetical central commands to fingers, *modes* (Danion et al. 2003):

$$\mathbf{m} = [\mathbf{E}]^{-1}\mathbf{F} \quad (3\text{-}2)$$

where **m** and **F** are 4×1 vectors of finger modes and forces, respectively. The neural controller is assumed to be able to change finger modes one at a time, while this is not true for finger forces. The matrix of enslaving effects, [E] contains forces of individual fingers in separate trials with an individual finger trying to produce maximal force in each trial (a detailed description can be found in Latash 2006, chapter 4).

3.2 Analysis of Variance of Finger Forces and Modes

Before describing the quantitative analysis of synergy, I would like to introduce two important terms that are going to be used for many times in this thesis: *elemental variables and performance variables*. *Elemental variables* are variables produced by apparent elements of a multi-element system. The assumption is that the controller can change the elemental variables individually. The term *performance variable* will be used to describe a goal variable that is produced by elemental variables; moreover, performance variables play an important role for a group of tasks. For instance, total force can be considered as a performance variable becaasuse it is the sum of four finger forces (elemental variables).

Assume a redundant task such as finger pressing force-moment production; it involves four effectors and two constraints, $\{M_{TOT}, F_{TOT}\}$. As the relation between performance and elemental variables is linear, these two constraints can be considered as the Jacobian matrix. The solution space or, it is better to say, the null space of the Jacobian is two-dimensional in this example. This space is also called the uncontrolled manifold (UCM; Scholz and Schoner 1999).

The inter-trial variance in the space of elemental variables in the directions orthogonal to UCM (V_{ORT}; variance that affects performance) and within UCM (V_{UCM}; variance that keeps performance unchanged) can be computed at each instance of time. In the three studies presented here these quantities were computed at different phases corresponded to a time interval [t - 0.3, t - 0.2]s. Note that t can be any arbitrary instance of time. This analysis can only be done if sufficient repletion of a same task is available (usually more than twenty trials). The variance indices computed at each phase must be normalized by the dimensionality of the corresponding space, which for this example would be two. This normalization makes the comparison of the two variances possible. A detailed description of the analysis can be found in Latash et al. 2001; Scholz et al. 2002.

Various scales have been presented for quantifying the synergy (Latash 2006). The index of synergy (ΔV) used in this thesis was defined as the difference between V_{UCM} and V_{ORT} normalized by total variance (V_{TOT}), also quantified per dimension:

$$\Delta V = \frac{{}^{V_{UCM}}/_{n_{UCM}} - {}^{V_{ORT}}/_{n_{ORT}}}{{}^{V_{TOT}}/_{n_{TOT}}} \quad (3\text{-}3)$$

where V_{TOT} stands for total variance which is the sum of the two variances. *n* with subscripts, stand for the dimensionality of the corresponding spaces. Since ΔV by its computation is bounded, for statistical analysis ΔV values were log-transformed using the modified Fisher's z-transform (Solnik et al. 2013).

3.3 Analysis of Motor Equivalence

The analysis of motor equivalence (ME) is another useful tool for studying the stability of a complex system. To describe the outcome of this analysis with a simple example; assume someone is asked to produce a level of total force by two fingers, then for any reason the total force is changed to a new level. Mathematically, the sufficient way to make this change is by taking the shortest possible movement in the space of finger forces (orthogonal to the UCM); however, this is not what usually happens. ME analysis quantifies the amount of displacement occurs along and orthogonal to the UCM. Therefore, one can see what the tendency of the system is in reaching a new condition.

To do ME analysis we need to have our task defined in the matrix form:

$$\mathbf{CF} = \mathbf{P} \tag{3-4}$$

where, **C** is the constraint matrix defining the task, **F** is the vector of finger forces (elemental variables in our analysis), and **P** is the vector of performance variables. Changes in the elemental and performance variables:

$$\mathbf{J}\Delta\mathbf{F} = \Delta\mathbf{P} \tag{3-5}$$

where $\Delta\mathbf{F}$ is the vector of changes in the finger force between two phases. Since equations 3-4 and 3-5 are linear, the Jacobian (**J**) of the system is the same as the **C** matrix.

Performance remains unchanged ($\Delta\mathbf{P} = 0$) if the change in elemental variables occurs in the null space of the **J** [$\mathbf{e} = \text{null}(\mathbf{J})$]. Hence, the projection of $\Delta\mathbf{F}$ onto the null-space is defined as the ME component, while the projection of $\Delta\mathbf{F}$ orthogonal to the null-space is defined as the nME components. ME and nME components should be normalized by the square root of the corresponding space dimensionality to make the comparison possible (cf. Mattos et al. 2011). This analysis can be done in both mode and force space.

3.4 Analytical Inverse Optimization (ANIO)

The purpose of this method it to use the data collected during an experiment for approximating a hypothetical objective function for the explored range of the elemental variables (see Martin et al. 2013). Mathematical proofs and computational details can be found in Terekhov et al. 2010; Terekhov and Zatsiorsky 2011. In this study, we determined the cost function explaining the distribution of the normal component of finger force in the force-moment production task. $g_i(F_i^n)$ The constraints were the prescribed total force and total moment, $\{F_{TOT}, M_{TOT}\}$ combination. Thus, the ANIO problem was defined in the following way:

$$\underset{F^n}{argmin} J = \sum_{i=1}^{4} g_i(F_i^n) \tag{3-6}$$

$$F_1^n + F_2^n + F_3^n + F_4^n = F_{TOT} \tag{3-7}$$

$$r_1F_1^n + r_2F_2^n + r_3F_3^n + r_4F_4^n = M_{TOT} \tag{3-8}$$

where $F^n = [F_1^n, F_2^n, F_3^n, F_4^n]^T$ is the vector of normal finger forces ($F_i^n \geq 0, i = 1, \ldots, 4$); the numbers 1 to 4 stand for the index, middle, ring, and little finger, respectively, g_i is an arbitrary continuously differentiable function (g_i belongs to C^n with $n \geq 1$ in the feasible region); $r = [r_1, r_2, r_3, r_4]^T$ is the vector of moment arms, which was $[-0.045, -0.015, 0.015, 0.045]^T$ meters in this experiment. Pronation (PR) was considered as the negative moment. The equations can be written in matrix form:

$$CF^n = b \tag{3-9}$$

where,

$$C = \begin{bmatrix} 1 & 1 & 1 & 1 \\ r_1 & r_2 & r_3 & r_4 \end{bmatrix} \tag{3-10}$$

$$b = \begin{bmatrix} F_{TOT} \\ M_{TOT} \end{bmatrix} \tag{3-11}$$

First, we verified that the problem was not "splittable" (Terekhov et al. 2010), which means that our optimization problem could not be represented as a set of smaller optimization problems solved independently. Second, we tested whether the experimental data are distributed in a plane using PCA (see Methods) as it was observed in several earlier studies (Park et al. 2010; Niu et al. 2012a,b). If this was true, then the unknown cost function had to be a second-order polynomial (Terekhov et al. 2010; Martin et al. 2013).

The third step was computing the coefficients of the objective function within the class of second-order polynomials:

$$J^a = \frac{1}{2}\sum_{i=1}^{4} k_i(F_i^n)^2 + \sum_{i=1}^{4} w_i F_i^n \tag{3-12}$$

where, J^a is the objective function reconstructed from the data, k_i is the i^{th} quadratic term coefficient, and w_i is the i^{th} linear term coefficient. Indices i = 1, 2, 3, and 4 refer to the index, middle, ring, and little finger, respectively.

Writing the Lagrange principle for the problem $\langle J^a, C \rangle$ in matrix form we get:

$$\hat{C}J^{a'} = 0 \tag{3-13}$$

where,

$$\hat{C} = I - C^T(CC^T)^{-1}C \tag{3-14}$$

$\hat{C}$ is a matrix of rank 2, and $J^{a'}$ is a vector consisting of partial derivatives of J^a (gradient vector). Substituting Eqs 7 in 8 gives the plane of optimal solutions:

$$\hat{C}KF^n + \hat{C}w = 0 \quad (3\text{-}15)$$

where K is the diagonal matrix of quadratic coefficients, and w is the vector of linear coefficients. Rank of $\hat{C}$ is 2; therefore, equation 3-14 defines a plane in the four-dimensional space. ANIO finds the coefficients by minimizing the dihedral angle (D-angle) between the optimal plane defined by equation 3-15 and the experimental data plane determined by the first two PCs (see Martin et al. 2013). The objective functions were constructed for each participant separately. The "fmincon" function ("active-set" algorithm) from the Matlab optimization toolbox was used to minimize the D-angle. The coefficients of the objective function were normalized by the square root of the sum of squared quadratic coefficients (as in Terekhov and Zatsiorsky 2011; Martin et al. 2013). Equation 3-12 was used to compute the cost values (C_{ANIO}) within the phase of interest.

Chapter 4

On the Nature of Unintentional Actions

If a person is instructed to produce a constant force magnitude in isometric conditions by an effector (e.g., pressing with a finger) with the help of visual feedback, turning the feedback off results in a slow consistent drift of the force, typically to lower magnitudes (Slifkin et al. 2000; Vaillancourt and Russell 2002; Shapkova et al. 2008). This drop in force can reach large magnitude, up to 30% of the initial force level over 20-30 s, without the subject being aware of the force drop. This phenomenon has been interpreted as a reflection of a limitation of the working memory with the possible contribution of fatigue (Slifkin et al. 2000, Vaillancourt and Russell 2002). A few recent studies questioned this interpretation (Ambike et al. 2015; Jo et al. 2015), in particular, based on an observation that resting for a similar time interval does not result in a consistent change in the force level reproduced without visual feedback after the rest interval.

An alternative explanation has been suggested based on an approach to human motor actions as reflections of natural motion of a physical/physiological system (including both neural and muscle elements and the external forces) toward its most stable state corresponding to the minimum of potential energy (Latash 2010; Ambike et al. 2015). According to this view, force production by a finger in isometric conditions is associated with setting a referent coordinate (RC) for the fingertip and a magnitude of apparent stiffness (*k*, which is also a reflection of shifts in spatial RCs for the participating muscles) (Pilon et al. 2007; Feldman 2015; Ambike et al. 2016b). Given the constant actual coordinate of the effector (AC), force magnitude $F = k(RC - AC)$. A slow drop in force means that RC drifts toward AC (for simplicity, we do not consider here possible changes in *k*).

The main purpose of this study has been to explore this interpretation using a task of four-finger accurate production of a combination of total force (F_{TOT}) and total moment (M_{TOT}). Assume that the fingertips perform a pressing task, and all the points of force vector application are in a horizontal plane. M_{TOT} production with respect to an axis may be viewed as a shift of the referent orientation of the plane of fingertip coordinates (RO) away from its actual orientation (AO) scaled with an apparent stiffness coefficient (k_O): $M_{TOT} = k_O(RO - AO)$. This is illustrated in Figure 4-1. Based on the suggested interpretation, we expected that drifts of RC toward AC and of RO toward AO would lead to a parallel drop in both F_{TOT} and M_{TOT} magnitudes (Hypothesis 1). As a result, depending on the role of individual fingers in the M_{TOT} production, some fingers are expected to show a drift toward lower forces (fingers that contribute to M_{TOT} production in the initial condition) while others may show a drift to higher forces (fingers that act against the instructed M_{TOT}, "moment antagonists", Zatsiorsky et al. 2002) (Hypothesis 2).

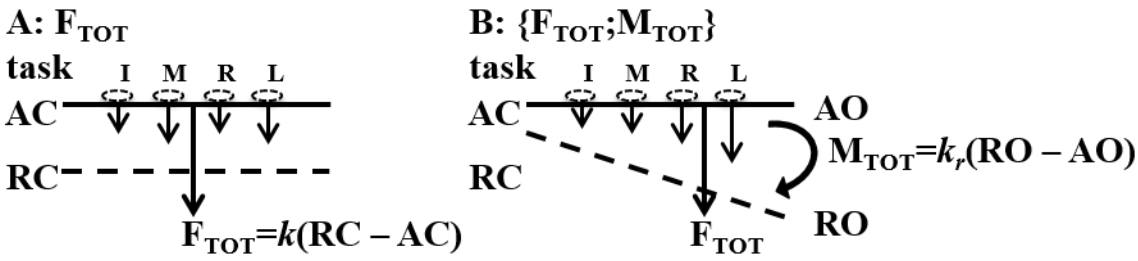

Figure 4-1. A: The production of a magnitude of total force (F_{TOT}) with a set of fingers (I – index; M – middle; R – ring, and L – little) in isometric conditions is associated with setting a referent coordinate (RC) for the fingertip and a magnitude of apparent stiffness k. Given the constant actual coordinate of the effector (AC), $F_{TOT} = k(RC - AC)$. B: The production to a magnitude of the moment of force, M_{TOT} is associated with a shift of the referent orientation of the plane of fingertip coordinates (RO) away from its actual orientation (AO) scaled with an apparent stiffness coefficient (k_O): $M_{TOT} = k_O(RO - AO)$.

We also explored whether multi-finger synergies stabilizing F_{TOT} and M_{TOT} in the initial state (under visual feedback) persist during the process of unintentional F_{TOT} and M_{TOT} drift. The word *synergy* has been used in the literature in different meanings (reviewed in Latash and Zatsiorsky 2015). We use this word to imply task-specific neural organization of abundant sets of elements (Gelfand and Latash 1998; Latash 2012) that ensure the stability of a salient performance variable (Latash et al. 2007). Several recent studies have shown that synergies stabilizing salient performance variables persist during unintentional movements (or force changes) in response to a transient external perturbation (Wilhelm et al. 2013; Zhou et al. 2014). While no studies explored synergies during spontaneous force drift, we hypothesized that synergies would indeed persist during F_{TOT} and M_{TOT} drifts (Hypothesis 3).

We used the framework of the uncontrolled manifold (UCM) hypothesis (Scholz and Schöner 1999) to quantify multi-finger synergies stabilizing F_{TOT} and M_{TOT} before and at the end of the time interval without visual feedback. The UCM hypothesis allows quantifying inter-trial variance within a space leading to no changes in a particular performance variable (V_{UCM}) and in the orthogonal subspace where this variable changes (V_{ORT}). The inequality $V_{UCM} > V_{ORT}$ has been used as a signature of a synergy stabilizing the performance variable (Latash et al. 2002). A spontaneous drift in a performance variable, $F_{TOT,}$ and/or M_{TOT} is expected to lead to an increase in the corresponding V_{ORT} compared to the condition with feedback (Hypothesis 4). No data allow predicting changes in V_{UCM}; so, this was an exploratory goal.

We also explored the direction of the spontaneous drift in the spaces of finger force and finger modes (hypothetical commands to fingers, Latash et al. 2001; Danion et al. 2003). Two components of the drift were quantified, along the UCM (motor equivalent, ME) and ORT (non-motor equivalent, nME) (Mattos et al. 2011, 2014). The expected drift in F_{TOT} and M_{TOT} suggests a corresponding consistent nME

drift; however, ME drift by definition has no effect on performance. We had no predictions with respect to its magnitude; this was an exploratory goal.

4.1 Methods

4.1.1 Subjects

Nine right-handed male (age: 21.44±0.18 years, weight: 77.71±2.67 kg, height: 176.39±2.67 cm) participated in this study voluntarily after signing a consent form. All subjects were healthy, and none of them reported any history of neuropathy. The procedures were approved by the Office for Research Protections of the Pennsylvania State University.

4.1.2 Apparatus

Four six-component Nano-17 sensors (ATI Industrial Automation, Garner, North Carolina, USA) were mounted on an aluminum plate clamped to a table. Sensors were covered with sandpaper with the friction coefficient of 1.4-1.5 (Savescu et al. 2008). A 19'' monitor was placed on the table about 60 cm in front of the subjects and used for visual feedback. A scheme of the experiment setup is depicted in Figure 4-2.

A 12-bit analog-to-digital converter (PCI-6031, National Instruments, Austin, TX) was used for digitizing twenty-four analog signals (four sensors × six components) at 100 Hz. Data acquisition software was written in Labview 2010.

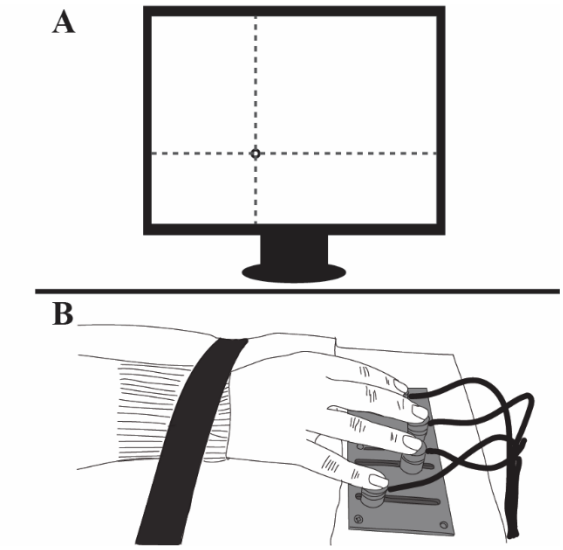

Figure 4-2. An illustration of the experimental setup. A: The monitor presented total force (F_{TOT}) and total moment (M_{TOT}) feedback. B: The hand configuration of the sensors.

4.1.3 Experimental procedure

The subject sat comfortably at the table and placed the fingertips of a hand on the force sensors. The sensor position was adjusted in the anterior-posterior direction for the hand anatomy to ensure comfort. Two Velcro straps were used to secure the hand and forearm position during the experiment. Both hands were tested in a random order.

Before each trial, the subject was asked to relax the hand with the fingertips on the sensors; then the sensor readings were set to zero so that during data collection only the actively generated downward finger forces were recorded.

The experiment was done in three parts for each hand. *Part-1* involved maximal voluntary contraction by all four fingers (MVC-4) and by the index finger alone (MVC-I). In each MVC task subjects had 6 s to reach maximal force with the instructed finger(s), and then they relaxed. There were 30-s rest intervals between trials. Both MVC tasks were repeated twice, and the maximum value across the two trials was used to set further tasks. The maximal force from individual fingers in the MVC-4 task was also measured.

Part-2 of the experiment involved accurate force ramp tasks performed by individual fingers. Each ramp task was 10 s long; it started with zero force and ended with 40% of the maximal individual finger forces observed in the MVC-4 task. The ramp started 2 s after the trial initiation and took 6 s to reach the final level. The subjects saw both the ramp template and the actual force by the instructed finger on the

screen. One trial was performed by each finger. The data from this part were used later to quantify the finger force interdependence (enslaving, Zatsiorsky et al. 2000).

Part-3 was the main part of the experiment. The *y*-axis on the screen showed the total force (F_{TOT}) produced by the four fingers while the *x*-axis showed the total moment (M_{TOT}) by the normal forces computed with respect to the axis passing in the anterior-posterior direction in-between the sensors for the middle and ring fingers. The pronation (PR) moment was considered negative, and the supination (SU) moment was considered positive. When the hand was relaxed, the cursor stayed at the mid-bottom of the screen. Two targets were used with F_{TOT} always equal to 20% of MVC-4 and M_{TOT} equal to 1.5PR or 1.5SU. One PR or SU was defined as 7% of the moment produced by MVC-I given its nominal level arm of 4.5 cm (as in Park et al. 2013).

Each trial started with the hand relaxed. Then the subject was given 5 s to reach the specified target. After 5 s, the visual feedback was turned off (the cursor became invisible), and the subject was required to keep performing the task for 20 s more. The instruction to subjects was to continue performing the task ("keep doing what you have been doing") throughout the trial. Twenty-two trials for each of the two targets were performed with 10-s rest intervals. There were 1-min rest intervals between the conditions. The two hands were tested in a random order, and the tasks were presented for each hand in a block-random order. Prior to data collection, each subject performed five practice trials to get familiar with the experiment.

4.1.4 Data processing

All finger forces were low-pass filtered at 5 Hz using a zero lag, fourth-order Butterworth filter. All force and moment variables were normalized by the task magnitude, i.e. by 20%MVC for force variables and by |1.5PR| for moment variables. Two phases were defined for *Part-3* of the experiment: *Phase-1* corresponded to the time interval 4.7–4.8 s; *Phase-2* was defined as the time interval 24.7–24.8 s. These two intervals were chosen to reflect the steady states under the original two constraints (*Phase-1*) and at the end of the trial (*Phase-2*). Figure 4-3 illustrates the two phases using the F_{TOT} time series from a representative trial by a typical subject.

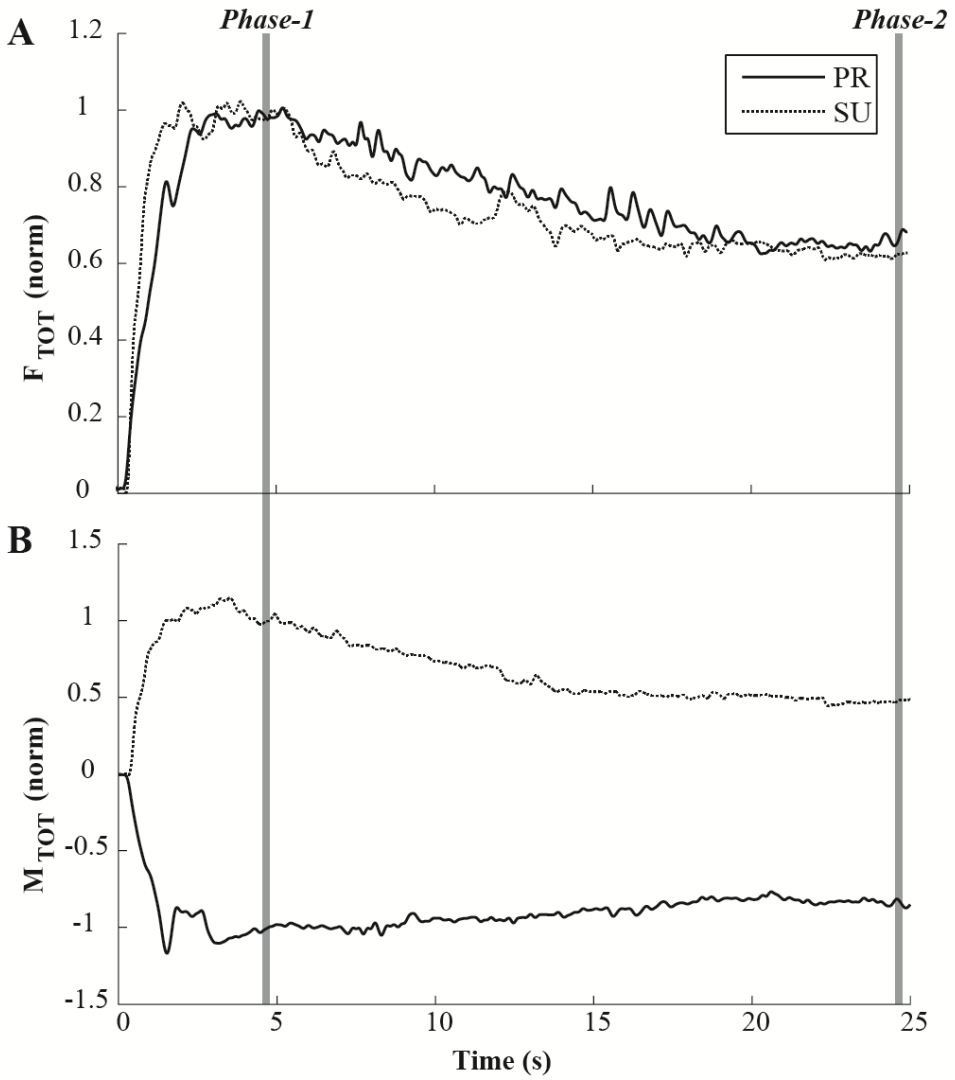

Figure 4-3. The time series of the normalized F_{TOT} and M_{TOT} for a representative subject in a trial when no feedback was presented after 5 s. PR – pronation; SU - supination. Phase-1 was defined as the time interval 470-480 ms; Phase-2 was defined as the time interval 2470-2480 ms. Note the downward drift in both F_{TOT} and M_{TOT} magnitudes.

4.1.5 Enslaving and Finger Modes

When a person is instructed to press with one finger, other fingers of the same hand also produce force. This phenomenon is called enslaving or lack of finger individuation (Kilbreath and Gandevia 1994; Zatsiorsky et al. 2000; Schieber and Santello 2004). Single-finger ramp tasks (*Part-2*) were used to quantify enslaving. For each trial, linear regression of F_{TOT} against individual finger forces was performed:

$$F_{i,j} = F_i^0 + k_{i,j} \times F_{TOT,j} \quad (4\text{-}1)$$

where *i*, *j* are indicating fingers (I – index, M – middle, R – ring, and L – little), $F_{TOT,j}$ is the total force produced by all fingers when finger *j* was the instructed finger, and $F_{i,j}$ is the force produced by finger *i* when *j* was the instructed finger. The values of $k_{i,j}$ arranged into the 4×4 enslaving matrix, **E**. The intercept values, F_i^0 were very small and not analyzed here. The inverse of **E** was used to compute hypothetical central commands to fingers, *modes* (Danion et al. 2003):

$$\mathbf{m} = [\mathbf{E}]^{-1}\mathbf{F} \quad (4\text{-}2)$$

where **m** and **F** are 4×1 vectors of finger modes and forces, respectively. The neural controller is assumed to be able to change finger modes one at a time, while this is not true for finger forces.

4.1.6 Analysis of Force and Moment Drift

Changes in total force (ΔF_{TOT}) and total moment (ΔM_{TOT}) over the time without visual feedback were computed as the differences in the averaged values of F_{TOT} and M_{TOT} over *Phase-2* and *Phase-1* in each trial. Further, these values were converted into fractions of the task magnitudes of F_{TOT} and M_{TOT}.

4.1.7 Analysis of Variance of Finger Forces and Modes

Each task was redundant: It involved four effectors and two constraints, {M_{TOT}, F_{TOT}}. Hence, the solution space for each task was two-dimensional; it has been addressed as the uncontrolled manifold (UCM; Scholz and Schoner 1999). We quantified the inter-trial variance in the space of finger forces and the space of finger modes in the directions orthogonal to UCM (V_{ORT}; variance that affects performance) and within UCM (V_{UCM}; variance that keeps performance unchanged). The UCM was estimated as the null-space of the corresponding Jacobian matrix. V_{UCM} and V_{ORT} were computed over each set of 22 trials using averaged over *Phase-1* and *Phase-2* finger force data in each trial, for each phase, each subject, and each condition separately. A detailed description of the analysis can be found in Latash et al. 2001; Scholz et al. 2002. Each variance index was normalized by the dimensionality of the corresponding space, which was always two.

An index of synergy (ΔV) was defined as the difference between V_{UCM} and V_{ORT} normalized by total variance (V_{TOT}), also quantified per dimension:

$$\Delta V = \frac{V_{UCM}/_2 - V_{ORT}/_2}{V_{TOT}/_4} \quad (4\text{-}3)$$

This computation makes ΔV bounded between –2 to +2; therefore, for statistical analysis ΔV values were log-transformed using the modified Fisher's z-transform (Solnik et al. 2013). The described analysis was performed for sets of trials performed by each subject, each hand, and each initial target location separately.

4.1.8 Analysis of Motor Equivalence

This analysis quantified changes in the mode and force vectors (Δ**m** and Δ**F**) between *Phase-2* and *Phase-1* within the UCM and ORT spaces. The vector component within the UCM results in no change in the corresponding performance variable and is called motor equivalent (ME). The component within ORT affected the performance variable and is addressed as non-motor equivalence (nME) (Mattos et al. 2011, 2014). These components were quantified in each trial and then averaged across the 22 trials within a set for each subject, each hand, and each condition separately. The analysis was performed with respect to three performance variables, F_{TOT}, M_{TOT}, and {M_{TOT}, F_{TOT}} combined. The UCM and ORT spaces were defined as the null-space and its orthogonal complement for the corresponding Jacobian matrices. The analysis was performed with respect to three possible Jacobians [force (J_F), moment (J_M), and force-moment (J_{FM})]. ME and nME components were normalized by the square root of the dimensionality of the respective spaces (cf. Mattos et al. 2011).

4.1.9 Statistics

The data are presented in the text and figures as means ± standard errors unless stated otherwise. Two-way analysis of variance with repeated measures (ANOVA) was used to test the effects of *Moment* (PR and SU) and *Hand* (Left and Right) on the main outcome variables such as drifts in ΔF_{TOT}, ΔM_{TOT}, variance components (V_{UCM} and V_{ORT}), index of synergy (ΔV_Z), and ME and nME components quantified within the mode and force spaces (factor *Space*). A two-way multivariate analysis of variance with repeated measures (MANOVA) was used to test the effect of *Moment* (PR and SU) and *Hand* (Left and Right) as within-subject factors, and *Finger* (I, M, R, L) as between-subject factors on the drifts in individual finger forces. In all of the analyses, significant effects of ANOVA and MANOVA were further explored using pairwise contrasts with Bonferroni adjustments. All the data sets were checked for normality and sphericity using the Mauchly criterion. In cases of sphericity violations, the Greenhouse-Geisser correction was applied. The critical p-value in all of the analysis was set at 0.05.

4.2 Results

4.2.1 General patterns of performance

In the MVC four-finger task, peak force values (MVC-4) were 84.22±9.06 and 75.03±5.99 N for the right and left hand, respectively. In the MVC index finger tasks, MVC-I was 41.48±4.66 and 41.95±4.09 N for the right and left hand, respectively.

Both F_{TOT} and M_{TOT} showed consistent drifts after the visual feedback was turned off; the drifts were seen in both initial moment condition, PR and SU. The drifts were consistently in the direction of a drop in the magnitude of both F_{TOT} and M_{TOT}. Typical examples of the drifts in F_{TOT} and M_{TOT} for an individual subject are shown in Figure 4-3. Note the similar F_{TOT} drifts for the PR and SU conditions, and the counter-directional drifts in M_{TOT} depending on the initial M_{TOT} level.

The drifts of both F_{TOT} and M_{TOT} were, on average, larger during tasks performed by the right hand. This is illustrated in Figure 4-4 using averaged across subjects data with error shades. While the drift in F_{TOT} was not significantly different between the moment conditions, the absolute magnitude of the drift in M_{TOT} was significantly larger for the SU condition.

Figure 4-5 illustrates these findings using the averaged across subjects differences in F_{TOT} and M_{TOT} (ΔF_{TOT} and ΔM_{TOT}) between *Phase-2* (end of trial) and *Phase-1* (just before turning visual feedback off). On average, ΔF_{TOT} was 23.03% ± 4.71% and 25.69% ± 5.32% for the left-hand PR and SU conditions, respectively. For the right-hand PR and SU conditions, ΔF_{TOT} was significantly higher, 33.52% ± 6.33% and 32.92% ± 6.79, respectively (effect of *Hand*, $F_{[1, 8]} = 10.067$, $p < 0.05$, without an effect of *Moment*). In contrast, there were no significant effects of *Hand* on ΔM_{TOT}, while the magnitude of ΔM_{TOT} was significantly larger for the SU condition (47.56% ± 7.65% and 68.60 ± 7.61% for left and right hands, respectively) compared to the PR condition (18.59% ± 6.46% and 29.83% ± 6.45% for left and right hands, respectively) (effect of *Moment*, $F_{[1, 8]} = 53.349$, $p < 0.001$).

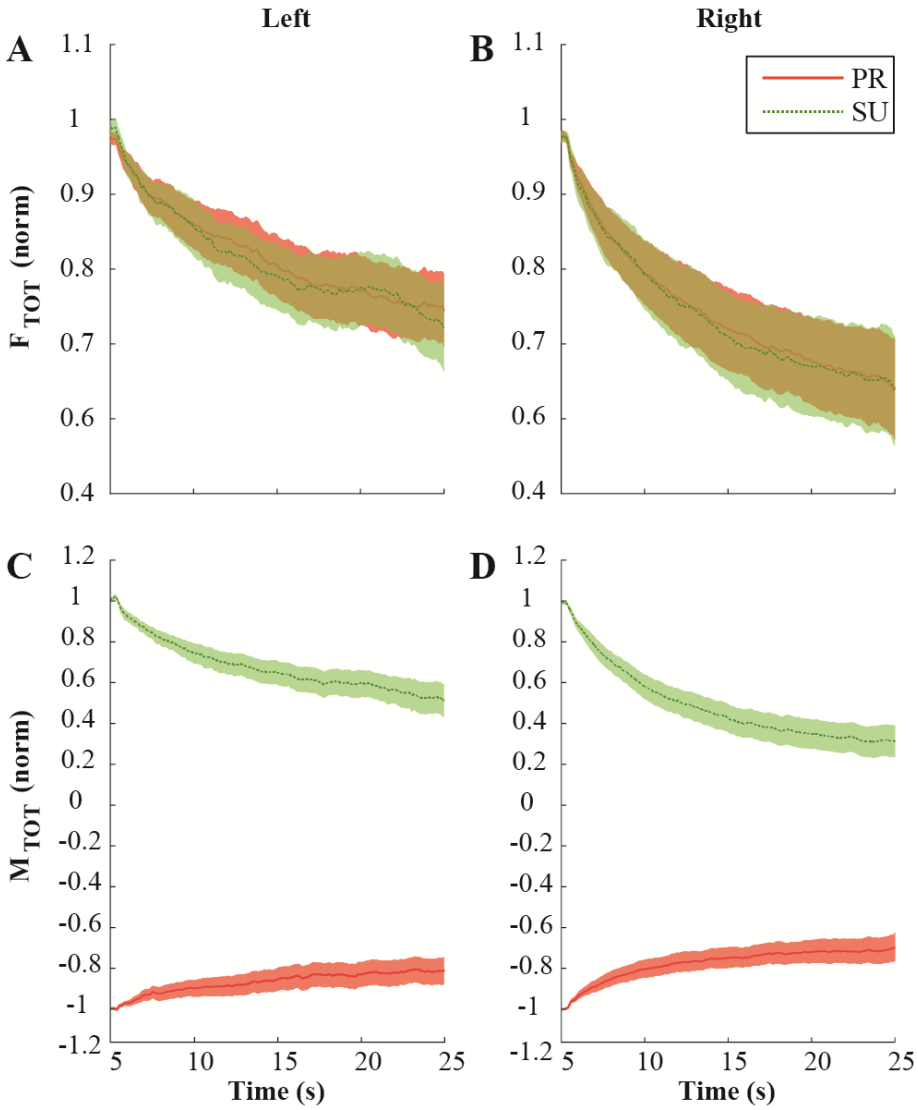

Figure 4-4. The averaged across subjects time series of normalized F_{TOT} and M_{TOT} for the left hand (panels A and C) and the right hand (panels B and D) with standard error shades. Note the larger drop in F_{TOT} in the right hand for both initial moment magnitudes (PR – pronation, SU – supination). Both hands showed a larger M_{TOT} drift for the initial SU moment.

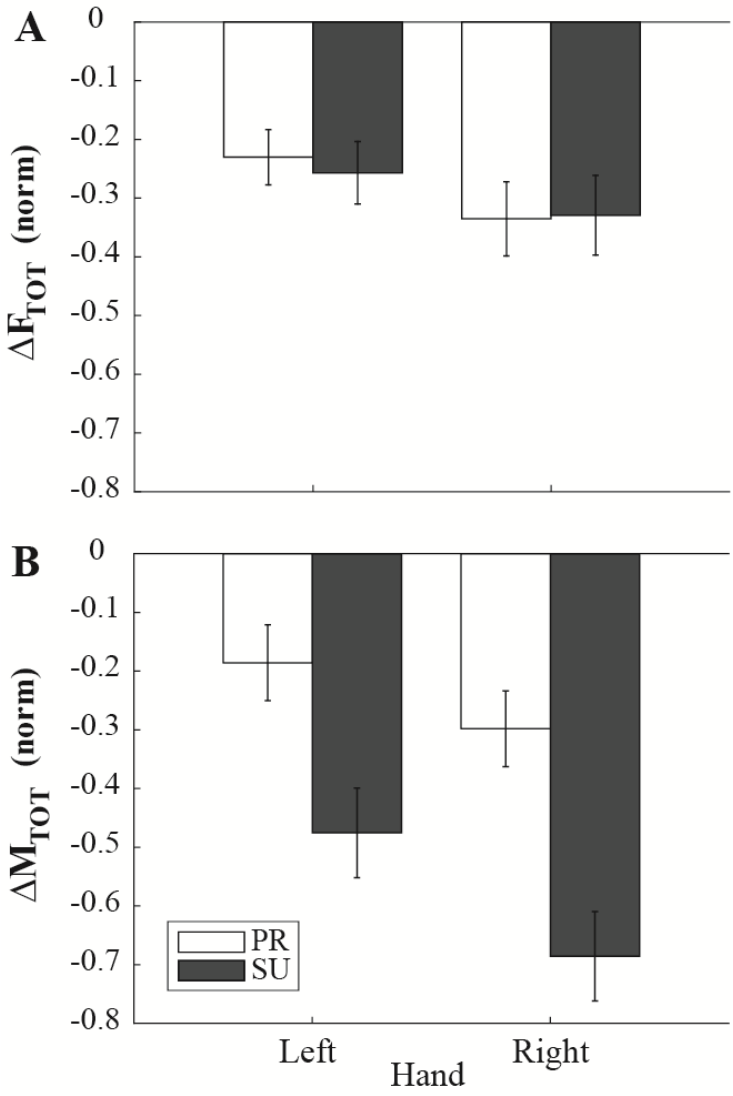

Figure 4-5. The changes in F_{TOT} and M_{TOT}, ΔF_{TOT} and ΔM_{TOT} (both normalized by the initial values) for each hand and moment condition. Averaged across subjects values are shown with standard error bars. Note the larger ΔF_{TOT} in the right hand (panel A) with no effect of the moment direction (PR – pronation; SU – supination). The drift in M_{TOT} was much larger for the SU moments (panel B).

Drifts in the individual finger forces showed a more complex pattern that depended strongly on the initial moment condition and the role of the fingers in producing the initial moment. In particular, the index and middle fingers, which produced the PR moment, showed a decrease in force in the PR condition and an increase in force under the SU condition. The pattern was reversed for the ring and little fingers. This overall pattern was consistent in the force and mode spaces as illustrated in Figure 4-6.

A two-way MANOVA with *Hand* × *Moment* as within subject factor and *Finger* as a between-subject factor on ΔF_{finger} confirmed a significant effect of *Moment* ($F_{[1, 32]} = 7.453$, $p < 0.01$) and *Moment* ×

Finger interaction ($F_{[3, 32]} = 17.442$, $p < 0.001$). Pairwise contrasts revealed the significant difference between the index and all other fingers ($p < 0.05$). Similar patterns were observed in Mode space as illustrated in Figure 4-6B.

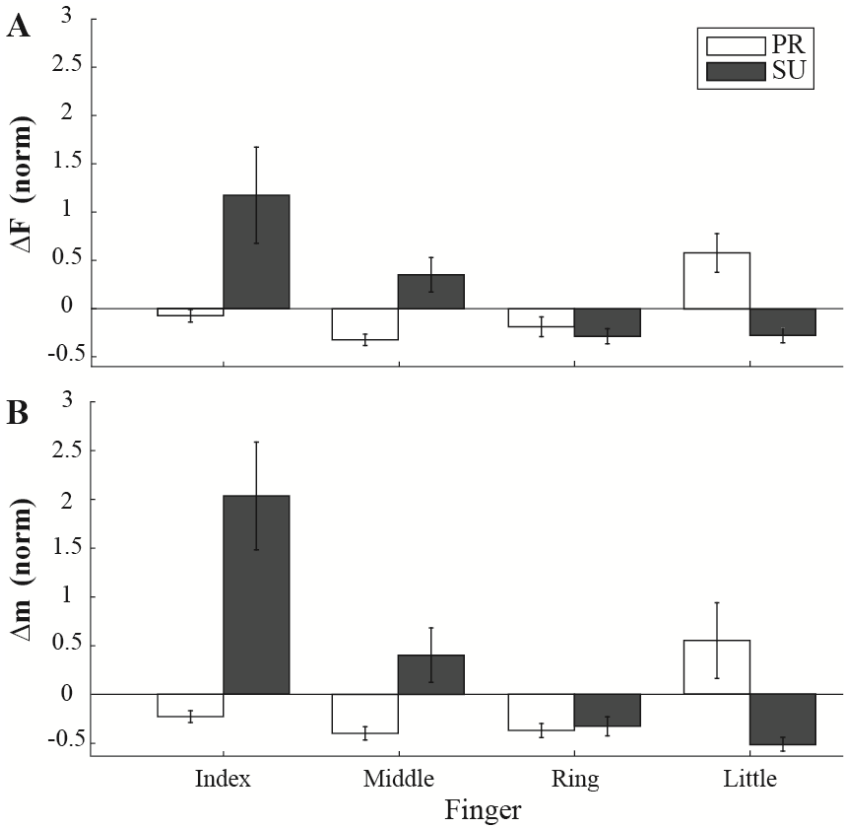

Figure 4-6. The changes in the individual finger forces (A) and modes (B) for each moment condition (PR – pronation; SU – supination). Averaged across subjects values are shown with standard error bars. Positive values correspond to an increase in the finger force (mode) while negative values indicate a drop in the finger force (mode). Note that positive values were typical for "moment antagonist" fingers, i.e. those producing moment against the required moment direction.

4.2.2 Analysis of the structure of variance

The structure of variance was analyzed in both finger force and mode spaces at both *Phase-1* and *Phase-2*. In *Phase-1*, $V_{UCM} > V_{ORT}$ across conditions. Figure 4-7 illustrates these results for the analysis performed with respect to $\{F_{TOT}; M_{TOT}\}$ (J_{FM} Jacobian, see Methods). At the end of the force drift, in *Phase-2*, V_{ORT} was larger than in Phase-1, while V_{UCM} changes were inconsistent across hands and initial conditions. A three-way ANOVA with repeated measures with factors *Hand* (right and left), *Space* (UCM and ORT), and *Phase* (*Phase-1* and *Phase-2*) were run on both mode and force data. For PR, the only

significant effect was for the interaction *Plane* ×*Phase* ($F_{[1, 8]}$ = 32.465, p < 0.001). For SU, *Phase* and *Plane* × *Phase* interaction effects were significant ($F_{[1, 8]}$ = 6.594, p < 0.05; and $F_{[1, 8]}$ = 23.741; p < 0.001]. The analysis for J_F and J_M showed similar results.

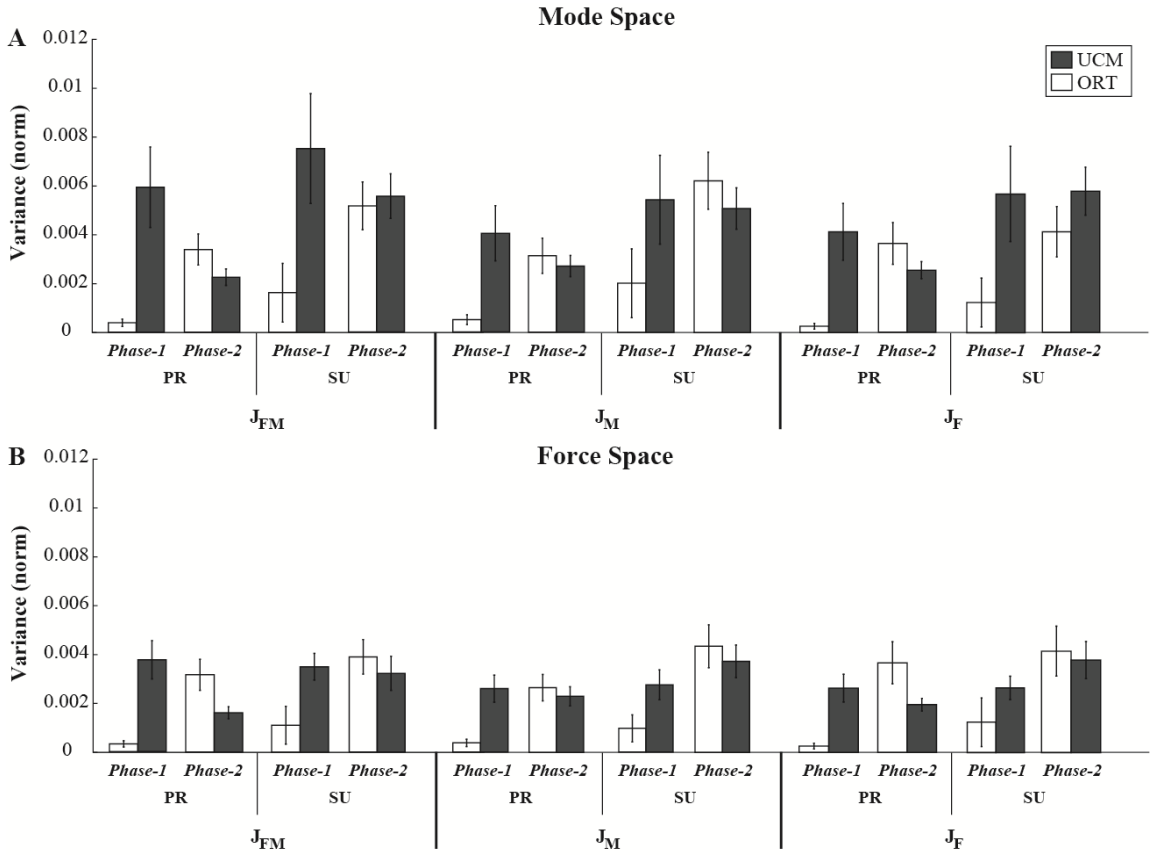

Figure 4-7. Two components of the normalized variance across trails, within (V_{UCM}) and orthogonal (V_{ORT}) to the UCM for the right hand. Averaged across subjects values are shown with standard error bars. The results of the analysis for Phase-1 and Phase-2 for both hands and both moment conditions are shown in the force space (A) and the mode space (B). The analysis was performed for the Jacobians computed with respect to F_{TOT} (J_F), M_{TOT} (J_{FM}), and both {F_{TOT}; M_{TOT}} (J_{FM}). In Phase-1, across conditions and analyses, there were synergies stabilizing both F_{TOT} and M_{TOT} (V_{UCM}>V_{ORT}, for all Jacobians) while there were no such synergies in Phase-2. Similar results were observed for the left hand. PR – pronation; SU – supination.

Analysis of the changes in the two variance components, $\Delta V_{UCM,}$ and ΔV_{ORT}, between *Phase-1* and *Phase-2* was run in both force and mode spaces. A two-way ANOVA indicated a larger change in V_{ORT} compared to the change in V_{UCM} in both spaces ($F_{[1, 8]}$ > 23.7, p < 0.001).

The log-transformed index of multi-finger synergy, ΔV_Z is illustrated in Figure 4-8 for the analysis with respect to J_{FM}. In *Phase-1*, ΔV_Z was consistently positive reflecting $V_{UCM} > V_{ORT}$. In contrast, in Phase-2, ΔV_Z was close to zero because of the increase in V_{ORT}. The effect of *Phase* was strongly significant in both force and mode spaces ($F_{[1, 8]}$ > 65.94; p < 0.001). The three-way repeated measure ANOVA *Hand* ×

Moment ×*Phase* also showed a significant *Moment* ×*Phase* interaction in both spaces ($F_{[1, 8]} > 61.04$; $p < 0.001$) reflecting the bigger phase-related difference for the PR condition. The analysis for J_F and J_M showed similar results.

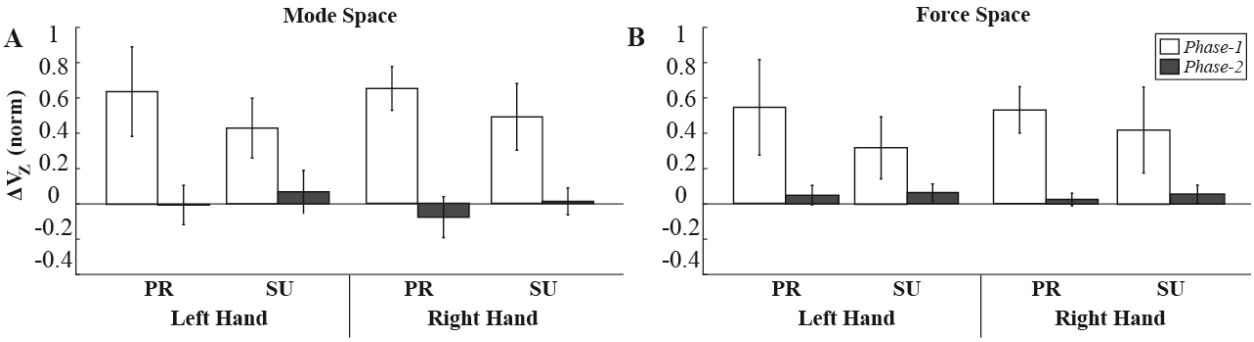

Figure 4-8. The magnitudes of the z-transformed index of synergy (ΔV_Z) for the mode (A) and force (B) space analyses are shown at Phase-1 (open bars) and Phase-2 (black bars) for all the hand and moment conditions. Averaged across subjects values are shown with standard error bars. Note that $\Delta V_Z > 0$ in Phase-1 but not in Phase-2. The panels show the results for the $\{F_{TOT}; M_{TOT}\}$-based Jacobian (J_{FM}). Similar results were obtained for the analyses with respect F_{TOT}-based (J_F) and M_{TOT}-based (J_M) Jacobians. PR – pronation; SU – supination.

4.2.3 Analysis of motor equivalence

The analysis of two components of the finger force drift, ME, and nME, was done using three different Jacobians reflecting three distinct performance variables, F_{TOT}, M_{TOT} and the combination of both $\{F_{TOT}; M_{TOT}\}$. The results for the ME and nME components are depicted in Figure 4-9. For the J_{FM}- and J_M-based analyses, the nME component was consistently larger for the SU moment (*Moment* × *Space* interaction; $F_{[1, 8]} > 12.7$, $p < 0.01$), while for the J_F-based analysis the nME component was approximately the same for both moment conditions. Note also the larger ME and nME components for the right hand (effect of *Hand* significant for the J_M- and J_F-related analyses; $F_{[1, 8]} > 5.45$; $p < 0.05$). The effect of *Hand* was typically larger for the nME component as reflected in the *Hand* ×*Space* interactions significant across all three Jacobians ($F_{[1, 8]} = 13.21$, $p < 0.01$).

A complete description of the results of three-way repeated-measures ANOVAs with *Hand* × *Moment* ×*Space* in presented in Table 1. Note that the analyses were run with respect to three Jacobians (J_F, J_M, and J_{FM}) and two spaces (force and mode).

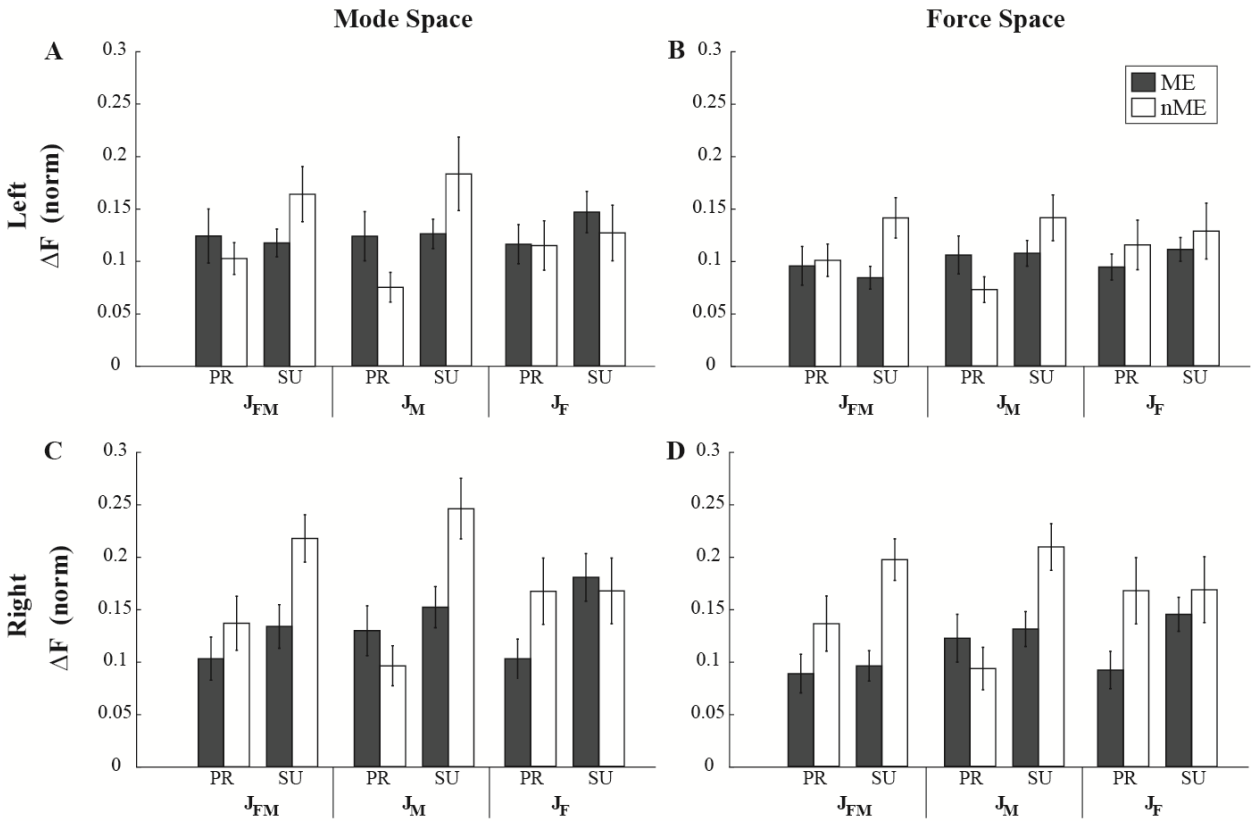

Figure 4-9. The motor equivalent (ME) and non-motor equivalent (nME) components of the vector of mode (panels A and C) and force (panels B and D) difference between Phase-2 and Phase-1. Averaged across subjects values are shown with standard error bars for the left hand (panels A and B) and the right hand (panels C and D). Both ME and nME components were normalized by the square root of corresponding degrees of freedom. Note the larger nME for the right hand compared to the left hand and for the SU (supination) condition compared to the PR (pronation) condition.

Table 4-1. Results of statistical analysis

		Hand	Moment	Space	Hand × Moment	Hand × Space	Moment × Space	Three-way
J_F	Force	**$F_{[1,8]} = 7.96$ $p < 0.05$**	**$F_{[1,8]} = 5.81$ $p < 0.05$**	$F_{[1,8]} = 3.05$ $p = 0.12$	$F_{[1,8]} = 1.06$ $p = 0.33$	**$F_{[1,8]} = 12.23$ $p < 0.01$**	$F_{[1,8]} = 2.4$ $p = 0.16$	$F_{[1,8]} = 3.26$ $p = 0.11$
	Mode	**$F_{[1,8]} = 5.47$ $p < 0.05$**	**$F_{[1,8]} = 12.52$ $p < 0.01$**	$F_{[1,8]} = 0.16$ $p = 0.7$	$F_{[1,8]} = 4.19$ $p = 0.08$	**$F_{[1,8]} = 25.16$ $p < 0.001$**	$F_{[1,8]} = 5.06$ $p = 0.06$	$F_{[1,8]} = 3.32$ $p = 0.11$
J_M	Force	**$F_{[1,8]} = 7.26$ $p < 0.05$**	**$F_{[1,8]} = 11.68$ $p < 0.01$**	$F_{[1,8]} = 0.74$ $p = 0.41$	$F_{[1,8]} = 3.23$ $p = 0.11$	$F_{[1,8]} = 3.95$ $p = 0.82$	**$F_{[1,8]} = 34.59$ $p < 0.001$**	**$F_{[1,8]} = 6.67$ $p < 0.05$**
	Mode	**$F_{[1,8]} = 17.88$ $p < 0.05$**	**$F_{[1,8]} = 16.70$ $p < 0.05$**	$F_{[1,8]} = 3.73$ $p = 0.09$	$F_{[1,8]} = 0.21$ $p = 0.66$	**$F_{[1,8]} = 17.90$ $p < 0.01$**	**$F_{[1,8]} = 15.14$ $p < 0.01$**	$F_{[1,8]} = 1.57$ $p = 0.25$
J_{FM}	Force	$F_{[1,8]} = 4.97$ $p = 0.06$	$F_{[1,8]} = 3.03$ $p = 0.12$	**$F_{[1,8]} = 13.91$ $p < 0.01$**	$F_{[1,8]} = 2.36$ $p = 0.16$	**$F_{[1,8]} = 13.97$ $p < 0.01$**	**$F_{[1,8]} = 27.80$ $p < 0.001$**	$F_{[1,8]} = 0.01$ $p = 0.93$
	Mode	$F_{[1,8]} = 3.21$ $p = 0.11$	**$F_{[1,8]} = 7.33$ $p < 0.05$**	**$F_{[1,8]} = 11.89$ $p < 0.01$**	**$F_{[1,8]} = 6.83$ $p < 0.05$**	**$F_{[1,8]} = 13.21$ $p < 0.01$**	**$F_{[1,8]} = 12.72$ $p < 0.01$**	$F_{[1,8]} = 0.20$ $p = 0.67$

Results of the three-way ANOVA, Hand × Moment × Space of deviations in the force and mode spaces between Phase-1 and Phase-2 performed with respect to three Jacobians, J_F, J_M, and J_{FM}. Significant effects are in bold.

4.3 Discussion

The first two hypotheses have been supported by the data. Indeed, after the visual feedback had been turned off, there was a consistent drop in both F_{TOT} and M_{TOT} magnitude as predicted by Hypothesis 1. Note that the direction of M_{TOT} drift depended on its initial quantity: The drift was in the direction of PR for the initial SU task and the direction of SU for the initial PR task. Individual fingers showed drifts in different directions depending on their role in the production of the initial M_{TOT}. "Moment agonists" (i.e., fingers that produced moments of force in the direction of required M_{TOT}) typically showed a force drop, while "moment antagonists" (cf. Zatsiorsky et al. 2002) demonstrated a force increase as predicted by Hypothesis-2. The results were more ambiguous with respect to Hypotheses 3 and 4 that predicted changes in the inter-trial variance in the spaces of finger force and finger modes (hypothetical commands to fingers, Danion et al. 2003) analyzed within the UCM hypothesis (Scholz and Schöner 1999). Indeed, the component of inter-trial variance leading to a change in the task-related performance variables, V_{ORT}, increased at the end of the time interval without visual feedback (in support of Hypothesis 4). Synergies stabilizing those variables disappeared or became much weaker thus falsifying Hypothesis 3. This was

associated with no consistent change in the component of inter-trial variance that did not affect task-related performance variables, V_{UCM}; in fact, V_{UCM} showed a tendency to drop. The exploration of the magnitude of the ME and nME drifts (drifts within the UCM and ORT sub-spaces) has suggested no consistent differences in the magnitude of the ME and nME deviations. This result has important implication for an earlier hypothesis on the origin of the unintentional force drift (Ambike et al. 2015, 2016a) discussed later in this section.

4.3.1 Origins of unintentional change in performance

Some studies have shown that humans show spontaneous changes in performance when they are instructed to "continue doing what you have been doing", in particular when they do not have the benefit of visual feedback on performance. For example, when a person is asked to walk toward an obstacle and step over it, repeating the task leads to a slow drop in the clearance between the foot and the obstacle, particularly pronounced for the trailing foot, and sometimes the trailing foot hits the obstacle (Heijnen et al. 2012, 2014). Force production in isometric conditions leads to a slow drop in force when the subject is deprived of visual feedback; this is observed for moderate force levels that are not expected to lead to fatigue (Slifkin et al. 2000; Vaillancourt and Russell 2002; Ambike et al. 2015). These spontaneous changes in performance have been explored in only a handful of studies despite their potential importance for understanding the system for movement production demonstrated, for example, by studies that showed a significantly faster performance drift in patients with Parkinson's disease (Vaillancourt et al. 2001; Jo et al. 2015).

Early studies invoked limitations of working memory as a possible reason for the force drop without visual feedback (Slifkin et al. 2000; Vaillancourt and Russell 2002). This interpretation has been criticized because problems with memory are expected to lead to higher variance in the performance but not necessarily to its unidirectional drift. Besides, no consistent force drift was reported in a pilot study when the subjects were asked to memorize a force level and then to reproduce it after resting for 20 s, which is a typical time of force drop in continuous force production trials (Jo et al. 2015). This observation suggests that memory limitation, by itself, was not the defining factor in the unintentional force drop.

An alternative explanation has been formulated within the physical approach to motor control (Kugler and Turvey 1987; Latash 2010, 2014). This approach assumes that the central nervous system (CNS) manipulates parameters of physical laws to perform intentional actions. The system for movement production behaves like any physical system; in particular, it shows a natural tendency to move toward a

state with minimal potential energy (and maximal stability). As described in the Introduction, force production may be viewed as a consequence of defining a referent coordinate (RC) for the effector, which is different from its actual coordinate (AC). The difference between the two translates into active force toward RC. If the effector is released, it moves toward RC. If AC cannot move (e.g., in isometric conditions), a natural drift of RC toward AC is expected (coined "RC-back-coupling", Zhou et al. 2014) reducing the difference between RC and AC and moving the system toward a state with lower potential energy. If visual feedback is available, the subject corrects the drift and no net force change in observed. Without the benefit of visual feedback, a drift of RC toward AC takes place resulting in a force drop.

This interpretation allows making non-trivial predictions with respect to unintentional force drifts in an abundant system such as four fingers producing total force and/or total moment. In particular, M_{TOT} production is associated with a difference between the fixed actual orientation (AO) of the plane of fingertip contacts and its referent orientation (RO) (Latash et al. 2010; see Figure 4-1). A drift of RO toward AO is expected to lead to a drop in M_{TOT} magnitude associated with a drop the forces of "moment agonist" fingers and an increase in the forces of "moment antagonist" fingers. This pattern, which is not predicted by any alternative hypotheses, was observed in the experiment.

Figure 4-10 illustrates the production of F_{TOT} and M_{TOT} with changing RC and RO. Note the different effects of the RC and RO drift on individual fingers resulting in different changes in the finger forces. Of course, this is a cartoon offering only one of the many possible solutions because of the abundance of the four-finger system with respect to the $\{F_{TOT}; M_{TOT}\}$ task. The hypothesized RC and RO drifts are shown in the right panel. Note that a drift in RC contributes to a drop in all finger forces. In contrast, a drift in RO is expected to contribute to a drop in the forces of "moment agonist" fingers and an increase in the forces of "moment antagonists". Actual finger forces are expected to depend on the relative rate of the RC and RO drifts. In our study, the relative drop in M_{TOT} was consistently higher than the drop in F_{TOT} (Figure 4-5) suggesting a relatively larger drift in RO compared to RC. This is expected to lead to an increase in the forces of "moment antagonist" fingers as illustrated in the right panel of Figure 4-10. Of course, this is a simplified analysis; in particular, it does not consider possible drifts in the apparent stiffness coefficients, *k* (see Introduction).

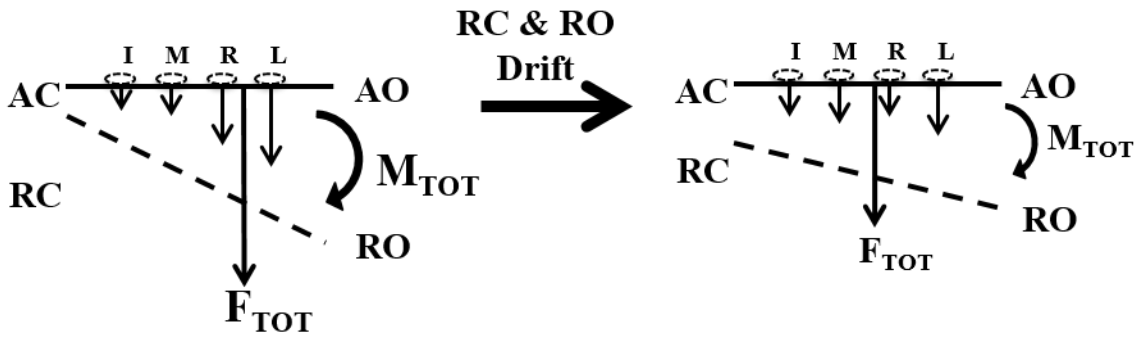

Figure 4-10. An illustration of the production of F_{TOT} and M_{TOT} with changing RC and RO. After a drift in RC and RO (the right panel), a drop in the magnitude of both F_{TOT} and M_{TOT} is expected. Note consistent changes in the forces of "moment agonist" fingers (force reduction) while changes in the forces of "moment antagonists" may depend on the relative rate of the RC and RO drifts. They can lead to an increase in the forces of those fingers.

Our computation of M_{TOT} was performed with respect to the midpoint between the middle and ring fingers. This is potentially biased some of the results because the point of application of the resultant force during natural four-finger pressing tasks is shifted toward the middle finger reflected in the typical sharing patterns of total force among the fingers (Li et al. 1998). This factor could bring about some of the observed effects of initial moment of force, in particular, the larger drift for the SU moment compared to the PR moment (Figure 4-5).

4.3.2 Two types of unintentional force change

Another example of unintentional movements and force changes was demonstrated in studies that applied smooth transient perturbations during a static task while the subjects were instructed not to react to the perturbations ("do not interfere", Feldman 1986; Latash 1994). Such experiments involved hand positional tasks and transient changes in the force acting on the hand (Zhou et al. 2014, 2015) as well as multi-finger force production tasks and transient positional perturbations applied to one of the fingers (Wilhelm et al. 2013; Reschechtko et al. 2014, 2015) with the "inverse piano" device (Martin et al. 2011). In these experiments, if the application and removal of a perturbation were interrupted with a dwell time, the final position (force level) undershot the initial level, i.e. equifinality was violated (cf. Kelso and Holt 1980; Schmidt and McGown 1980; Latash and Gottlieb 1990; Lackner and DiZio 1994). The drift in the final position (force) was fast and large: It could reach up to 50% of the original change in position (force) induced by the perturbation with the typical times of 1-2 s. Within the idea of control with RCs, these

observations suggest a much faster RC drift compared to the one assumed to happen during spontaneous force drifts, similar to those described in the current study.

Interpretation was suggested for the two types of RC drift within the framework of the UCM hypothesis (Scholz and Schöner 1999). Note that the UCM-based framework is applicable even to apparently non-redundant tasks, such as force production by a single finger because all natural tasks are abundant at other, hidden, levels of analysis (e.g., at the level of muscle involvement). The interpretation is based on the idea that different stability within the UCM and ORT sub-spaces (Schöner 1995) is associated with various typical times of natural relaxation processes within these sub-spaces, fast in the more-stable ORT and slow in the less-stable UCM (Ambike et al. 2015). Spontaneous slow drifts are expected to happen primarily within the UCM while perturbation-induced fast drifts are supposed to originate in ORT. A degree of coupling between the two sub-spaces was hypothesized leading to drifts in ORT (such as F_{TOT} and M_{TOT} changes) induced by the slow process in the UCM.

This hypothesis received indirect support in an experiment with cyclical force production (Ambike et al. 2016a). Cyclical force production may be viewed as a combination of setting a steady midpoint RC coordinate and a cyclic oscillation of RC about that point (cf. Hogan and Sternad 2007). The oscillation, by definition, happens within the ORT subspace for total force, and its drift is expected to be fast. The midpoint does not move intentionally, and hence, its drift is expected to be slow. These predictions have been confirmed: Turning visual feedback off led to a slow drift in the mid-point of the force range (similar to the one observed in our study) and a much faster drifts in the peak-to-peak amplitude of force changes resembling the fast drifts induced by perturbations (e.g., in Zhou et al. 2014; Reschechtko et al. 2014). We will return to this hypothesis in relation to our current data further in the Discussion.

4.3.3 Synergies stabilizing intentional and unintentional actions

An earlier study of intentional and unintentional hand movements produced by transient perturbations with dwell time has shown that the unintentional actions are associated with multi-joint synergies stabilizing salient performance variables such as hand coordinate and orientation (Zhou et al. 2015). While unintentional movement led to larger V_{ORT} computed with respect to the final hand coordinate compared to intentional movements (a predictable result given that intentional movements were performed to a visual target), the inequality $V_{UCM} > V_{ORT}$ held for both types of movement. This inequality also held for the analysis with respect to F_{TOT} produced by the four fingers measured after the drift induced by a finger positional perturbation with a dwell time (Wilhelm et al. 2013; Reschechtko et al. 2014, 2015).

Given those results, we expected to see multi-finger synergies stabilizing both F_{TOT} and M_{TOT} after the drift in our current study. Unexpectedly, no synergies stabilizing F_{TOT} and M_{TOT} were seen at the end of the trial (*Phase-2*), while such synergies were consistently strong early in the trial when visual feedback was available (*Phase-1*). The analysis of the two variance components, $V_{UCM,}$ and V_{ORT}, has shown that the force drift led to a large increase in V_{ORT} without much of a change in V_{UCM}; as a result, the two variance indices became close to each other in magnitude, and the synergy index (ΔV) became close to zero.

These observations suggest that synergies stabilizing performance in tasks performed under visual control are crucially dependent on visual information. Our subjects had the benefit of haptic and proprioceptive information throughout the trial, but it was obviously insufficient to organize {F_{TOT}; M_{TOT}}-stabilizing synergies. Note that the importance of feedback loops for synergic control has been assumed in several models based on different theoretical approaches to synergies (Todorov and Jordan 2002; Latash et al. 2005; Martin et al. 2009). Our observations suggest that, at least in the studied conditions, synergies without visual information disappear.

It is possible that the formulation of the task biases subjects toward using specific sensory systems to ensure stable performance. Since our task was presented under visual feedback, the subjects were biased to use primarily this sensory channel to organize {F_{TOT}; M_{TOT}}-stabilizing synergies. This is a testable hypothesis. For example, subjects can be trained to produce certain force levels under haptic/proprioceptive information only. After the training is over, they can be asked to keep the remembered force over 30 s. The hypothetical RC-back-coupling may be expected to lead to drift in F_{TOT} while F_{TOT}-stabilizing synergies may be expected to persist throughout the trial.

4.3.4 Direction of force drift in an abundant system

We also explored the magnitude of the drift in the space of finger forces (and finger modes, Danion et al. 2003) in directions that span the UCM and in directions that span the ORT. The former led to ME motion of the system while the latter led to nME motion (Mattos et al. 2011, 2014). While the nME motion was expected to reflect the drift in the task-specific salient variables, $F_{TOT,}$ and M_{TOT}, ME drift, by definition, had no effect on performance and could be of any magnitude. In our experiments, ME drift was typically of about the same magnitude as nME drift (Figure 4-9). In other words, the drift had about equal components in the UCM and ORT sub-spaces.

Within the aforementioned hypothesis that slow drift originates in the UCM space (Ambike et al. 2015), the observations of about equal ME and nME deviations suggests a very strong coupling between

relaxation processes within the UCM and ORT spaces. This conclusion seems to be at odds with the basic assumptions of the UCM hypothesis and numerous observations of much larger variance within UCM compared to variance within ORT (reviewed in Latash et al. 2007; Latash 2008).

To reconcile the current results with the body of experimental data supporting the main assumptions of the UCM-hypothesis (reviewed in Latash et al. 2007; Latash 2012), we invoke the notion of hierarchical control with RCs (Latash 2010). The drift in performance, e.g. in F_{TOT}, suggest a drift at the highest level of the hierarchy, at which F_{TOT} results from a combination of two commands reflected in RC and *k* (apparent stiffness) defined for a virtual finger (VF, an imagined digit with the same resultant force as all the actual digits combined, Arbib et al. 1975). A recent study has shown large inter-trial variations in RC and *k* that kept variance of F_{TOT} very low (Ambike et al. 2016b). During the slow F_{TOT} drift, a larger drift is expected within the UCM for F_{TOT} in the {RC; *k*} space compared to the drift in ORT. This is a testable prediction that we plan to check in a future study. At the next level of the hierarchy {RC; *k*} for the VF are distributed among {RC; *k*} pairs for individual fingers. This transformation may lead to larger or smaller ME displacements compared to the nME displacements, or about equal displacements observed in our experiment.

While studying effects of hand dominance was not a goal of our study, some of the effects allow interpretation within the dynamic dominance hypothesis (Sainburg 2005, 2014). According to this hypothesis, the dominant hand and its neural control are specialized for dealing with quick action, while the non-dominant hand is specialized for steady-state tasks. A number of earlier studies demonstrated higher synergy indices during steady-state accurate force production tasks in the left hand of right-handed persons compared to similar tasks performed by the right hand (Park et al. 2012; Jo et al. 2015). Some of our results confirm higher stability of performance by the left (non-dominant) hand. In particular, the right hand showed a larger drift in both F_{TOT} and M_{TOT} (Figure 4-5), although only the former effect was statistically significant. Along similar lines, there were larger magnitudes of both nME and ME motion in the right hand (Figure 4-9). Both results can be interpreted as a sign of lower stability of performance by the right hand.

4.3.5 Concluding comments

To summarize, our results confirm the hypothesis that unintentional changes in force/moment observed after turning visual feedback off, represent consequences of a drift of referent coordinates for the effector. This framework allowed predicting non-trivial observations such as counter-directional changes in the individual finger forces in the force/moment production tasks. Some of the results, such as the lack

of synergies stabilizing total force and a total moment after the drift and the similar magnitudes of drift in the ME and nME directions, suggest important new hypotheses that can be tested in future studies. Overall, this study illustrates the richness of the theoretical framework offered by the combination of the UCM hypothesis and the hypothesis on the control of movements with shifts in spatial referent coordinates (Latash 2010; Feldman 2015).

Chapter 5

Optimality and stability of intentional and unintentional actions: I. Origins of drifts in static performance

The unintentional drift of performance is a well-documented phenomenon. It is observed during both unperturbed continuous trials (Slifkin et al. 2000; Vaillancourt and Russell 2002), in response to transient force perturbations (Wilhelm et al. 2013; Zhou et al. 2014), and over repeated trials (Heijnen et al. 2012). For example, when a person is asked to maintain accurate constant force by an effector under visual feedback, and then the feedback is removed, a slow drift in force, typically to lower values, is observed (Vaillancourt and Russell 2002; Shapkova et al. 2008). A similar, but much faster, drift is observed when the effector is subjected to a transient perturbation (Wilhelm et al. 2013; Reschechtko et al. 2014). If a person is asked to walk toward an obstacle, step over it, and continue walking, over repeated trials the clearance between the foot and the obstacle gets smaller (particularly for the trailing foot), and sometimes the foot touches the obstacle (Heijnen et al. 2012, 2014). Earlier studies offered interpretations of these phenomena based on a variety of concepts such as limitation of the working memory, boredom, inattention, minimization of energy expenditure, and fatigue.

Recently, we have offered an alternative interpretation for unintentional drifts in performance based on two concepts. The first concept suggests that the control of the voluntary actions is performed by changing the referent configurations (RCs) of the involved effectors (Feldman and Levin 1995; Feldman 2015). For example, when squeezing an object in the hand, the RC of the hand is situated inside the squeezed object. The squeezing force is then determined by the distance between the actual configuration of the hand (AC) and RC. The second is the idea of synergic control of redundant systems (note that all natural actions involve redundant sets of effectors, Bernstein 1967) based on the principle of abundance (Latash 2012). Within this scheme, producing a constant force by an effector is associated with setting its RC (and possibly apparent stiffness, Latash and Zatsiorsky 1993) and keeping it unchanged with the help of visual feedback. When the feedback becomes unavailable, RC drifts toward the actual coordinates and causes a slow decrease of the produced force. This hypothetical mechanism has been referred to as RC-back-coupling (Reschechtko et al. 2014; Ambike et al. 2015; Zhou et al. 2015).

When the task involves a redundant set of effectors, the effector space can be decomposed into two subspaces based on the effect that the effectors have on the performance variable. The uncontrolled manifold (UCM, Scholz and Schöner 1999) subspace is such that when the change of the effector commands belong to this subspace, these changes have no effect on the performance variable. The subspace, orthogonal to the UCM, (ORT) is in opposite, the one through which the effectors can change

the performance variable. During steady-state tasks, processes in the UCM are usually less stable as compared to ORT (reviewed in Latash et al. 2002, 2007). As a result, slower drift is expected within the while faster drift is expected within ORT. When the system is perturbed leading to a change in the salient performance variable, e.g. total force, the perturbation by definition affects the ORT space resulting in a fast RC-back-coupling process and fast change in the performance variable. During continuous steady-state tasks, relaxation processes are slow reflecting the lower stability of the UCM. A degree of coupling between the two sub-spaces has been hypothesized leading to the slow total force drift observed during continuous tasks (Ambike et al. 2015).

The concepts of RC and synergic control were used to explain the overall change in the salient performance variable and its stability as reflected, for example, in the structure of inter-trial variance within the UCM and ORT spaces. In this study, we focus on the third characteristic of actions by abundant systems, namely the average across trials sharing of the salient performance variable among the elements. We consider only the systems where effects of the individual variables on the performance variable are additive, such as producing a total force and total moment with several fingers. Sharing has been addressed based on optimality principles (reviewed in Prilutsky and Zatsiorsky 2002). Recently, a method of analytical inverse optimization (ANIO) has been introduced (Terekhov et al. 2010) that allows computing a cost function based on observed behavior of a redundant system over a broad range of task constraint values.

Our main hypothesis is that unintentional changes in performance variables during continuous static tasks without visual feedback are due to two processes. First, there is the aforementioned RC-back-coupling leading to a drift of the RC towards the actual coordinate of the effector. Second, there is a drift within the UCM toward a minimum of the cost function reflected in coordinated drifts of the elemental variables. We tested the main hypothesis in multi-finger isometric pressing tasks that required the accurate production of a combination of total moment and total force, $\{M_{TOT}; F_{TOT}\}$ (similar to Park et al. 2010, 2013).

To test the first set of predictions, we quantified the drifts in F_{TOT} and M_{TOT} observed when the subjects continued performing such tasks without visual feedback. We predicted that F_{TOT} would drop (similarly to Vaillancourt and Russell 2002; Ambike et al. 2015a) while M_{TOT} drift would depend on the initial magnitude and direction of M_{TOT} and directed toward its zero magnitude corresponding to the horizontal actual orientation of the hand. To test the second set of predictions, we required our subjects to vary their preferred sharing of the task among the four fingers using visual feedback. Namely, we asked them to produce the same $\{M_{TOT}; F_{TOT}\}$ combination but with the force of the middle finger (F_{MID}) reduced by 50%. After visual feedback had been turned off, we expected the forces to drift towards their preferred sharing pattern corresponding to a minimum of the cost function reconstructed using the ANIO method.

Since no perturbations were used, we expected all the processes to be relatively slow with characteristic times of 10-20 s (cf. Ambike et al. 2015a,b). To explore the interaction among the hypothesized processes, we quantified the drifts in performance under a variety of visual feedback conditions, from no feedback at all to feedback presented selectively on only a subset of the three constraints, F_{TOT}, M_{TOT}, and F_{MID}. We expected consistent drifts in the no-feedback variables only.

5.1 Methods

5.1.1 Subjects

Six male and five female subjects (age 27.27 ± 5.44 years, mass 74.18 ± 14.73 kg, height 171.18 ± 8.30 m), all right-handed, volunteered to participate in the study. All subjects were healthy and without any history of neuropathy or any other upper-limb disorders. Nine subjects performed the experiment entirely. For technical reasons, for one of the conditions, the data for two subjects were unavailable (see later in Methods). All the procedures were approved by the Office for Research Protection of the Pennsylvania State University.

5.1.2 Equipment

Four force transducers (Nano-17 sensors, ATI Industrial Automation, Garner, NC, USA) were mounted on an aluminum plate, which was attached to a wooden board. The whole setup was fixed with a clamp to a table (Figure 5-1). The sensors were covered with sandpaper, the friction coefficient with human fingerpads is approximately 1.4-1.5 (Savescu et al. 2008). Visual feedback was shown on a 19'' monitor placed at the eye level, about 0.6 m away from subjects.

Twenty-four analog signals (4 sensors × 6 components) were digitized at 100 Hz by a 12-bit analog-digital converter (PCI-6031, National Instruments, Austin, TX). The programs for visual feedback and data collection were written in LabVIEW 2010. Off-line analysis was done using MATLAB 2014.

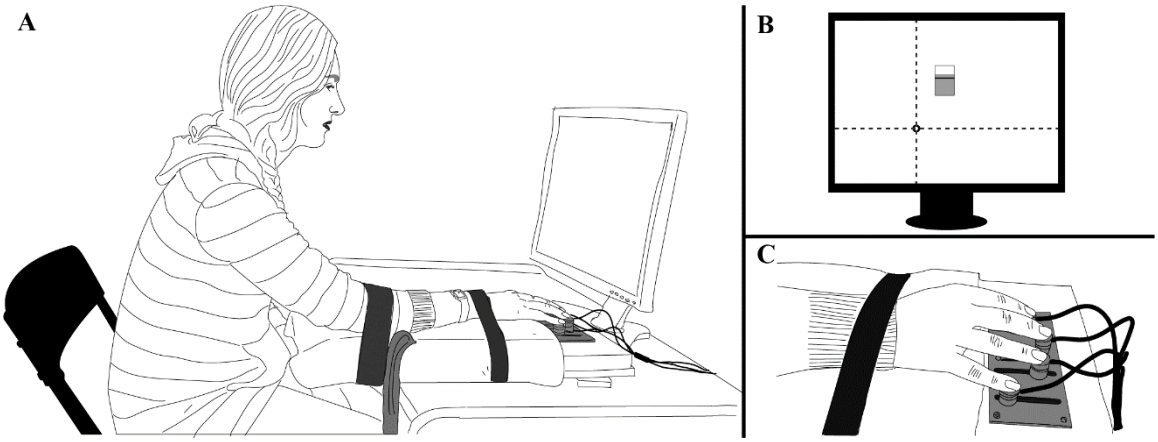

Figure 5-1. Experiment setup. (a) The complete setup. All subjects were tested with this setup. Their arm comfortably fixed to the platform and they were pressing on the force sensor to follow the visual feedback shown on the screen in front of them. (b) A sample of the visual feedback that was shown to subjects. The small hollow circle indicates a {M_{TOT}, F_{TOT}} combination. The x-axis and y-axis are total moments, and total force, respectively. The tank in the middle of the screen is the feedback on middle finger force. The level is the value that subjects must reach before *Phase-2*. The dotted cross is being controlled by subjects' {M_{TOT}, F_{TOT}} production, and must be held within the circle. (c) Hand placement on the sensors.

5.1.3 Experimental procedure

During the test, subjects sat in a chair at the table and placed the right-hand fingertips on the sensors. Two Velcro straps were used to maintain a steady hand and forearm position (Figure 5-1). The wooden plate was covered with a soft sponge layer for comfort. Sensor position in the anterior-posterior direction was adjusted for subject's hand anatomy.

At the beginning of every trial, the experimenter asked the subject to place the fingertips on the sensors and relax the hand. The sensor readings were set to zero so that during data collection only the downward active force of the fingers was recorded.

The vertical axis on the visual feedback monitor screen showed the total pressing force (F_{TOT}, the sum of the pressing forces of all four fingers), and the horizontal axis showed the total moment of force (M_{TOT}) computed about the anterior-posterior axis passing in-between the sensors for the ring and middle fingers (Figure 5-1). Note that M_{TOT} was a nominal moment value computed based on the vertical force magnitudes that did not take into account possible effects of the shear forces. As shown in Figure 5-1, subjects controlled the cursor position by adjusting F_{TOT} and M_{TOT}. (M_{TOT}, F_{TOT}) = (0, 0) corresponded to a cursor location in the mid-bottom of the screen. Pronation (PR) moment was considered negative while supination (SU) moment was positive.

The experiment consisted of three parts. The first part involved the maximum voluntary contraction (MVC) by all four fingers (MVC-4) and by the index finger alone (MVC-I). During these trials, the subjects were given a feedback on the force produced by all four fingers (in MVC-4), or by the index finger (in MVC-I). Subjects performed two trials at each task with at least 30 s between the trials; the trial with the maximal value of the instructed force was chosen to set further tasks.

The second part involved data collection for analytical inverse optimization (ANIO). In this part, the subjects were required to press with the four fingers in a natural way, with minimal effort, to reach a target shown on the screen corresponding to a combination of M_{TOT} and F_{TOT}, $\{M_{TOT}; F_{TOT}\}$. To set tasks, we defined the unit of M_{TOT} as 7% of MVC-I multiplied by the index finger nominal lever arm (0.045 m). Nine total force levels (5-45% of MVC-4 with steps of 5%), and seventeen-moment levels (0-4PR and 0-4SU with steps of 0.5) were used resulting in a total of eighty-one $\{M_{TOT}; F_{TOT}\}$ combinations that filled a triangular shape with {(4PR, 45%MVC), (0, 5%MVC), (4SR, 45%MVC)} as vertices (as in Park et al. 2013). Subjects had 6 s to reach the target and stay there. There were 10-s intervals between trials, and additional 1-min rest periods after each 10-trial block.

The third part involved the main task. During this task, subjects were required to press with four fingers to reach the presented $\{M_{TOT}; F_{TOT}\}$ target in a natural way, as in the second part. Three targets were used with F_{TOT} always equal to 20% of MVC-4, while M_{TOT} was 1.5PR, 0, or 1.5SU.

All the subjects were able to reach the prescribed $\{M_{TOT}; F_{TOT}\}$ target within 3 s. After 5 s from the trial initiation, an additional feedback was shown on the screen as a tank chart located in the middle of the screen (not interfering with the original feedback on $\{M_{TOT}; F_{TOT}\}$). The additional feedback showed the force of the middle finger, F_{MID}. The subjects were required to reduce F_{MID} to 50% of the average F_{MID} level they had been producing over the 4.5–5 s time interval from the trial initiation (computed online). They were given 10 s to reach a new steady finger force combination that would satisfy the original $\{M_{TOT}; F_{TOT}\}$ constraint and the new F_{MID} constraint.

At that time (15 s into the trial), visual feedback was manipulated. There were seven feedback conditions: no feedback on any of the three variables (None), feedback on F_{TOT} only, feedback on M_{TOT} only, feedback on F_{MID} only, feedback on F_{TOT} and F_{MID} (F_{TOT}+F_{MID}), feedback on F_{TOT} and M_{TOT} (M_{TOT}+F_{TOT}), and feedback on M_{TOT} and F_{MID} (M_{TOT}+F_{MID}). For nine of the subjects, an eighth condition was also used, in which all the feedback remained on the screen until the end of the trial (All). For technical reasons, data for the remaining two subjects for the “All” condition were unavailable. The subjects were always instructed to continue pressing with the same finger forces: “keep doing what you have been doing”. The conditions were presented in a fully randomized order. Three trials were performed under each condition.

Before starting the data collection, subjects performed ten practice trials to get acquainted with the main task. Conditions for the practice trials were selected randomly. No data were recorded in those trials.

A 10-s break was enforced between trials to prevent fatigue. After every ten trials, a one-minute break was given. Subjects were encouraged to ask for more rest during the experiment as needed. None of the subjects reported fatigue after the experiment.

5.1.4 Data processing

All data analysis was done in MATLAB software. The finger forces were low-pass filtered at 5 Hz using a zero lag, fourth-order Butterworth filter. Three phases were selected in each trial for data analysis. *Phase-1* corresponded to the time interval between 4.7 and 4.8 s; *Phase-2* corresponded to the time interval between 14.7 and 14.8 s, and *Phase-3* corresponded to the time interval between 29.7 and 29.8 s. These three 100-ms long time intervals were selected to reflect the steady states under the original two constraints, $\{M_{TOT}; F_{TOT}\}$, under the combination of three constraints, $\{M_{TOT}; F_{TOT}\}$ and F_{MID}, and at the end of the trial. Figure 5-2 illustrates these three phases for a sample trial using the F_{TOT} time series.

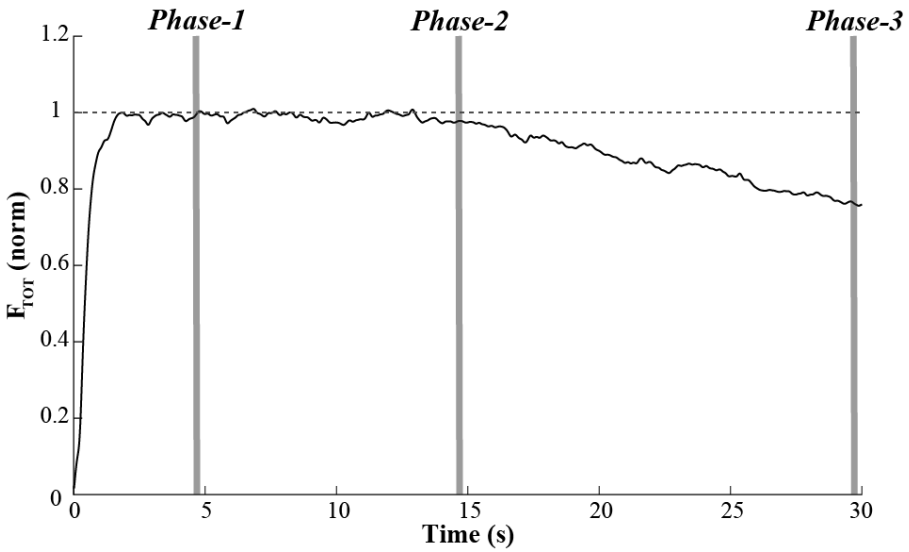

Figure 5-2. A sample of total force profile. In this figure, the three important phases described in the context was show in a total force profile.

5.1.5 Analysis of the drift in performance variables

The drift in the main performance variables, F_{TOT}, M_{TOT}, and F_{MID} was estimated as the difference in the values of these variables averaged over *Phase-3* and *Phase-2* (ΔF_{TOT}, ΔM_{TOT}, and ΔF_{MID}, respectively). For each subject, the average drift values were computed across three repetitions over each condition separately. For across-subjects comparisons, the drifts in all performance variables and finger forces were normalized by the corresponding average values within *Phase-2*.

5.1.6 ANIO and computation of the cost function

The Analytical Inverse Optimization (ANIO) method (Terekhov et al. 2010) was used for approximating the cost function. The method used the data collected in the second part of the study, that is, during accurate production of 81 different {M_{TOT}; F_{TOT}} tasks. For each trial, we computed the average finger forces during the time interval {5.7 s; 5.9 s} from the trial initiation. We tested the planarity of the collected data sets within each subject using principal component analysis (PCA). Based on previous studies, we used the criterion of >80% of the variance explained by the first two PC vectors. All the subjects, except one, produced data sets that satisfied this criterion (see Table 1). This allowed using a second-order polynomial of finger forces as a cost function (Terekhov et al. 2010; Park et al. 2011):

$$J = \frac{1}{2}\sum_i k_i (F_i^n)^2 + \sum_i w_i F_i^n \qquad (5\text{-}1)$$

where *i* stands for fingers (index, middle, ring, and little), k_i and w_i are coefficients selected to provide the best fit to the original data. Further, the cost functions were used to compute optimal solutions for the same {M_{TOT}; F_{TOT}} tasks for each subject. For consistency, we used this equation also for the data of the only subject who failed to satisfy the 80% criterion. The dihedral angle (D-angle) between the plane of optimal solutions for the same {M_{TOT}; F_{TOT}} combinations and the plane of original data (spanned by PC1 and PC2) was computed. The D-angle is a metric reflecting the goodness of fit provided by the computed cost function. A more detailed description of the method can be found in the Section 3.4.

Equation 5-1 was further used to compute the cost values (C_{ANIO}) within *Phase-2* and *Phase-3* for the data collected during the main part of the experiment. The change in C_{ANIO} was computed between the two phases (ΔC_{ANIO}). The average values of ΔC_{ANIO} across the three repetitions at each condition were used for statistical purposes.

5.1.7 Statistical analysis

Data are presented in the text and figures as means ± standard errors unless stated otherwise. To test the first hypothesis, a two-way repeated measure ANOVA was run on ΔF_{TOT}, ΔM_{TOT}, and ΔF_{MID}, separately with the factors *Feedback* (None, F_{TOT}, M_{TOT}, F_{MID}, F_{TOT}+F_{MID}, F_{TOT}+ M_{TOT}, M_{TOT}+F_{MID}, and All) and *Moment* (PR, ZE, and SU). To include the "All" condition, the analysis was repeated for nine subjects who had performed all of the conditions; however, the main effects were studied for 11 subjects without including the "All" feedback condition. To test the second hypothesis, the same ANOVA design was applied to ΔC_{ANIO}.

Furthermore, to study changes in finger forces during the main task, a two-way MANOVA with repeated measures was used with the factors *Finger* (index, middle, ring, and little), *Feedback* and *Moment*. In all of the analysis, significant effects of ANOVA and MANOVA were further explored using pairwise contrasts with Bonferroni adjustments.

All the data sets were checked for normality and sphericity using the Mauchly criterion. In cases of sphericity violations, the Greenhouse-Geisser correction was applied. The critical p-value in all of the analysis was set at 0.05.

5.2 Results

5.2.1 Analytical Inverse Optimization (ANIO)

Principal component analysis (PCA) applied to the individual finger force data collected over the sets of 81 trials with different combinations of total moment and total force, {M_{TOT}; F_{TOT}}, led in all subjects, except one, to well over 80% of total variance accounted for by the first two PCs (Table 1). Only subject #4 failed to satisfy the 80% criterion while the average value across subjects was 87.4±1.43%.

For consistency, we applied ANIO to the data of all subjects including subject #4. The second column in Table 1 shows the coefficients (k_i) at the second-order terms of the cost function; see Equation (1) in Methods. Note that all these coefficients were positive, which is an important criterion for applicability of ANIO (Terekhov et al. 2010; Terekhov and Zatsiorsky2011). The positive k_i values mean that ANIO found a solution for the inverse optimization problem.

The dihedral angle (D-angle), the goodness of fit index (see Methods) was, on average 5.49±1.25°. Two subjects showed larger values of the D-angle (>10°); one of them was subject #4 who also showed the lowest percentage of variance accounted for by the two PCs.

5.2.2 Drifts in task-related performance variables

All the subjects were able to perform the {M_{TOT}; F_{TOT}} tasks, even after the additional constraint on F_{MID} had been added. Figure 5-2 shows the individual finger time series during a typical trial with an initial pronation moment, as well as the computed performance variables related to the task constraints, F_{TOT}, M_{TOT}, and F_{MID}. During the early portion of the task (until *Phase-1*), the subject achieved a certain finger force combination that satisfied the {M_{TOT}; F_{TOT}} constraint. By *Phase-2*, the subject was able to reduce F_{MID} by 50% (as required by the task) while still producing the same {M_{TOT}; F_{TOT}} combination. After the visual feedback on all three performance variables, F_{TOT}, M_{TOT}, and F_{MID}, was turned off, the finger forces showed consistent drifts leading to a drop in F_{TOT}, a drop in the magnitude of M_{TOT}, and an increase in F_{MID} (see *Phase-3* in Figure 5-2).

Keeping visual feedback on some of the performance variables helped the subjects to avoid drift in those variables, while drifts in the variables without visual feedback persisted. Figure 5-3 illustrates a typical trial with the initial moment into supination. After *Phase-2*, visual feedback on F_{TOT} only was preserved, while the feedback on M_{TOT} and F_{MID} was turned off. The Figure shows a consistent level of F_{TOT} throughout the trial, while the magnitude of M_{TOT} drifts to lower values and the magnitude of F_{MID} drifts toward higher values.

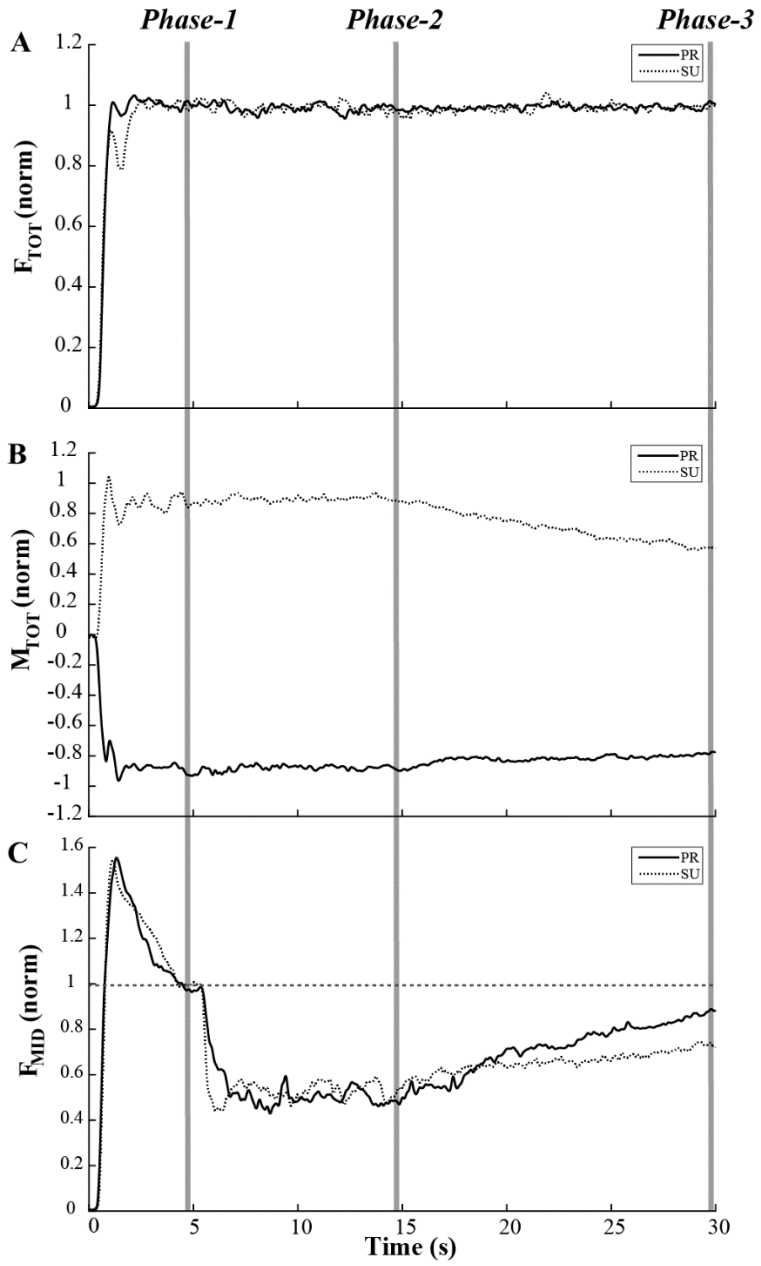

Figure 5-3. A typical trial observed when only F_{TOT} feedback was preserved after *Phase-2*. (a) F_{TOT} signal. No drift was expected as the feedback was provided on this task variable. (b) M_{TOT} signal was shown in this panel, and as expected M_{TOT} value decreases unintentionally by time in the absence of visual feedback. (c) F_{MID} signal. F_{MID} increases in the absence of visual feedback.

Overall patterns of the drifts in the three task-related variables are illustrated in Figure 5-4. Panel A of Figure 5-4 shows the averaged across subjects magnitude of the drift in F_{TOT} (ΔF_{TOT}) from *Phase-2* to *Phase-3* as a function of feedback condition. Note the very low drift magnitudes when F_{TOT} feedback was present and large consistent drifts to lower F_{TOT} values (negative ΔF_{TOT}) when F_{TOT} feedback was turned

off. The drift in F_{TOT} showed only minor changes with the initial M_{TOT} magnitude, but it showed smaller values when M_{TOT} feedback was present.

Two-way ANOVA, *Moment* × *Feedback*, on ΔF_{TOT} over the time of modified feedback confirmed a significant effect of *Feedback* ($F_{[2.574, 25.741]} = 22.394$, $p < 0.001$). Pairwise contrasts confirmed that the drop was larger in conditions without F_{TOT} feedback (on average, 12.76 ± 1.68% of the target F_{TOT}), compared to conditions when F_{TOT} feedback was kept over the whole trial (on average, 0.19 ± 0.037% of the target F_{TOT}, $p < 0.001$). It also confirmed larger magnitudes of ΔF_{TOT} for the "None" and "F_{MID}" condition (no feedback on F_{TOT} and M_{TOT}) compared to the "M_{TOT}" and "M_{TOT}+F_{MID}" conditions ($p < 0.05$).

The drift in M_{TOT} depended strongly on both the initial M_{TOT} value and feedback. As illustrated in panel B of Figure 5-4, this drift was very small and inconsistent when feedback on M_{TOT} was available throughout the trial. The drift was large when M_{TOT} feedback was unavailable for both initial PR (black bars) and SU (gray bars) M_{TOT} values. The difference in the sign of ΔM_{TOT} in the PR and SU conditions reflected the fact that M_{TOT} drifted toward zero value. The average decrease in M_{TOT} in the absence of visual feedback was 11.84%±6.45%, 1.56%±0.59%, and 24.83%±4.84% of the original value in PR, ZERO, and SU moment condition, respectively. When the feedback was shown, these values decreased to 1.20%±0.69%, 0.15%±0.03%, and 2.63%±0.94% of the original value, respectively.

Two-way ANOVA, *Moment* × *Feedback*, on ΔM_{TOT} confirmed a significant effect of *Moment* ($F_{[1.324, 13,236]} = 28.314$ $p < 0.001$) and a significant *Moment* × *Feedback* interaction ($F_{[3.668, 36.684]} = 11.374$, $p < 0.001$). The effect of *Moment* reflected significant differences within each pairs of the three levels, PR, SU and ZERO ($p < 0.05$). The interaction reflected the different magnitudes of the drift between conditions with and without M_{TOT} feedback ($p < 0.001$). Effect of *Feedback* was not significant because of the opposite effects depend on the initial moment.

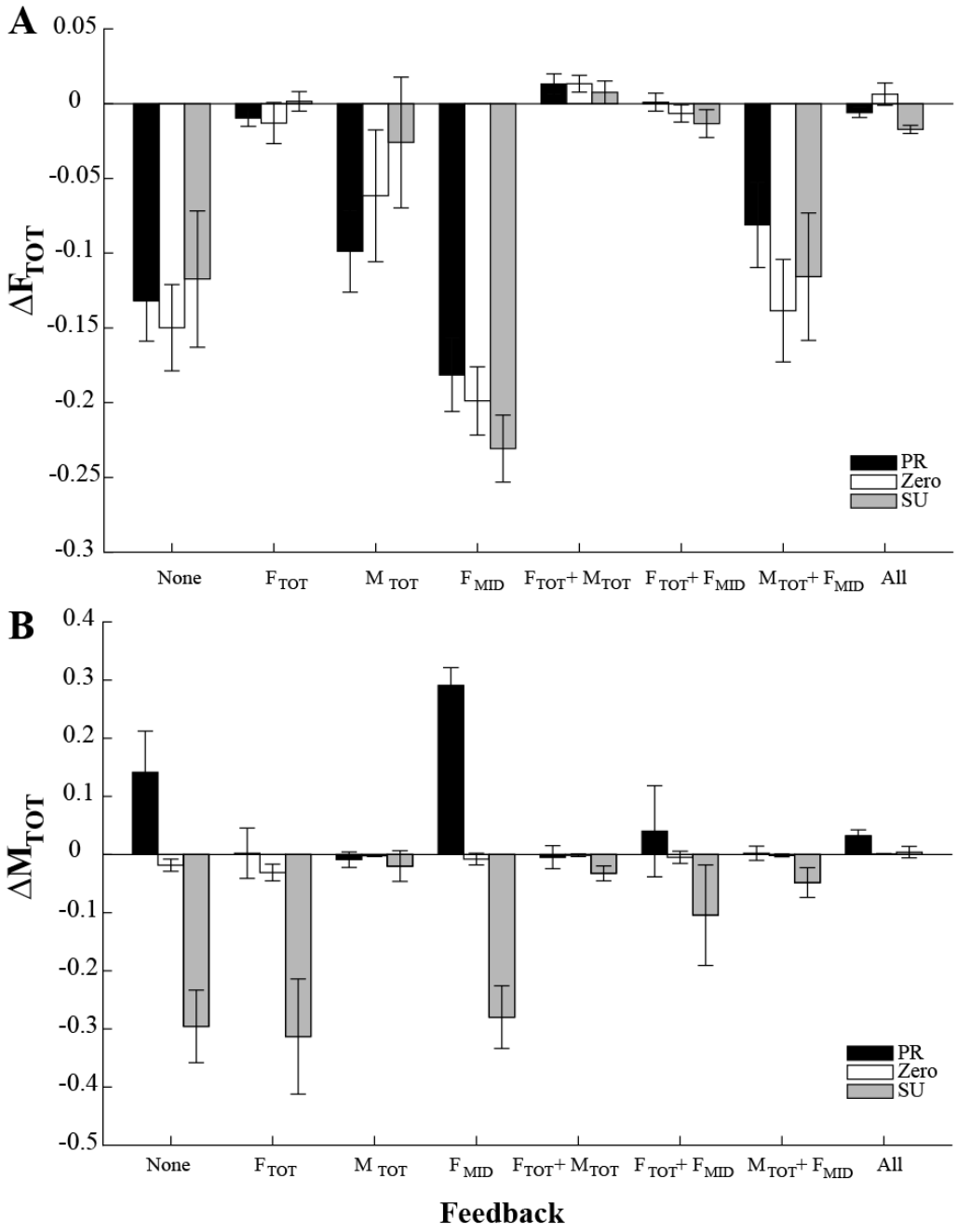

Figure 5-4. (a) Mean and standard error representing ΔF_{TOT} across trials for all *Moment* and *Feedback* conditions. The difference between F_{TOT} in *Phase-3* and *Phase-2* were considered as ΔF_{TOT}. Similarly, in (b) the ΔM_{TOT} was computed as the difference between M_{TOT} in *Phase-3* and *Phase-2*. Three different colors show various *Moment* conditions.

5.2.3 Drifts in finger forces

The regularities in the drifts of F_{TOT} and M_{TOT} were reflected also in drifts of the individual finger forces. Panel B of Figure 5-5 illustrates the drifts in the middle finger force, F_{MID}. In trials, when visual feedback on F_{MID} was provided, no consistent drifts in F_{MID} were observed. In contrast, when F_{MID} feedback was unavailable, F_{MID} showed a consistent tendency to increase. These effects were the strongest in the SU tasks (gray bars in Figure 5-5B) and weakest in the PR tasks (black bars in Figure 5-5B). In the absence of feedback on F_{MID}, 20.89%±8.27%, 31.01%±4.73%, and 64.21%±12.17% increase in F_{MID} was observed in the PR, ZERO, and SU conditions, respectively.

Two-way ANOVA, *Moment* × *Feedback*, on ΔF_{MID} confirmed significant effects of both *Moment* ($F_{[2, 20]} = 11.028$, $p < 0.001$) and *Feedback* ($F_{[2.710, 27.102]} = 13.582$, $p < 0.001$). There was also a significant *Moment* × *Feedback* interaction ($F_{[4.644, 46.439]} = 3.143$, $p < 0.05$).

Pairwise comparisons confirmed the larger ΔF_{MID} for SU compared to both PR and ZERO conditions ($p < 0.05$). The effect of *Feedback* reflected larger drift values for conditions without feedback on F_{MID} compared to conditions with F_{MID} feedback ($p < 0.05$). The interaction reflected the smaller effects of *Moment* on ΔF_{MID} for the "None" condition as compared to other conditions without F_{MID} feedback ($p < 0.05$).

In contrast to the ΔF_{MID} patterns, the forces produced by the other three fingers (index, ring, and little) typically showed drifts toward smaller values (panels A, C, and D of Figure 5-5). These drifts were smaller for the trials under "All" and "F_{TOT}+M_{TOT}" visual feedback conditions and larger under the "None" and "F_{MID}" conditions. These observations were supported by a significant effect of *Feedback* ($F_{[3.624,144.962]} = 15.910$, $p < 0.001$). There was also a significant effect of *Moment* reflecting the tendency of more positive (less negative) values of force changes for the SU tasks ($F_{[2, 80]} = 7.964$, $p < 0.001$), particularly pronounced for the index finger (*Moment* × *Finger* interaction, $F_{[6, 80]} = 6.880$, $p < 0.01$). Other significant effects, including the three-way interaction *Moment* × *Feedback* × *Finger* ($F_{[17.649, 235.316]} = 2.895$, $p < 0.01$) reflected the complex pattern of individual finger force adjustments. Since these effects were not directly related to the specific hypotheses and their discussion, we do not present these results.

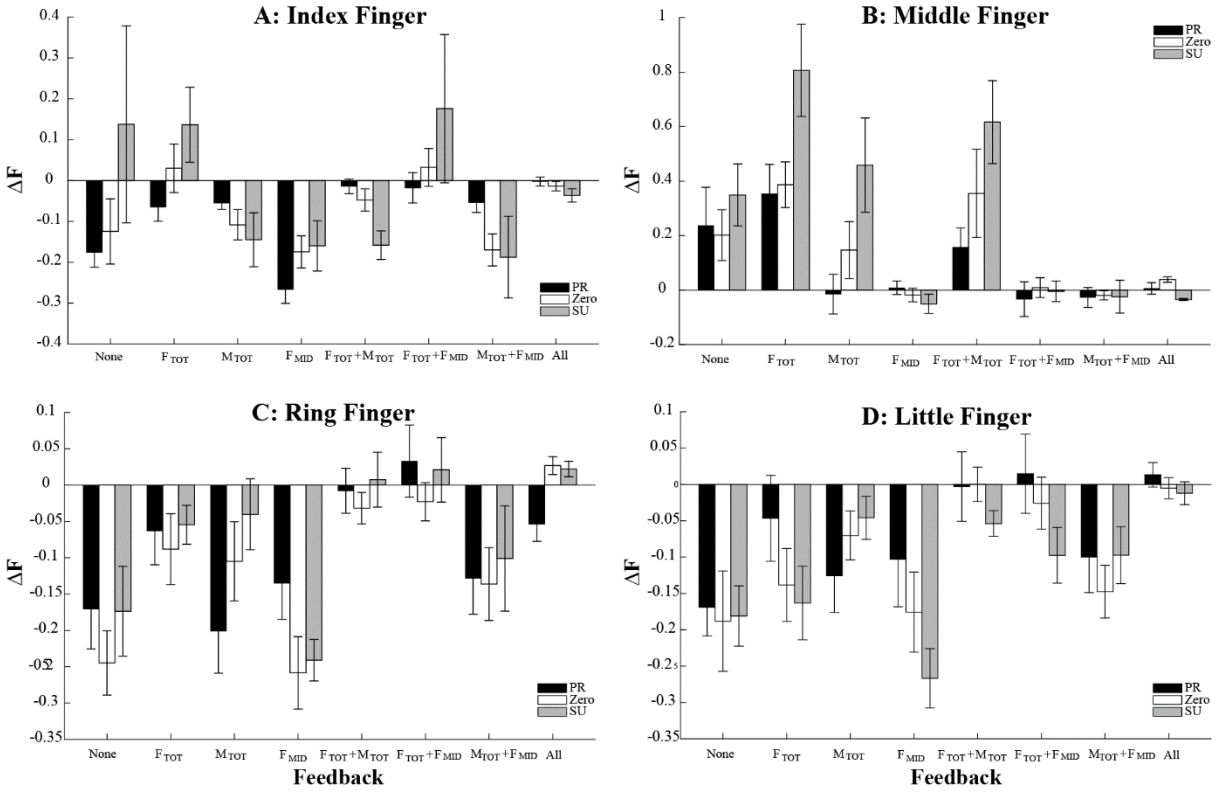

Figure 5-5. Drift in finger forces represented by mean and standard error. Index, middle, ring and little finger forces were computed as the difference between the finger force value in Phase-3 and Phase-2

5.2.4 Cost value drifts

To test the second hypothesis on the drift within the UCM toward a minimum of the cost function, we quantified changes in the cost function, ΔC_{ANIO} over the time interval between *Phase-2* and *Phase-3* (with modified visual feedback). Under most conditions, the cost function showed a drop as illustrated by the negative values in Figure 5-6. The largest magnitudes of ΔC_{ANIO} were seen under the "F_{MID}" and "None" conditions while the smallest changes, close to zero, were observed under the "All", "F_{TOT}+M_{TOT}" and "F_{TOT}+F_{MID}" conditions. These patterns did not show any clear effects of initial moment value. These results were reflected in the significant effect of *Feedback* in the *Moment* × *Feedback* ANOVA ($F_{[1.347,\ 13.474]}$ = 5.550, $p < 0.05$). No other effects reached significance.

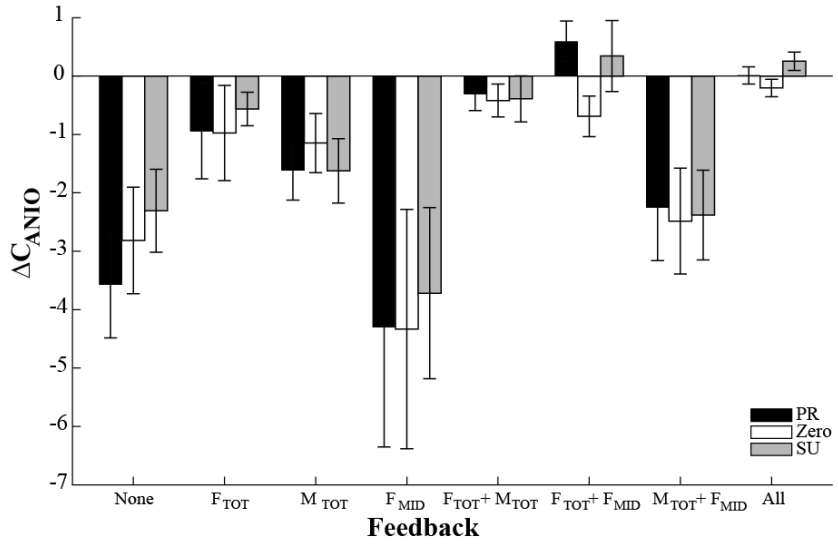

Figure 5-6. Mean and standard error representing ΔC_{ANIO} across trials for all *Moment* and *Feedback* conditions. ΔC_{ANIO} was computed by subtracting the C_{ANIO} at *Phase-2* from the value at *Phase-3*. Three different colors show various *Moment* conditions.

5.3 Discussion

The results of our study provide support for the main hypotheses formulated in the Introduction. We suggested that two factors contributed to the observed drift in finger forces in the absence of visual feedback. First, drift of the referent coordinate (RC) for a salient task-specific variable toward its actual coordinate was assumed (cf. Ambike et al. 2015). The experiments showed a drift of total force (F_{TOT}) to lower values across conditions without F_{TOT} feedback. They also showed a drift of the total moment of force (M_{TOT}) towards lower absolute values when no M_{TOT} related feedback was shown; the direction of the drift depended on the initial M_{TOT} magnitude. The idea of control with RC implies, in particular, that active force is approximately proportional to the difference between the referent and actual fingertip coordinates, while active moment is proportional to the difference between the referent and actual hand orientation (Latash et al. 2010). Given that the actual finger position and configuration were always the same, our current observations support the assumed RC drift toward actual fingertip coordinates and hand orientation.

Second, we also assumed that a drift would happen within the uncontrolled manifold (UCM; Scholz and Schöner 1999) for the salient performance variables toward a state corresponding to minimum of the cost function defined in the space of elemental variables. The initial cost of the finger force combination computed based on the cost function reconstructed with analytical inverse optimization (ANIO, Terekhov et al. 2010) dropped across conditions. Moreover, we observed an atypical drift of the middle finger force

(F_{MID}) to higher values in trials when the subjects reduced F_{MID} intentionally as compared to the preferred finger force combination. Note that all earlier studies reported downward drifts of finger forces after turning visual feedback off unless the initial forces were very low (Slifkin et al. 2000; Vaillancourt and Russell 2002; Ambike et al. 2015).

5.3.1 Factors that define unintentional changes in performance

Unintentional motor performance has been known for many years. One of the classical examples of the so-called Kohnstamm phenomenon (Kohnstamm 1915; Ivanenko et al. 2006): An unintentional motion of an extremity following a long-lasting strong isometric contraction. Unintentional changes in locomotion have been reported following walking on a rotating platform (the podokinetic effect, Weber et al. 1998; Scott et al. 2011) and under vibration applied to the leg muscles (Gurfinkel et al. 1998; Ivanenko et al. 2000).

Recently, the phenomenon of unintentional finger force drop has been studied in experiments with accurate force production with the help of under visual feedback, when the feedback was later turned off (Slifkin et al. 2000; Vaillancourt and Russell 2002; Shapkova et al. 2008). Similar effects have been observed in grasping studies following a slow transient change in the aperture (Ambike et al. 2014), while faster unintentional changes in arm position and finger forces were reported in experiments with transient perturbations applied to the effectors (Wilhelm et al. 2014; Zhou et al. 2014, 2015).

Some of the earlier studies invoked the notion of working memory limitations as the cause for the unintentional force drop (Vaillancourt et al. 2001; Vaillancourt and Russell 2002). This idea was challenged in later studies (Ambike et al. 2015; Jo et al. 2016) based on two observations. First, finger forces changed consistently across subjects while problems with working memory are expected to lead to inconsistent force production. Second, resting during a comparable time interval led to no consistent force drift. Ambike et al. (2015) also reported a force drift in the opposite direction, to higher values, but only in fingers that started the task with very low forces. These trends were weak (although statistically significant in some cases). While they remind the F_{MID} drift to higher forces in our study, the initial F_{MID} magnitudes in our experiment were typically higher (about 10% of the MVC force) than the values leading to finger force drift toward higher force reported by Ambike and colleagues (under 5% of that finger's MVC force). Besides, the magnitude of the F_{MID} drift in our study was of about the same magnitude as the more typical downward force drift in other fingers (Figure 5-5), while in the Ambike et al. study the upward force drift was an order of magnitude smaller than the typical downward drifts.

Several earlier studies (Ambike et al. 2014, 2015; Zhou et al. 2015) interpreted the unintentional force drift within the hypothesis assuming that the neural control of movements is based on shifts of referent spatial coordinates for salient variables (the RC-hypothesis, reviewed in Feldman 2015). Within the RC-hypothesis, force production in isometric conditions is associated with setting RC for the effector that differs from its actual coordinate (AC). The difference between AC and RC produces force via a scaling coefficient, apparent stiffness (cf. Pilon et al. 2007). An unintentional drop in force means that RC moves towards AC and/or the apparent stiffness decreases; for simplicity, we consider only the former mechanism. Note that when RC = AC, the system produces no force, and muscle activation is minimal for the given effector configuration. This state may be viewed as the state with minimal potential energy of the effector. A hypothesis has been suggested that, when the CNS does not implement sensory-based corrections, the physical/physiological system participating in the task relaxes toward a state with minimal potential energy, i.e., AC attracts RC leading to a force drift toward smaller magnitudes. Our current results on the F_{TOT} and M_{TOT} drifts provide support for this idea.

A novel hypothesis offered in this study is that, when an abundant set of effectors participates in a task, a drift toward preferred solution is expected in the space of elemental variables. We estimated preferred solutions using the analytical inverse optimization (ANIO) method (Terekhov et al. 2010) and then used the computed cost functions to estimate the changes in cost associated with the changing finger force combinations. Asking the subjects to perform the $\{F_{TOT}; M_{TOT}\}$ tasks with a reduced contribution from the middle finger forced them to deviate from the naturally preferred solution corresponding to a minimum of the cost function. The observed downward drift of the cost supports the idea that a drift took place in the space of finger forces leading to more natural finger force combinations (closer to the minimum of the cost function).

Taken together, our observations suggest superposition of two processes: a drift of RC toward AC and a drift in the space of finger forces directed at reducing the cost of the action. Figure 5-7 illustrates this idea for a two-finger task of producing a value of total force: $F_1 + F_2 = F_{TOT}$. Assume that the subject has a preferred pattern of sharing F_{TOT} between the two fingers, e.g., 50:50 (the large black dot), corresponding to a minimum of the cost function (shown with parabolic dashed lines). Other solutions for the task are possible shown by the lines with negative slope – UCMs for this task. The initial force level corresponds to a certain distance between RC and AC. Imagine now that the subject was asked to perform this task with an unusual force combination, i.e. lower contribution of finger #1 (the open circle). This point corresponds to a higher cost of the action (see the dashed circle, a projection of the point on the cost function). After visual feedback on both F_{TOT} and F_1 has been turned off, two processes will take place. First, RC will drift towards AC illustrated by the drift of the solution space (UCM) toward smaller F_{TOT} values (compare the

thick and thinner UCM lines in Figure 5-7). At the same time, a drift in the $\{F_1; F_2\}$ space will take place moving the actual finger force values closer to the bottom of the cost function. The resultant drift is shown as the dashed line with the arrow. Our observations suggest that the two processes proceed at comparable time scales, but this issue requires further investigation. Note that unintentional drifts at two time scales have been reported so far, slow (typical times of 10-20 s; Vaillancourt and Russell 2002; Ambike et al. 2014, 2015) and fast (typical times of 1-2 s; Wilhelm et al. 2013; Zhou et al. 2014, 2015; Ambike et al. 2016).

5.3.2 Hierarchical control with referent coordinates

The RC-hypothesis implies a hierarchical system of control with the RC for salient, task-specific variables defined at the highest level of the hierarchy. Further, this low-dimensional set of RCs maps on RCs at lower, higher-dimensional levels and defines RCs for limbs, joints, digits, and muscles. Such transformations are associated with synergic adjustments among RCs within abundant sets at lower levels, possibly via back-coupling loops (Latash et al. 2005; Martin et al. 2009). This scheme predicts relatively consistent behavior in the space of salient task-specific variables combined with a relatively variable behavior at the level of elements (Schöner 1995).

This prediction has been tested in a number of studies within the UCM hypothesis (Scholz and Schöner 1999). Some of those studies (reviewed in Latash et al. 2007; Latash 2008) compared inter-trial variance within a space where salient variables do not change (within UCM, V_{UCM}) and within a space where those variables change (orthogonal to the UCM, V_{ORT}). The inequality $V_{UCM} > V_{ORT}$, where both indices quantified per dimension in the corresponding spaces, has been used as a signature of a synergy stabilizing those salient variables. Another group of studies quantified deviations along the UCM and along the ORT space during quick corrective actions (Mattos et al. 2011, 2014). Note that deviations along the UCM by definition cannot correct deviations of salient variables. Nevertheless, large such deviations have been observed reflecting the lower stability of the system within the UCM as compared to the ORT directions.

In our study, we observed most consistent across subjects patterns of unintentional drifts in the task-related variables such as F_{TOT} and M_{TOT} when the corresponding feedback was turned off (Figure 5-4). The drifts in some of the individual finger forces were less consistent (Figure 5-5) suggesting that much of the finger force drifts took place within the UCM for F_{TOT} and M_{TOT}. This issue is analyzed in a companion study presented in Chapter 6.

5.3.3 Is optimization real?

The original formulation of the problem of motor redundancy (Bernstein 1935) stated explicitly that the main problem of motor control was the elimination of redundant degrees of freedom. This could be done by adding constraints to the system (for example, self-imposed, intentional constraints, e.g. Hu and Newell 2011), or by using optimization approaches, i.e., looking for a solution from an infinite set that minimizes (or maximizes) a cost function. A number of cost functions have been explored (reviewed in Nelson 1984; Prilutsky and Zatsiorsky 2002), such as minimal time, minimal energy expenditure, minimal jerk, minimal fatigue, minimal discomfort, and many others. Researchers selected specific cost functions rather arbitrarily, typically reflecting their intuition and experience.

Two questions emerge. First, can arbitrary choice of cost functions be avoided and replaced with a computational, data based, method? Second, are optimization approaches useful for analysis of natural, biological movements?

An answer to the first question was offered by the ANIO method (Terekhov et al. 2010: Terekhov and Zatsiorsky 2011). This method allows computing a cost function based on experimental observations under certain assumptions, in particular that the cost function is additive with respect to outputs of the elements. A number of studies have shown that ANIO produces consistent cost functions that allow describing multi-finger tasks with better accuracy than typical cost functions used in the literature (Niu et al. 2012), and that this method is sensitive to fatigue, healthy aging, and neurological disorders (Park et al. 2010, 2011b, 2012). Our current study makes another step in supporting applicability of ANIO to actions by abundant systems. As in the cited earlier studies, ANIO was able to reconstruct cost functions that generated solutions approximating the experimental data with good accuracy: The angle between the planes of actual solutions and ANIO-based solutions was, on average, about 5 degrees. Moreover, unintentional finger force changes after the visual feedback had been turned off led to a significant drop in the cost of the action based on the ANIO results.

With respect to the second question, we view the drift of the cost (ΔCANIO; see Figure 5-6) to lower values, as providing strong support for the idea that the CNS is indeed driven by some kind of an optimization process, i.e., it is naturally moved to solutions corresponding to minimum values of a cost function. Optimization does not have to be absolute, just “good enough” (Simon 1956; Loeb 1999). Our instruction to the subjects to drop FMID by 50% before the visual feedback was turned off (Phase 2) apparently took the subjects away from the “good enough” region. As a result, a drift leading to lower cost values was seen including, in particular, the non-trivial drift of FMID to higher values in contrast to the dominant downward trend in the other finger forces.

5.3.4 Concluding comments

The main results of our study include support for the hypothesis on two sources of the observed unintentional finger force drift: The drift of RC towards AC and the drift of cost toward lower values. The speed of all the observed drifts was relatively slow, corresponding to earlier reports on the force drift in the absence of visual feedback (Vaillancourt and Russell 2002; Shapkova et al. 2008; Ambike et al. 2015). It suggested processes within a subspace characterized by relatively low stability of the elements, i.e. primarily within the UCM for the task. Since the effects were observed in the salient performance variables, these observations also suggest a degree of coupling between the UCM and ORT spaces, a hypothesis (Ambike et al. 2015, 2016) that is still in need of more direct experimental confirmation.

Chapter 6

Optimality and stability of intentional and unintentional actions: II. Structure of variance and motor equivalence

In this study, we address the famous problem of motor redundancy (Bernstein 1967): For all natural actions, the number of variables produced by elements involved in an action (elemental variables) is larger than the number of constraints. This results in an infinite number of possible solutions, and the problem has traditionally been formulated as: How does the central nervous system (CNS) select specific solutions for such tasks? Recently, this problem has been revisited based on the principle of abundance (Gelfand and Latash 1998; Latash 2012). According to this principle, the CNS does not select specific solutions, but families of solutions are facilitated equally able to solve the task. This results in different stability properties in different directions within the space of elemental variables.

The related notion of task-specific stability introduced by Schöner (1995) suggests that the CNS acting in a multi-dimensional space of elemental variables can selectively stabilize processes in directions leading to changes in salient task-specific performance variables. For a given performance variable, the space of elemental variables may be viewed as composed of two sub-spaces, the uncontrolled manifold (UCM, Scholz and Schöner 1999) where the performance variable stays unchanged, and the orthogonal to the UCM (ORT) space where this variable changes. Processes in the ORT space are expected to show high stability leading to low variance across repeated trials, while processes within the UCM are expected to show low stability and high inter-trial variance, $V_{UCM} > V_{ORT}$ (each variance index is computed per degree-of-freedom in the corresponding space). The notion of a synergy stabilizing a performance variable has been introduced, and a synergy index (ΔV) has been used reflecting the normalized difference between V_{UCM} and V_{ORT} (reviewed in Latash et al. 2007; Latash 2008). Note that the synergy index may be viewed as a proxy of stability of the selected performance variable.

Different stability within different sub-spaces in a multi-dimensional space of elemental variables is also reflected in the phenomenon of motor equivalence (Mattos et al. 2011; Scholz et al. 2011). Any action leading to a change in a salient performance variable may be viewed as composed of two components, within the UCM and within ORT. Motion of elemental variables within the UCM by definition has no effect on the salient performance variable and is addressed as motor equivalent (ME). Motion within ORT changes the performance variable and is called non-motor equivalent (nME). Large amounts of ME motion have been documented in kinematic, kinetic, and electromyographic spaces in tasks that required quick corrections of performance variables in response to external perturbations (Mattos et al. 2011, 2013,

2015). These large ME motions have been interpreted as reflecting the low stability of processes within the corresponding UCMs.

In this study, we explored stability of performance variables during their unintentional drifts. So far, only one experiment with multi-joint positional tasks and external transient perturbations addressed this issue (Zhou et al. 2015). This is the first study to explore indices of performance stability during unintentional drifts in performance in steady-state tasks. Our first hypothesis was that selective stability of performance variables would be observed even when the magnitudes of those variables drift unintentionally. We tested this hypothesis with respect to variables that showed no drift (because of the presence of visual feedback) and with respect to variables that drifted (because their visual feedback was turned off, Slifkin et al. 2000; Vaillancourt et al. 2002). In the experiments, the subjects were required to produce accurate total force and total moment of force $\{F_{TOT}; M_{TOT}\}$ combinations and then to modify their preferred pattern of sharing the task among the four fingers by decreasing the middle finger force (F_{MID}) by 50% while producing the same $\{F_{TOT}; M_{TOT}\}$ magnitudes. We used the ME and nME indices as quantitative proxies of stability; note that the more commonly used analysis of inter-trial variance was not possible given only a few trials per feedback condition.

We also explored whether stability of a variable depended on the number of explicit task constraints. Earlier studies explored this issue indirectly by varying the number of explicitly involved elemental variables (e.g., Latash et al. 2001). They showed, in particular, that some performance variables showed higher stability indices (similar to ΔV) with an increase in the number of elemental variables. In our current study, no change in the number of elemental variables took place – the subjects always performed all tasks with four fingers of the right (dominant) hand. However, adding a constraint related to the required magnitude of F_{MID} was expected to reduce the range of available solutions. Based on the aforementioned earlier studies, we hypothesized that indices of stability for $\{F_{TOT}; M_{TOT}\}$ would drop after the subjects purposefully reduced F_{MID} to 50% of its preferred value.

6.1 Methods

6.1.1 Subjects

Eleven subjects voluntarily participated in this study, five females and six males (age: 27.27 ± 5.44 years, mass: 74.18 ± 14.73 kg, height: 171.18 ± 8.30 m). All our subjects were right-handed and healthy. All subjects signed the consent form approved by the Office of Research Protections of The Pennsylvania State University.

6.1.2 Apparatus

The setup is described in more detail in section 5.1.2 (Parsa et al. REF; see Figure 6-1). The subject sat in front of the monitor used to provide visual feedback and define tasks. The four fingers of the right hand were placed comfortably on six-component force sensors (ATI) while the right lower arm was fixed comfortably to the wooden plate with two sets of Velcro tapes (Figure 6-1A,C). The screen provided feedback on three variables (Figure 6-1B): The total normal force (F_{TOT}) produced by the fingers (along the Y-axis), the total moment (M_{TOT}) produced by the normal fingers forces with respect to a horizontal line in a sagittal plane passing in-between the middle and ring fingers, and the normal force produced by the middle finger (F_{MID}) as the level in a tank-with-water graph (see Figure 6-1B) located in such a way that it did not interfere with the first two feedback signals. The latter feedback was used at particular times only (described later).

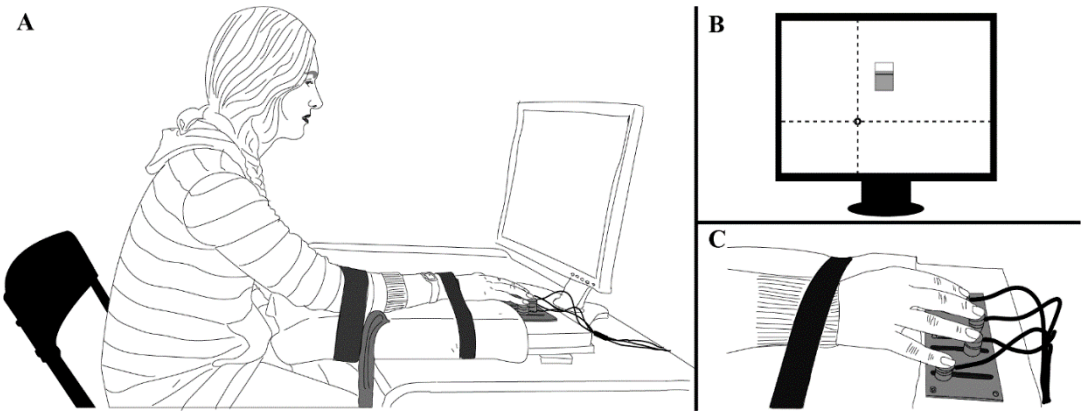

Figure 6-1. The setup. A: The subject's position. B: Visual feedback defined total force and total moment target, {F_{TOT}, M_{TOT}}, as the intersection of two lines. The "tank with water" in the middle of the screen presented the feedback on the middle finger force. C: Hand placement on the sensors.

Twenty-four analog signals (4 sensors × 6 components) were digitized by a 12-bit analog-digital converter (PCI-6031, National Instruments, Austin, TX) at 100 Hz. A Labview program was written for data acquisition and to provide visual feedback. All further data analyses were done using MATLAB 2014.

6.1.3 Experimental procedure

Subjects first placed their fingertips on the sensors and relaxed; then the sensor readings were set to zero; as a result only active downward forces were measured. The experiment consisted of three parts. The first two parts involved maximal force production trials (MVC) and trials with accurate production of various combinations {F_{TOT}; M_{TOT}} described in detail in Chapter 5. The data presented and analyzed in this study were collected in the third part.

Each trial started with a {F_{TOT}; M_{TOT}} target shown on the screen (Figure 6-1B). F_{TOT} was always equal to 20% of the four-finger MVC while M_{TOT} could be 1.5PR, 0, or 1.5SU. A unit of the moment into pronation (PR) or supination (SU) was defined as 7% of the index finger MVC multiplied by the index finger nominal lever arm (0.045 m). The subjects were given 5 s to match the {F_{TOT}; M_{TOT}} task combination.

Five seconds after the trial initiation, a third feedback on F_{MID} appeared on the screen and subjects were instructed to adjust their middle finger force to match the level shown by the tank feedback without changing the {F_{TOT}; M_{TOT}} level. The target level for F_{MID} was set at half of the average force this finger produced within the time interval 4.7-4.8 s from the trial initiation. The subjects were given 10 s to reach a new steady finger force combination that would satisfy the original {F_{TOT}; M_{TOT}} constraint and the new F_{MID} constraint.

At that time (15 s into the trial), visual feedback was manipulated. We had eight main conditions: no feedback on any of the three variables (None), feedback on one of the three performanca variables (F_{TOT}; $M_{TOT,}$ or F_{MID}), feedback on two of the performance variables (F_{TOT}&F_{MID}, M_{TOT}&F_{TOT}, and M_{TOT}&F_{MID}), and all the feedback remaining on the screen until the end of the trial (All). For technical reasons, data for two subjects for the “All” condition were unavailable. Under each condition, three trials were performed in a row with 10-s intervals.

6.1.4 Data processing

Finger force data were low-pass filtered at 5 Hz using a zero lag, fourth-order Butterworth filter. We selected three phases in each trial for data analysis to represent three steady states: Under the original set of constraints, {F_{TOT}; M_{TOT}}, under the combination of three constraints, {F_{TOT}; M_{TOT}} and F_{MID}, and at the end of the time with modified visual feedback. Correspondingly, Phase-1 was defined as the time interval between 4.7 and 4.8 s; Phase-2 corresponded to the time interval between 14.7 and 14.8 s, and Phase-3 corresponded to the time interval between 29.7 and 29.8 s.

6.1.4.1 Analysis of motor equivalence

The task constraints can be represented as a set of linear equations:

$$F_I + F_M + F_R + F_L = 0.2MVC \quad (6\text{-}1)$$

$$-0.045F_I - 0.015F_M + 0.015F_R + 0.045F_L = M_{TOT} \quad (6\text{-}2)$$

$$F_{MID} = 0.5F_{MID}^* \quad (6\text{-}3)$$

where F_I, F_M, F_R, and F_L stand for the index, middle, ring, and little finger forces; M_{TOT} could be 1.5PR, 1.5SU, or Zero depending on the task; and F_{MID}^* is the middle finger force by the subjects at the end of *Phase-1*. We can rewrite the task in a matrix form:

$$\mathbf{CF} = \mathbf{P} \quad (6\text{-}4)$$

where, **C** is the constraint matrix defining the task, **F** is the vector of finger forces (elemental variables in our analysis), and **P** is the vector of performance variables. Changes in the elemental and performance variables:

$$\mathbf{J}\Delta\mathbf{F} = \Delta\mathbf{P} \quad (6\text{-}5)$$

where $\Delta\mathbf{F}$ is the vector of changes in the finger force between two phases. It could be computed between Phase-2 and Phase-1 ($\Delta\mathbf{F}_{21}$) and between Phase-3 and Phase-2 ($\Delta\mathbf{F}_{32}$). Since equations 6-4 and 6-5 are linear, the Jacobian (**J**) of the system is the same as the **C** matrix.

Performance remains unchanged ($\Delta\mathbf{P} = 0$) if the change in elemental variables occurs in the null space of the **J** [$\mathbf{e} = \text{null}(\mathbf{J})$]. Hence, the projection of $\Delta\mathbf{F}$ onto the null-space was defined as the ME component, while the projection of $\Delta\mathbf{F}$ orthogonal to the null-space was defined as the nME components. ME and nME components were normalized by the square root of the corresponding space dimensionality.

6.1.4.2 Analysis of inter-trial variance

The UCM hypothesis (Scholz and Schöner 1999) allows the partitioning of the inter-trial variance within a redundant space of elemental variables into two components, one of them keeps salient

performance variables unchanged (V_{UCM}) while the other component leads to changes in these variables (V_{ORT}). We pooled the data from all trials in Phase-1 and Phase-2 because in those phases the visual feedback was always available for the task-specific performance variables. At each time sample, the inter-trial variance was computed within the null-space of **J** (which is the UCM for tasks with linear constraints) and within its orthogonal complement (ORT space). Further, an index of synergy (ΔV) was defined as the normalized difference between V_{UCM} and V_{ORT}:

$$\Delta V = \frac{{}^{V_{UCM}}/_{n_{UCM}} - {}^{V_{ORT}}/_{n_{ORT}}}{{}^{V_{TOT}}/_{n_{TOT}}} \quad (6\text{-}6)$$

Where V_{TOT} stands for total variance and *n* with subscripts, stand for the dimensionality of the corresponding spaces. Since ΔV by its computation is bounded, for statistical analysis ΔV values were log-transformed using the modified Fisher's z-transform (Solnik et al. 2013).

6.1.4.2 Statistics

We present the data in the text and figures as means ± standard errors unless stated otherwise. All data sets were tested for normality and sphericity using the Mauchly criterion, and in cases of sphericity violations, the Greenhouse-Geisser correction was used. We set the critical p-value at 0.05 for all the analysis.

We tested the effects of adding a constraint on the ME vs. nME indices and the structure of inter-trial variance computed for the {F_{TOT}; M_{TOT}} task between Phase-2 (two constraints) and Phase-1 (three constraints). Note that full feedback was available in both phases. The analysis of motor equivalence used repeated-measures ANOVA with factors *Component* (ME, nME), *Phase* (1 and 2), and *Moment* (PR, Zero, SU). The analysis of the z-transformed synergy index ΔVZ was done with a two-way ANOVA, *Phase* × *Moment*. We also explored the effects of adding the F_{MID} constraint on the two variance components using an additional factor Variance (V_{UCM} and V_{ORT}). The variance components and ΔV_Z were also computed in Phase-2 with respect to all three constraints: F_{TOT}, M_{TOT}, and F_{MID}.

Changes in the ME and nME components under different feedback conditions were tested between Phase-3 and Phase-2. We computed the two components with respect to the Jacobian representing variables that received visual feedback ($\mathbf{J}_{VISION}$) as well as with respect to the Jacobian representing variables that stopped receiving visual feedback ($\mathbf{J}_{NO\text{-}VISION}$). Both analyzes are used three-way repeated-measures ANOVA with the factors *Component* (ME, nME), *Moment* (PR, Zero, SU), and *Feedback* (seven levels). The "All" condition was left out of the $\mathbf{J}_{NO\text{-}VISION}$ analysis because **J** becomes empty while the "None" feedback condition was left out of the $\mathbf{J}_{VISION}$ analysis because **J** becomes empty. Significant effects were further explored with pairwise comparison with Bonferroni corrections.

6.2 Results

All the subjects were able to adjust their finger forces from Phase-1 to Phase-2 to accommodate the additional constraint (reduce F_{MID} by 50%) while keeping the required magnitude of the total force and total moment, $\{F_{TOT}; M_{TOT}\}$. This change in the finger forces was associated with a large ME motion and minuscule nME motion reflecting the fact that accuracy of performance with respect to the original set of constraints was nearly unchanged. Turning visual feedback off resulted in drifts in the variables without feedback: F_{TOT} and M_{TOT} typically drifted toward lower absolute magnitudes, while F_{MID} typically drifted toward higher magnitudes. Variables with preserved feedback showed no visible drifts. These findings were reflected in the relative magnitudes of ME and nME motion.

Typical performance by a representative subject is illustrated in Figure 6-2 for the task involving pronation moment under two conditions, with feedback on F_{MID} only (the top panels) and with feedback on F_{TOT} and M_{TOT} (the bottom panels). The lines in the left panels show averaged across three trials time series of F_{TOT}, M_{TOT}, and F_{MID}. The right panels show the results of motor equivalence analysis (ME and nME) over all three phases and inter-trial variance analysis (V_{UCM} and V_{ORT}) over Phase-1 and Phase-2. Details on the magnitudes of drifts are discussed in Chapter 5. Here we focus on changes in the ME and nME components and structure of variance.

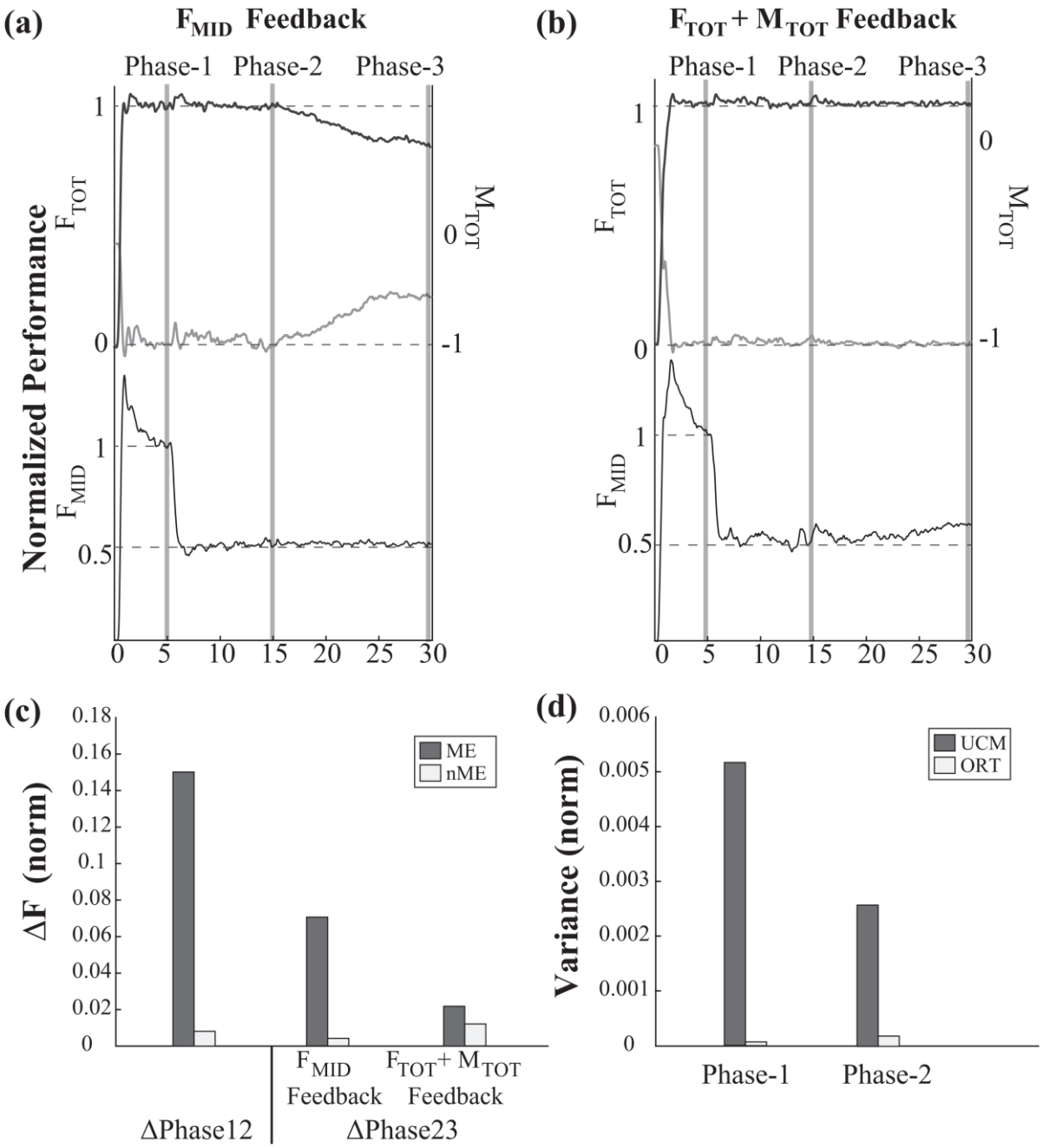

Figure 6-2. A typical example of F_{TOT}, M_{TOT}, F_{MID} was presented in (a) and (b) for F_{MID} and F_{TOT}+M_{TOT} feedback condition, respectively. Each of these time series were normalized to their targeted value at Phase-1. In (c) the ME and nME components computed considering Force-Moment Jacobian for the same subject and tasks was shown for two time intervals (ΔPhase12 and ΔPhase23). (d) shows the average value for the variance components (V_{UCM} and V_{ORT}) on Force-Moment Jacobian in Phase-1 and Phase-2.

6.2.1 Motor equivalence analysis

The magnitudes of the ME and nME components computed with respect to the {F_{TOT}; M_{TOT}} set of constraints are shown in Figure 6-3. Averaged across subjects' data with standard error bars are shown for the three tasks with different initial M_{TOT} magnitudes, PR, Zero, and SU. The left side of each panel shows the results over the interval from Phase 1 to Phase 2 ($\Delta Phase_{12}$), while the right side shows the results over the interval from Phase 2 to Phase 3 ($\Delta Phase_{23}$). In all three panels, the magnitude of ME over $\Delta Phase_{12}$ is much larger than the magnitude of nME ($F_{[2,\ 16]} = 37.33$, $p < 0.001$). The difference between the two components was smaller for the Zero M_{TOT} condition (*Component* × *Moment* interaction; $F_{[1,\ 8]} = 5.15$, $p < 0.05$). The relative magnitudes of the ME and nME component differed depending on the available visual feedback over $\Delta Phase_{23}$ as illustrated in the right parts of Figure 6-3. Under conditions with feedback on both F_{TOT} and M_{TOT}, the nME component remained very low, much lower than the ME component. The difference between the two components became smaller if only one of the two original constraints received visual feedback, and nME became significantly larger than ME if feedback on F_{MID} only was available (*Component* × *Feedback* interaction; $F_{[2.40,\ 23.96]} = 7.87$, $p < 0.01$).

These effects were consistent across M_{TOT} conditions although the trials with $M_{TOT} = 0$ were characterized by lower ME and nME magnitudes ($F_{[2,\ 20]} = 9.41$, $p < 0.001$). A three-way ANOVA with repeated measures, *Component* × *Moment* × *Feedback* also confirmed significant effects of *Component* ($F_{[1,\ 10]} = 101.79$, $p < 0.001$) reflecting the overall larger ME magnitudes, and *Feedback* ($F_{[2.12,\ 21.19]} = 5.507$, $p = 0.011$) reflecting many pairwise differences clear from Figure 6-3.

Figure 6-4 contrasts the ME and nME components computed with respect to the Jacobian reflecting constraints with the feedback that remained on the screen throughout the trial (top row), and also with respect to the Jacobian reflecting constraints without feedback between *Phase-2* and *Phase-3* (bottom row). This graph shows clearly that ME > nME for variables with feedback (top row) while the inequality reverses, nME > ME, for variables without feedback (bottom row). Note also the special set of data for the "All" condition in the top row: When all three variables remained specified throughout the trial, the subjects showed slight ME motion compared to all other conditions when at least one of the constraints was without the corresponding feedback.

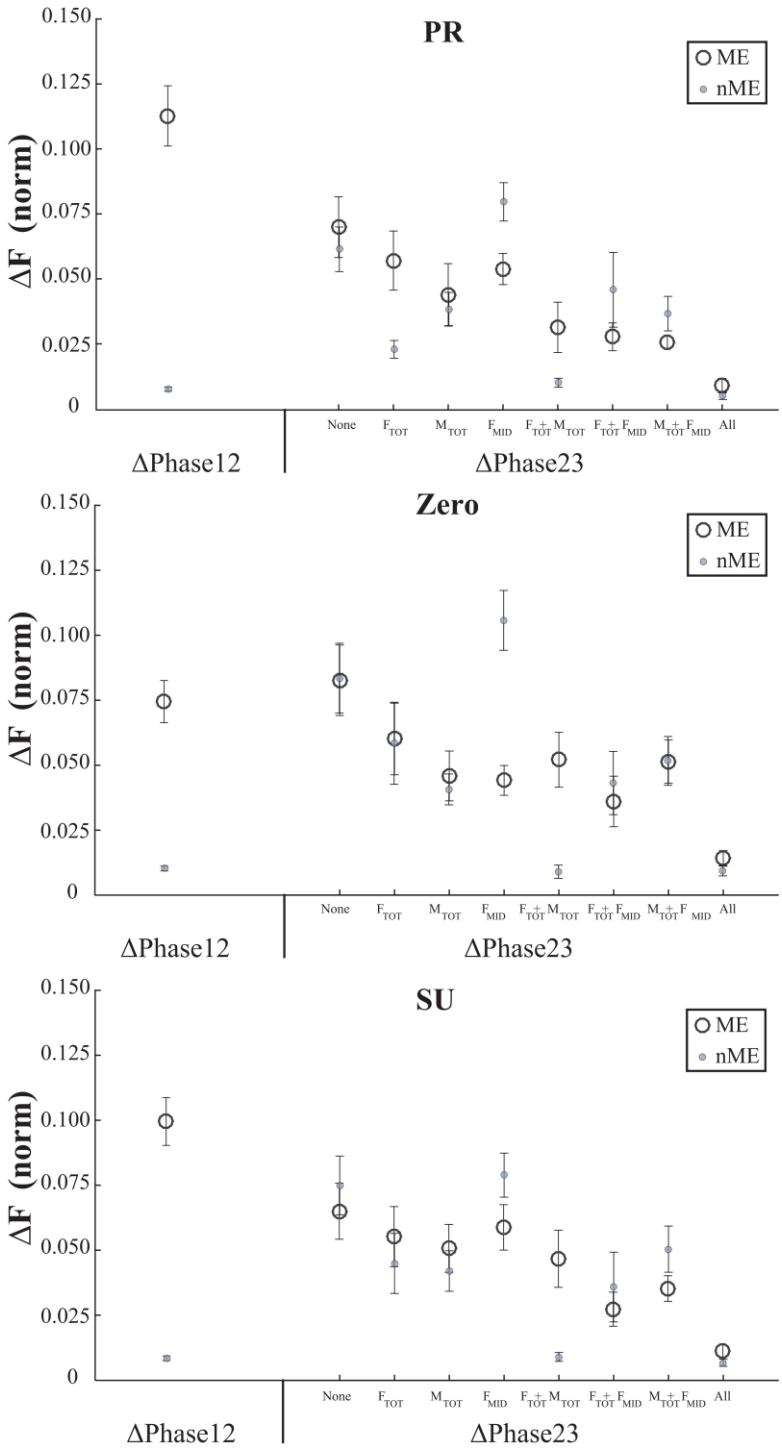

Figure 6-3. A typical example of F_{TOT}, M_{TOT}, F_{MID} was presented in (a) and (b) for F_{MID} and F_{TOT}+M_{TOT} feedback condition, respectively. Each of these time series was normalized to their targeted value at Phase-1. In (c) the ME and nME components computed considering Force-Moment Jacobian for the same subject and tasks was shown for two-time intervals (ΔPhase12 and ΔPhase23). (d) shows the average value for the variance components (V_{UCM} and V_{ORT}) on Force-Moment Jacobian in Phase-1 and Phase-2.

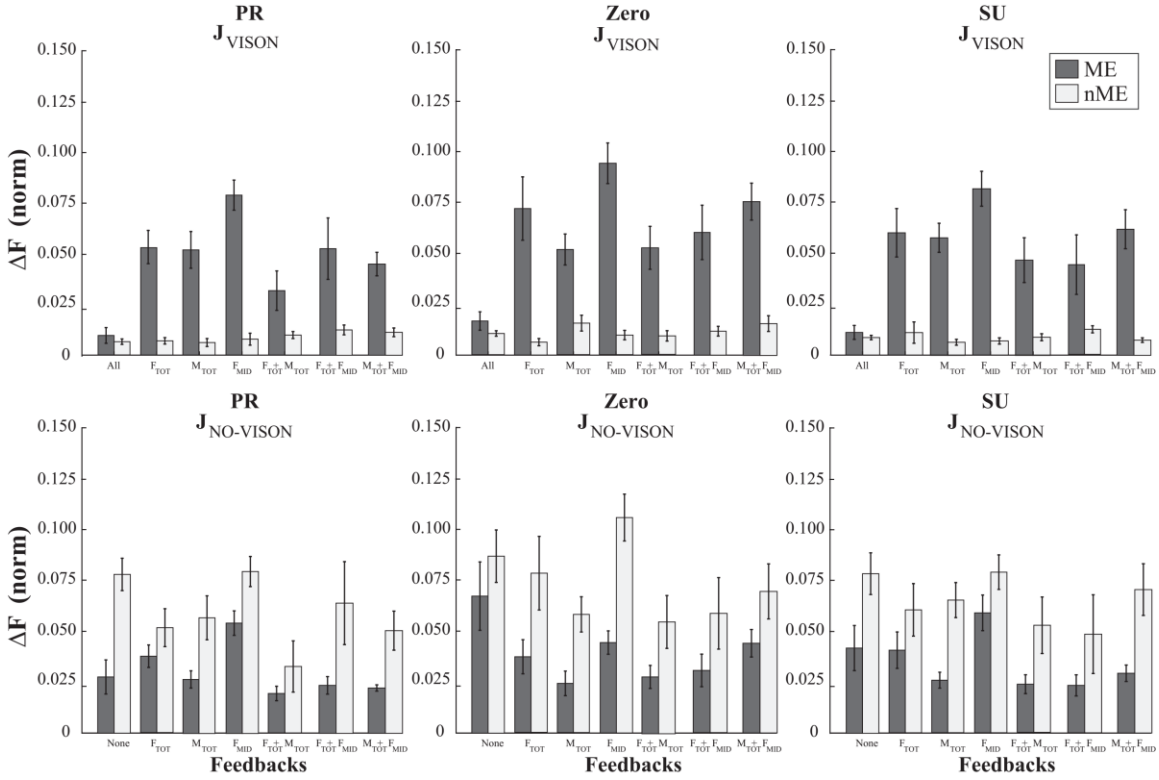

Figure 6-4. Averaged ME and nME components across all subjects for ΔPhase12 and ΔPhase23 for different moment conditions. Force-Moment Jacobian was used for all the conditions.

A three-way repeated measures ANOVA, *Jacobian* (feedback, no-feedback) × *Moment* × *Feedback* was run on ME and nME components separately. ANOVA on ME showed significant effects of *Moment* ($F_{[2, 20]} = 5.26$, $p < 0.05$), *Feedback* ($F_{[5, 50]} = 8.49$, $p < 0.001$), and *Jacobian* ($F_{[1, 10]} = 28.29$, $p < 0.001$), and a significant interaction *Moment* × *Jacobian* ($F_{[2, 20]} = 15.11$, $p < 0.001$). Pairwise contrast confirmed that the ME component was the largest when the feedback was provided on F_{MID} only compared to conditions with feedback on other subsets of constraints ($p < 0.05$). It is obvious from Figure 6-4 that the nME values were much larger for the No-Feedback Jacobian than for the Feedback Jacobian ($F_{[1, 10]} = 33.55$, $p < 0.001$). ANOVA showed no significant effect of *Feedback* while there was an effect of *Moment* ($F_{[2, 20]} = 7.29$, $p < 0.005$) reflecting larger nME magnitudes for the Zero M_{TOT} condition compared to the PR condition.

6.2.2 Analysis of the structure of variance

This analysis could only be run over Phase-1 and Phase-2 because only three trials were available for any given feedback conditions between Phase-2 and Phase-3. In both Phase-1 and Phase-2, strong synergies stabilizing the $\{F_{TOT}; M_{TOT}\}$ combination were observed. These synergies were reflected in the much higher inter-trial variance component leading to no changes in $\{F_{TOT}; M_{TOT}\}$ compared to the variance component leading to changes in $\{F_{TOT}; M_{TOT}\}$, $V_{UCM} > V_{ORT}$ ($F_{[1, 9]} = 35.76$; $p < 0.005$). Adding the new constraint (F_{MID}) led to very small effects on V_{ORT}; in contrast, there was a consistent drop in the magnitude of V_{UCM} (*Phase* × *Variance* interaction, $F_{[1, 9]} = 12.05$; $p < 0.01$). These results are illustrated in Figure 6-5. Note the very small V_{ORT} magnitudes (white bars) compared to the V_{UCM} (black bars) and a drop in V_{UCM} from Phase-1 to Phase-2.

These results were reflected in the synergy index ΔV values that were consistently positive across conditions and phases. The synergy indices were larger in Phase-1 (on average, z-transformed values were 1.85 ± 0.074 for Phase-1, and 1.56 ± 0.071 for Phase-2, $F_{[1, 9]} = 12.53$, $p < 0.01$). The synergy indices were the largest for $M_{TOT} = 0$ (*Moment* $F_{[2, 18]} = 6.423$, $p<0.01$), and the difference between the phases was the smallest for $M_{TOT} = 0$ (*Moment* × *Phase* interaction, $F_{[2,18]} = 3.65$, $p < 0.05$).

When the analysis in Phase-2 was run with respect to all three constraints (F_{TOT}, M_{TOT}, and F_{MID}), both the V_{ORT} and V_{UCM} values became significantly larger when normalized by dimensionality of the spaces (compare the data for "Phase-2" and "Phase-2*" in Figure 6-5; the data with * refer to the analysis with respect to all three constraints; $p < 0.05$). Note that V_{TOT} was the same for the two analyses. The difference between the phases was due to the fact that the UCM is two-dimensional for the analysis with respect to $\{F_{TOT}; M_{TOT}\}$, and it is one-dimensional with respect to the three constraints. So, the total V_{UCM} was in fact smaller for the analysis with respect to the three constraints, but the normalized values were larger. These results were reflected in the significantly larger ΔV_Z indices computed with respect to the two original constraints in Phase-2 as compared to the ΔV_Z indices computed with respect to all three constraints (1.55±0.38 vs. 0.93±0.41; $F_{[1, 9]} = 22.2$, $p<0.001$). As in the earlier analysis of ΔVZ data, there was a significant effect of *Moment* ($F_{[2, 18]} = 14.0$, $p<0.001$) and a significant *Moment* × *Jacobian* interaction ($F_{[2, 18]} = 18.7$, $p<0.01$) reflecting the largest values of ΔV_Z for $M_{TOT} = 0$ and the smallest difference between the two analyses for $M_{TOT} =0$.

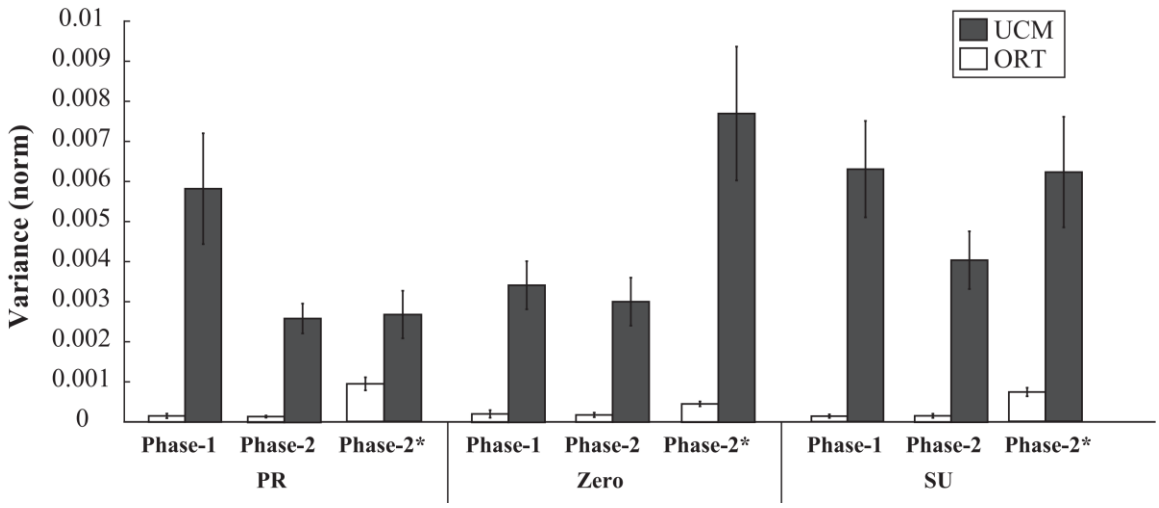

Figure 6-5. Averaged ME and nME components across all subjects for ΔPhase23. A Jacobian reflecting constraints with the feedback that remained on the screen throughout the trial (J_{VISION}) was used for each feedback condition in the top row. However, the reverse was done in the bottom row, ME and nME components were computed with respect to the Jacobian reflecting constraints without feedback ($J_{NO\text{-}VISION}$) between Phase-2 and Phase-3. As a result, we are observing large nME components in the bottom row. Both of the components were normalized by the corresponding dimension of the space in which they were computed.

We also explored correlations between the indices of motor equivalence during the transition from Phase-1 to Phase-2 and the inter-trial variance indices available for Phase-2. This analysis was done across all subjects. The only consistently significant correlations were observed between the nME index and V_{ORT} (R^2 ranged between 0.462 and 0.624; $p < 0.05$ for all three moment conditions). There were no significant correlations between V_{UCM} and ME and between ME/nME and ΔV_Z indices.

6.3 Discussion

Our first hypothesis was that selective stability of performance variables would be observed even when the magnitudes of those variables drifted unintentionally. This hypothesis has been falsified in the analysis of motor equivalence (cf. Mattos et al. 2011, 2015). Indeed, under complete visual feedback (between Phase-1 and Phase-2 and also under the "All" condition between Phase-2 and Phase-3), the finger force deviations led not only very small changes in the directions that changed the magnitudes of variables related to the task constraints (non-motor equivalent, nME). In contrast, finger force deviations were large in directions that led to no changes in those variables (motor equivalent, ME > nME). When the analysis was run for variables that stopped receiving visual feedback between Phase-2 and Phase-3, the ME deviations became smaller while the nME deviations increased leading to an inequality nME > ME. While quantitative analysis of the ME and nME indices has to be interpreted with care (cf. Scholz and Schöner 2014; also see later in the Discussion), the counter-directional changes in the two components suggest that visual feedback was crucial to ensure stability of the task-related variables.

Our second hypothesis was related to changes in the structure of inter-trial variance after adding a new constraint to the ongoing task of producing a combination of total force and total moment, $\{F_{TOT}; M_{TOT}\}$. We hypothesized that the synergy index (reviewed in Latash et al. 2007) would drop after the subjects purposefully reduced F_{MID} to 50% of its preferred value, and the results have supported this hypothesis. Indeed, while the inequality $V_{UCM} > V_{ORT}$ was present at both phases, during Phase-2, there was a significant drop in the synergy index (ΔV). Further, we discuss implications of these results for stability of performance variables that are produced with or without appropriate visual feedback.

6.3.1 Synergies and the number of constraints

Our understanding of synergies links this central concept in motor control (Babinski 1899; Bernstein 1947, 1967) to stability of performance (Schöner 1995). Stability is an absolutely crucial feature of functional movements because all such movements are performed in the presence of unpredictable, time-varying neural states in the unpredictable and time-varying environment. This makes the current concept of synergy different from those used in clinical studies (DeWald et al. 1995) and in studies of motor behavior that imply under this term sets of performance variables produced by effectors that show parallel changes (d'Avella et al. 2003; Ivanenko et al. 2004; Ting and Mcpherson 2005).

In earlier studies within the framework of the UCM hypothesis, inter-trial variance indices were used as proxies of stability (reviewed in Latash et al. 2002, 2007). To make the indices comparable between spaces with different dimensionalities, V_{UCM} and V_{ORT} were normalized per dimension. We used the same method to compare variance indices between Phase-1 (when the subject performed the task under the two original constraints, F_{TOT} and M_{TOT}) and Phase-2 (when the third constraint related to F_{MID} was added). Adding the third constraint forced the subjects to use a sub-space in the original UCM (in Phase-1) compatible with the required value of F_{MID}. This naturally was expected to lead to a drop in V_{UCM}, which was observed in the experiment, resulting in a drop in the synergy index ΔV.

Earlier studies with the production of accurate sine patterns of F_{TOT} with 2, 3, and 4 fingers of a hand led to an unexpected result (Latash et al. 2001; Scholz et al. 2002): When the subjects performed the task with two fingers only, they showed a pattern of variance compatible with stabilization of M_{TOT} although it was not specified as a performance variable, and the subjects had no visual feedback on M_{TOT}. This led to lack of synergies stabilizing F_{TOT}. Adding a third finger led to even stronger M_{TOT}-stabilizing synergies without F_{TOT}-stabilizing synergies. Only in the four-finger condition, the subjects showed stabilization of M_{TOT} (stabilized over the whole cycle) and of F_{TOT} (stabilized only within a narrow phase range corresponding to relatively high force magnitudes). Taken together, the results of those studies and of the current study confirm the idea that: (a) a new constraint is incorporated into the original solutions space leading to a reduction in the size of the solution space used by the CNS; and (b) reducing the number of elements leads to shrinking the solution space, which primarily affects stability of less salient variables.

Then analysis with respect to all three constraints in Phase-2 (data shown s Phase-2* in Figure 6-5) showed a somewhat counter-intuitive picture: Both V_{UCM} and V_{ORT} increased for the three-constraint analysis (as compared to the two-constraint analysis) while total variance obviously stayed the same. This was possible because of two factors, the different dimensionality of the UCM and ORT spaces in the two analyses and the very different magnitudes of the variance components ($V_{UCM} >> V_{ORT}$). Indeed, V_{UCM} dropped in the three-constraint analysis, while V_{ORT} increased by the same magnitude. Because of the normalization per dimension, the normalized magnitude of V_{UCM} increased. On the other hand, the added variance to V_{ORT} was so much bigger as compared to its original magnitude that, even after normalization by the increased dimensionality of ORT, it remained significantly larger as compared to the two-constraint analysis. The data in Figure 6-5 show that comparing variance indices across tasks with different numbers of constraints may lead to seemingly controversial results.

6.3.2 Stability and its reflections in motor equivalence and structure of variance

The two methods of analysis used in this study, structure of variance and motor equivalence, have been used in earlier studies as proxies of stability with respect to task-specific, salient performance variables (reviewed in Scholz and Schöner 2014; Latash and Zatsiorsky 2015). The two indices (ME/nME and ΔV) are not 100% equivalent. This was shown in earlier studies that documented somewhat different behaviors of the two indices (Mattos et al. 2011, 2014).

In our study, two inequalities ($V_{UCM} > V_{ORT}$ and ME > nME) were seen consistently for the data at Phase-1 and Phase-2 when the subjects had full feedback on all the relevant variables. The two inequalities are both consistent with the idea of selective stabilization of the two performance variables related to the original set of constraints, $\{F_{TOT}; M_{TOT}\}$. Correlation analysis, however, revealed significant correlations between V_{ORT} and nME only. In other words, subjects who showed larger nME deviations during the transition from the two-constraint phase to the three-constraint phase were also the ones who showed larger V_{ORT} at the end of this transition. Large nME reflects larger violations of the original $\{F_{TOT}; M_{TOT}\}$ constraints during the transition. These larger changes in $\{F_{TOT}; M_{TOT}\}$ led to larger inter-trial variance in those variables (V_{ORT}), possibly reflecting the so-called signal-dependent noise (Newell; Wolpert REF).

The lack of correlations between ME and V_{UCM} is non-trivial. Indeed, larger ME deviations imply larger changes of finger forces in directions that did not affect $\{F_{TOT}; M_{TOT}\}$. The idea of signal-dependent noise suggests that inter-trial variance in those directions should also be larger. This was not the fact, however: Correlations between V_{UCM} and ME across M_{TOT} conditions could be both positive and negative with the R^2 values always under 0.11. So, by itself, signal-dependent noise was not a defining factor in the patterns of finger force changes and the respected variance indices. The relations between the outcome variables of the ME and variance analyses remain unclear and have to be explored in future studies. While both sets of indices seem to reflect stability of relevant performance variables (cf. Mattos et al. 2011; Scholz and Schöner 2014), they should be viewed as complementary rather than redundant.

6.3.3 Stability during unintentional drift in performance

In Chapter 5, we present arguments in favor of a scheme that views unintentional drifts in performance as consequences of two processes. First, there is a drift of referent coordinates (RCs) for the salient task-specific variables toward their actual coordinates (ACs). This is a natural process expected in any physical system moving toward minimum of potential energy; it is expected within the hypothesis on

the neural control of movements with changes in RCs for salient variables (Latash 2010; Feldman 2015). Second, there is a drift of an abundant system toward states with smaller costs as defined within the ideas of optimal control: If a system is forced to perform using non-optimal contributions of elemental variables, it is expected to show a drift toward more optimal configurations. We modeled this situation by asking the subjects to produce $\{F_{TOT}; M_{TOT}\}$ values using finger force combinations that differed from the preferred ones, namely with the middle finger force reduced by 50%.

Within this general scheme, both ME and nME drifts are expected. The consistent drifts in F_{TOT} and M_{TOT} in the absence of visual feedback (cf. Slifkin et al. 2000; Vaillancourt and Russell 2002; Parsa et al. 2016) are leading to nME deviations. The drifts within the UCM, directed toward finger force combinations with smaller costs, lead to ME deviations. A priori, we could not predict the relative magnitude of the two drifts. Based, of earlier studies and on the general scheme of hierarchical control with RCs (Latash et al. 2010; Ambike et al. 2015), we expected to see synergies stabilizing variables that showed consistent drifts after the relevant visual feedback had been turned off. The main result, however, falsified this hypothesis. Indeed, visual feedback manipulations led to the typical inequality ME > nME for the variables that continued to receive feedback, while the inequality reversed, nME > ME, for the variables without visual feedback (Figure 6-4). This was associated with changes in both ME and nME. Overall, the ME components decreased after the removal of visual feedback, while the nME components increased.

Unfortunately, because of the large number of feedback conditions, we could not collect enough trials per condition to perform the analysis of the structure of inter-trial variance in Phase-3. So, in this study, we have only ME data reflecting stability of the variables that continues to receive visual feedback vs. those that stopped receiving this feedback. The contrast between the two is striking. It suggests that visual feedback plays a very important role in ensuring stability of performance variables. While the result is compatible with several hypotheses on the origin of synergies (Todorov and Jordan 2003; Latash et al. 2006; Martin et al. 2009), it suggests that the central back-coupling loops by themselves were unable to bring about stability of variables without the help of visual feedback. It is possible that the formulation of the task biased the subjects toward relying on visual feedback to ensure stable performance in our experiment. We plan to explore this possibility by using similar tasks performed primarily under somatosensory control and/or based on memory.

6.3.4 Concluding comments

To summarize, we learned the following main lessons from the results presented in this series of two papers (Chapter 5 and 6). Unintentional changes in performance can be seen in different performance variables – individual finger forces, total force, and total moment of force – following removal of the visual feedback. The variables showing the drift fail to show stabilization by the adjusted contributions of individual fingers, while variables that continue to receive visual feedback show signatures of selective stability. The drifts are consistent with two processes: (a) a drift of the referent coordinate for a variable toward its actual coordinate; and (b) a drift in the abundant space of elements toward configurations with lower cost. Adding a new constraint to an ongoing task results in a drop in the amount of variance within the original uncontrolled manifold leading to a drop in the synergy index. Overall, these results fit naturally the scheme of hierarchical control using changes in referent coordinates for relevant variables.

Chapter 7

Discussion

The study presented here tested seven specific hypotheses in three successive studies. Hypothesis 1 predicted that as a result of RC-back-coupling F_{TOT} and M_{TOT} would drift in the absent of visual feedback. However, some fingers might experience an increase in force as they need to satisfy the moment condition (Hypothesis 2). Hypothesis 3 predicted that synergies would persist during F_{TOT} and M_{TOT} drifts. Hypothesis 4 predicted that the drift in F_{TOT} and M_{TOT} would lead to an increase in the corresponding V_{ORT} compared to the condition with feedback. The similar effect on V_{UCM} was explored. As an increase in VORT was expected, it was also hypothesized that nME would consistently drift (hypothesis 5). However, again the change in ME component was explored.

In the second study, it was hypothesized that unintentional changes in performance variables during continuous static tasks without visual feedback are due to two processes: RC-back-coupling and a drift within UCM toward a minimum. Therefore, in addition to hypothesis 1 we hypothesized that in the case of having a good approximation for the cost function the value of it would decrease by time (hypothesis 6). Hypothesis 7 predicted that a selective stability of performance variables would be observed even when the magnitudes of those variables drift unintentionally. ME and nME indices were used as quantitative proxies of stability. It was also explored whether the stability of a variable depended on the number of explicit task constraints.

Some of the hypotheses mentioned above have been supported, while some have not. This study showed the richness of both UCM hypothesis and the hypothesis of control of the actions by controlling unique coordinates in describing humans' motor behavior. F_{TOT} and M_{TOT} drop in the absent of visual feedback while depending on the role of each finger in the initial moment condition they may decrease or increase. The drift at the moment itself depends on in the initial moment, but its absolute value falls. Observation of the drifts can also be interpreted based on the performance of the sensory system. In section 2.5.1.3 the characteristics of mechanoreceptors were briefly described. We know that Merkel's disks and Ruffini endings detect contact forces, and they are slowly adapting sensors. Therefore, they are playing an important role in the results of all experiments presented in this thesis. The drifts we observe can be a result of the Merkel's disks and Ruffini endings slow adaptation to the pressure on the fingertips. It also is good to be noted is that as the sensory input never gets to zero the forces produced by fingers never reaches zero; however, this is theoretically possible if the actual coordinates reach the referent coordinates.

As V_{ORT} increases without visual feedback and $V_{UCM,}$ tend to drop the synergy stabilizing those performance variables disappears in the absent of visual feedback. Moreover, along with the drift in performance variables (orthogonal to UCM), there is another ongoing drift within UCM which is purposeful. It is a minimum cost for the set of $\{F_{TOT}, M_{TOT}\}$ that is being experienced during the drift. This movement lets the system reach a preferred sharing while reaching the new RC. This phenomenon can also be observed if subjects get to a $\{F_{TOT}, M_{TOT}\}$ target and staying there for a while; they eventually will find the best set of finger sharing for that task.

More interesting is that when an additional constraint is added to a $\{F_{TOT}, M_{TOT}\}$ task like the given feedback on F_{MID}, it lead to a large ME component while taking any combination of the feedbacks away always result in an ME component less than that (Figure 6-2). Furthermore, it decreases the synergistic behavior within fingers by reducing V_{UCM}. This is a case in point that shows not all precise performance are an indication of having high synergy. To put it in another word, the system needs to have enough freedom to be able to compensate for any disturbance and reach stability. Therefore, highly constraining it will affect this ability and result in lower synergies.

Overall, what has been learned through this study is that observing promising results interpretable by UCM and RC hypotheses tells us that these can become useful quantitative tools for the measurement of people's performance. This quantitative measure can be very helpful for rehabilitation purposes that still suffer from that lack of a precise measure to categorize their patients correctly. However, this needs a broad set of targeted experiments with a large control/patient subject population to be able to make reliable conclusions.

On the other hand, bio-inspired robotics has become very popular recently. The focus of this field of science and engineering is to use the outcome of the neuroscience and motor control (the available models of human movement) for the design of their robots (Vitello et al. 2016, Ott et al. 2016, Huang and Wang 2016, Cauli et al. 2016). The findings from this line of research might be insightful for engineers, considering that the most significant challenge for a bi-pedal robot is maintaining its stability in the environmental disturbances. Variability gives the system more stable behavior. However, one should not overestimate this conclusion as designing a robot is very complicated and involves many different parts consisting hardware design, sensors, and software (including the controller). Therefore, some suggestions without a full knowledge of the underlying mechanisms might be tough if not possible to implement mathematically.

Researchers have become more interested in using subject-specific models (Scheys et al. 2011 Leitch et al. 2010, Winby et al. 2008). Although in almost all of these studies the primary goal was to determine the parameters of the musculoskeletal model as close as possible to subjects properties, this still

can indicate they tendency to design all parts of the model and mathematical methods for individual subjects. Having a subject-specific model is precious for the prediction of a musculoskeletal surgery. Or they can be used to investigate the optimal performance of an athlete for a particular competition. Our findings in this study demonstrate that ANIO can be helpful in finding a subject specific cost function.

Another area that is having a well-defined model of human movement can be very essential is animation production. One way to make a human character more believable is by making it move in similar patterns as humans do. Therefore, it is critical to be able to define the relations between joints and the strategy used for solving the redundant problem of movement as similar to humans. Findings in this study showed that UCM hypothesis is a promising perspective that helps to reduce the dimensionality of the elemental variable by teasing out the variables affecting the performance from those can be let free.

To be able to put the results of this study in practice one need to expand this study and use the same approach and test more complex movements. Therefore, I think the next experiment that worth doing could be on reaching tasks. To see if the same dual behavior (RC-back-coupling and the drift in cost) is still observed in the drift or not.

7.1 References

Ambike S, Mattos D, Zatsiorsky VM, Latash ML (2016a) The nature of constant and cyclic force production: Unintentional force-drift characteristics. *Experimental Brain Research* 234: 197-208.

Ambike S, Mattos D, Zatsiorsky VM, Latash ML (2016b) Synergies in the space of control variables within the equilibrium-point hypothesis. *Neuroscience* 315: 150-161.

Ambike S, Zatsiorsky VM, Latash ML (2015) Processes underlying unintentional finger force changes in the absence of visual feedback. *Experimental Brain Research* 233: 711-721.

Arbib MA, Iberall T, Lyons D (1985) Coordinated control programs for movements of the hand. In: Goodwin AW and Darian-Smith I, eds. *Hand Function and the Neocortex*. Berlin: Springer Verlag; pp. 111-129.

Berret B, Chiovetto E, Nori F, and Pozzo T, Evidence for composite cost functions in arm movement planning: an inverse optimal control approach, *PLoS Comput Biol*, vol. 7, p. e1002183, Oct .2011

Bottasso CL, Prilutsky BI, Croce A, Imberti E, and Sartirana S, A numerical procedure for inferring from experimental data the optimization cost functions using a multibody model of the neuro-musculoskeletal system, *Multibody System Dynamics*, vol. 16, pp. 154-123, .2006

Buchanan TS, Lloyd DG, K. Manal K, and Besier TF, Neuromusculoskeletal modeling: estimation of muscle forces and joint moments and movements from measurements of neural command, *Journal of applied biomechanics* ,vol. 20, p. 367, .2004

Buchanan TS and Shreeve DA, An evaluation of optimization techniques for the prediction of muscle activation patterns during isometric tasks, *Journal of biomechanical engineering*, vol. 118, p. 565, .1996

Danion F, Schöner G, Latash ML, Li S, Scholz JP, Zatsiorsky VM (2003) A force mode hypothesis for finger interaction during multi-finger force production tasks. *Biological Cybernetics* 88: 91-98.

Feldman, A.G. (2015) Referent control of action and perception: Challenging conventional theories in behavioral science. Springer, NY.

Forster E, Simon U, Augat P, and Claes L, Extension of a state-of-the-art optimization riterionto predict co-contraction, *J Biomech*, vol. 37, pp. 81-577, Apr .2004

Gelfand IM, Latash ML (1998) On the problem of adequate language in motor control. *Motor Control* 2:306-313

Heijnen MJ, Muir BC, Rietdyk S (2012) Factors leading to obstacle contact during adaptive locomotion. *Experimental Brain Research* 223: 219-231.

Heijnen MJ, Romine NL, Stumpf DM, Rietdyk S (2014) Memory-guided obstacle crossing: more failures were observed for the trail limb versus lead limb. *Experimental Brain Research* 232: 2131-2142.

Herzog W and Binding P, Predictions of antagonistic muscular activity using nonlinear optimization, *Math Biosci*, vol. 111, pp. 29-217, Oct 1992

Hogan N, Sternad D (2007) On rhythmic and discrete movements: reflections, definitions and implications for motor control. Experimental Brain Research 181:13-30

Jiang Z, Mirka GA, Application of an Entropy-Assisted Optimization Model in Prediction of Agonist and Antagonist Muscle Forces, in Proceedings of the Human Factors and Ergonomics Society Annual Meeting, 2007, pp. .927-923

Jo HJ, Ambike S, Lewis MM, Huang X, Latash ML (2016) Finger force changes in the absence of visual feedback in patients with Parkinson's disease. Clinical Neurophysiology 127: 684-692.

Jo HJ, Park J, Lewis MM, Huang X, Latash ML. (2015) Prehension synergies and hand function in early-stage Parkinson's disease. *Experimental Brain Research* 233: 425-440.

Kilbreath SL, Gandevia SC (1994) Limited independent flexion of the thumb and fingers in human subjects. *Journal of Physiology* 479: 487-497.

Kelso JA, Holt KG (1980) Exploring a vibratory systems analysis of human movement production. *Journal of Neurophysiology* 43: 1183-1196.

Kugler PN, Turvey MT (1987) Information, Natural Law, and the Self-Assembly of Rhythmic Movement. Hillsdale, NJ: Erlbaum

Latash ML (2008) *Synergy*. Oxford University Press: New York.
Latash ML (2010) Motor synergies and the equilibrium-point hypothesis. *Motor Control* 14: 294-322.
Latash ML (2012) The bliss (not the problem) of motor abundance (not redundancy). *Experimental Brain Research* 217: 1-5.
Lackner JR, DiZio P (1994) Rapid adaptation to Coriolis force perturbations of arm trajectory. *Journal of Neurophysiology* 72: 1-15.
Latash ML, Gottlieb GL (1990) Compliant characteristics of single joints: Preservation of equifinality with phasic reactions. *Biological Cybernetics* 62: 331-336.
Latash ML, Scholz JF, Danion F, Schöner G (2001) Structure of motor variability in marginally redundant multi-finger force production tasks. *Experimental Brain Research* 141: 153-165.
Latash ML, Shim JK, Smilga AV, Zatsiorsky VM (2005) A central back-coupling hypothesis on the organization of motor synergies: A physical metaphor and a neural model. *Biological Cybernetics* 92: 186-191.
Latash ML, Scholz JP, Schöner G (2007) Toward a new theory of motor synergies. *Motor Control* 11: 276-308.
Latash ML, Zatsiorsky VM (2015) *Biomechanics and Motor Control: Defining Central Concepts*. Academic Press: New York, NY.
Liu CK, Hertzmann A, and Popović Z, Learning physics-based motion style with nonlinear inverse optimization, in *ACM Transactions on Graphics (TOG)*, 2005, pp. .1081-1071
Martin V, Scholz JP, Schöner G (2009) Redundancy, self-motion, and motor control. *Neural Computations* 21:1371-1414
Mattos D, Latash ML, Park E, Kuhl J, Scholz JP (2011) Unpredictable elbow joint perturbation during reaching results in multijoint motor equivalence. *Journal of Neurophysiology* 106: 1424-1436.
Mattos D, Schöner G, Zatsiorsky VM, Latash ML (2015) Motor equivalence during accurate multi-finger force production. *Experimental Brain Research* 233: 487-502.
Mombaur K, Truong A, and Laumond JP, From human to humanoid locomotion—an inverse optimal control approach, *Autonomous robots* ,vol. 28, pp. 383-369, .2010
Park J, Wu Y-H, Lewis MM, Huang X, Latash ML. (2012) Changes in multi-finger interaction and coordination in Parkinson's disease. *Journal of Neurophysiology* 108: 915-924.
Parsa B, O'Shea DJ, Zatsiorsky VM and Latash ML. (2016) On the nature of unintentional actions: A study of force/moment drifts during multi-finger tasks. *Journal of Neurophysiology*
Siemienski A, Direct solution of the inverse optimization problem of load sharing between muscles, *arXiv preprint math*/0611502, .2006